Dosimetry of Technetium-99m Pyrophosphate: A Bone Imaging Radiopharmaceutical

by Dennis Lowe

A thesis presented to the University of Manitoba
in partial fulfillment of the requirements
for the degree of Master of Science
in the Department of Physics

Winnipeg, Manitoba, Canada

ISBN 0-315-47856-X

DOSIMETRY OF TECHNETIUM-99m PYROPHOSPHATE: A BONE IMAGING RADIOPHARMACEUTICAL

BY

DENNIS LOWE

A thesis submitted to the Faculty of Graduate Studies of the University of Manitoba in partial fulfillment of the requirements of the degree of

MASTER OF SCIENCE

I hereby declare that I am the sole author of this thesis.

I authorize the University of Manitoba to lend this thesis to other institutions or individuals for the purpose of scholarly research.

Dennis Lowe

I further authorize the University of Manitoba to reproduce this thesis by photocopying or by other means, in total or in part, at the request of other institutions or individuals for the purpose of scholarly research.

Dennis Lowe

The University of Manitoba requires the signatures of all persons who use or photocopy this thesis. Please sign below, and give address and date.

ACKNOWLEDGEMENTS

I would like to thank my supervisor, Dr. R. F. Palser, for his guidance and support. I would like to thank the members of my thesis committee, Dr. J. B. Sutherland, Dr. M. W. Billinghurst, and Dr. W. Huda. Finally, I would like to thank Mrs. C. Shyka for her help in obtaining the patient data.

The use of the facilities at the Manitoba Cancer Treatment and Research Foundation, the Winnipeg Health Sciences Center, and the University of Manitoba are acknowledged.

This work was funded in part by the Manitoba Cancer Treatment and Research Foundation and by Health and Welfare Canada.

ABSTRACT

The absorbed dose and effective dose equivalent were calculated in 25 patients injected with 740 MBq (20 mCi) of Tc-99m labelled pyrophosphate. The patients were referred for routine diagnostic bone scans. Four whole body scans were obtained over a 24 hour period after injection. Also, urine collections were obtained just before each scan. The imaging system consisted of a scanning table and two gamma cameras controlled by a mini-computer. Anterior and posterior images were obtained simultaneously, and were stored and analyzed on the mini-computer. Activity was quantified using the geometric mean method. Biodistribution data was obtained for the kidneys, bladder (urinary), bone (skeleton), and soft tissue (remainder of the body). The absorbed dose was calculated using the MIRD method. The effective dose equivalent was calculated using the ICRP 26 weighting factors.

The following results give the mean and standard deviation for 25 patients and are normalized to a 740 MBq (20 mCi) injection. The absorbed doses to the various organs were, in mGy: bone surface (56±17), bladder (21±11), kidneys (11±3), red marrow (9.0±1.6), total body (3.0±0.2), ovaries (2.8±0.5), testes (2.3±0.4) and the remaining organs (<4). The effective dose equivalent was (6.1±0.8) mSv. Although the absorbed doses vary among organs by up to ±50%, the effective dose equivalent varies among patients by no more than ±15%.

DOSIMETRY OF TECHNETIUM-99M PYROPHOSPHATE:
A BONE IMAGING RADIOPHARMACEUTICAL

PAGE CONTENTS

MATERIALS AND METHODS

PAGE CONTENTS

MATERIALS AND METHODS

PAGE FIGURES

DATA REDUCTION

PAGE CONTENTS

DATA REDUCTION

PAGE FIGURES

RESULTS AND DISCUSSION

PAGE CONTENTS

PAGE FIGURES

INTRODUCTION

Internal radiation dosimetry deals with the calculation of absorbed dose to an organ in the body due to radioactivity distributed within the body. This requires a knowledge of:

(1) the distribution of activity in the organs as a function of time (also called biodistribution data or time-activity data);
(2) the nature of the radiation emitted by the radionuclide and the energy carried by each different type of radiation; and
(3) the fraction of energy emitted by each source organ that is absorbed in the particular target organ.

Item (2) is known with high accuracy compared to items (1) and (3). Due to the variation of function, size, shape, linear attenuation coefficient and relative location of organs among people, items (1) and (3) are approximated by models based on some concept of an "average human". The calculation of the distribution of activity among the various organs in the body is, at best, an approximation based on measurements performed on available subjects of varying anatomies and degrees of health.

The purpose of the present study was to obtain biodistribution data with the view of improving the accuracy of dose calculations over that currently reported in the literature. Specifically, patients referred for bone scans using Tc-99m pyrophosphate were studied.

RADIATION DOSIMETRY

ABSORBED DOSE

A standard method of calculating the absorbed dose to an organ due to some distribution of activity in the body has been developed by the Medical Internal Radiation Dosimetry (MIRD) Committee of the Society of Nuclear Medicine (REF, Loevinger 1976). An organ with a high concentration or large amount of activity is defined as a source organ. An organ for which the absorbed dose is to be calculated is called a target organ. A source organ may also be a target organ. Note that the word "organ" is not used in the strict anatomic sense, but can describe any part of the body, including the whole body.

The absorbed dose to an organ is defined as the energy absorbed by the organ divided by its mass. The mean absorbed dose to a target organ from a source organ is given by:

$$D\ (t, s) = \tilde{A}_s \times S\ (t, s)$$

$D\ (t, s)$ mean absorbed dose to target organ "t" from source organ "s" (mGy). The mean is used because the absorbed dose varies over the volume of the target organ.

$S\ (t, s)$ S value, or mean absorbed dose to target organ "t" per unit cumulated activity of source organ "s" (mGy/MBq-hr)

$\tilde{A}_s$ cumulated activity of source organ "s" (MBq-hr)

The total absorbed dose D_t (or simply absorbed dose) to a target organ "t" is given by the sum of the mean absorbed doses over all source organs:

$$D_t = \Sigma_s D(t, s)$$

The cumulated activity, $\tilde{A}_s$, is obtained by integrating the time-activity curve of the source organ "s". The limits of integration are from the time of administration of activity to the time when all activity is removed from the body by biological and physical processes.

The S value, or mean absorbed dose per unit cumulated activity, describes the contribution of absorbed dose to a target organ from activity in a source organ, for a given radionuclide. The S value combines the physical data of the radionuclide (REF, Dillman 1975), the absorption data of the organs (REF, Snyder 1977), and Reference Man data (REF, ICRP 23 1975) all into one number for each pair of source-target organs (REF, Snyder 1973). The S values for 20 source organs and 20 target organs for Tc-99m are given in (P06, MIRD S VALUES FOR TECHNETIUM-99M). Several assumptions are made in the calculation of the S values, with the major ones being that:

(1) the activity in a source organ is uniformly distributed; and
(2) Reference Man is representative of the average human adult.

In practice, the activity in a source organ is never uniformly distributed. Also, the anatomy of a person never conforms exactly to the anatomy of Reference Man. As a result, the MIRD method only allows one to calculate the absorbed dose to an organ to within a factor of two to three (REF, Roedler 1981), so that the absorbed dose calculations are estimates at best.

EFFECTIVE DOSE EQUIVALENT

The absorbed doses to the target organs were combined into one number called the effective dose equivalent (REF, ICRP 26 1977). The effective dose equivalent for a given set of absorbed doses produces the same risk as a uniform whole body radiation dose which is numerically equal to the effective dose equivalent. The advantage of this concept is that it is a direct estimate of risk and is therefore additive, and allows direct comparison of the risks of diagnostic procedures which use ionizing radiation.

The effective dose equivalent is given by:

$$H_e = \Sigma_t w_t \times H_t$$

H_e effective dose equivalent (mSv)

w_t weighting factor for target organ "t"

H_t dose equivalent to target organ "t" (mSv), where $H_t = D_t \times Q$

D_t absorbed dose to target organ "t" (mGy)

Q quality factor

The weighting factors are defined for the seven most radiosensitive organs in the body (P08, ICRP 26 WEIGHTING FACTORS). The weighting factors for all organs except the gonads are proportional to the risk of induction of fatal cancers. The risk to the gonads is for serious genetic disorders in the first two generations of offspring. The "remainder" refers to five other organs with the highest absorbed doses, over which the remaining "risk" is distributed. The choice of five organs, instead of ten or more, is arbitrary and leads to an overestimate of the effective dose equivalent. The "breast" organ is not listed as a target organ in the table of MIRD S values. Instead, the "other (muscle)" organ is assumed to be equivalent to the breast for the purpose of absorbed dose calculations. The sum of the weighting factors is one.

The quality factor represents the relative biological effectiveness of the radiation, which in turn depends on the energy and type of radiation (REF, ICRU 40 1986). To a first approximation, electrons with energies greater than 30 keV and all gamma rays have a quality factor of one. As shown in (P40, DECAY SCHEME OF Tc-99M), Tc-99m emits gamma rays and electrons, where most of the electrons have a mean energy greater than 15 keV. Therefore, to a first approximation, the quality factors of the radiations emitted by Tc-99m are all unity, so that the dose equivalent is numerically equal to the absorbed dose.

MIRD S VALUES FOR TECHNETIUM-99M

S value, or absorbed dose per unit cumulated activity
with units of milligray per megabecquerel-hour
1 mGy/MBq-hr=(37/10000)*rad/μCi-hr

	SOURCE ORGANS									
TARGET ORGANS	Adrenals	Bladder Contents	Stomach Contents	Small Intestine Contents	Upper Large Intestine Contents	Lower Large Intestine Contents	Kidneys	Liver	Lungs	Other tissue (muscle)
Adrenals	8.4E-01	4.1E-05	7.3E-04	2.7E-04	2.5E-04	9.7E-05	3.0E-03	1.2E-03	7.3E-04	3.8E-04
Bladder wall	3.5E-05	4.3E-02	7.3E-05	7.0E-04	5.9E-04	1.9E-03	7.6E-05	4.3E-05	9.7E-06	4.9E-04
Bone surface ***	5.4E-04	2.5E-04	2.4E-04	3.5E-04	3.0E-04	4.3E-04	3.8E-04	3.0E-04	4.1E-04	2.6E-04
GI (stom wall)	7.8E-04	7.3E-05	3.5E-02	1.0E-03	1.0E-03	4.9E-04	9.7E-04	5.1E-04	4.9E-04	3.5E-04
GI (small intest)	2.2E-04	8.1E-04	7.3E-04	2.1E-02	4.6E-03	2.5E-03	7.8E-04	4.3E-04	5.1E-05	4.1E-04
GI (ULI wall)	2.5E-04	5.9E-04	9.5E-04	6.5E-03	3.5E-02	1.1E-03	7.8E-04	6.8E-04	5.9E-05	4.3E-04
GI (LLI wall)	5.9E-05	2.0E-03	3.2E-04	2.0E-03	8.6E-04	5.1E-02	1.9E-04	6.2E-05	1.9E-05	4.6E-04
Kidneys	3.0E-03	7.0E-05	9.5E-04	8.6E-04	7.6E-04	2.3E-04	5.1E-02	1.1E-03	2.3E-04	3.5E-04
Liver	1.3E-03	4.6E-05	5.4E-04	4.9E-04	7.0E-04	6.8E-05	1.1E-03	1.2E-02	6.8E-04	3.0E-04
Lungs	6.5E-04	6.5E-06	4.6E-04	5.9E-05	7.0E-05	2.1E-05	2.3E-04	6.8E-04	1.4E-02	3.5E-04
Marrow (red) ***	9.7E-04	5.9E-04	4.3E-04	1.2E-03	1.0E-03	1.4E-03	1.0E-03	4.3E-04	5.1E-04	5.4E-04
Other (muscle)	3.8E-04	4.9E-04	3.8E-04	4.1E-04	4.1E-04	4.6E-04	3.5E-04	3.0E-04	3.5E-04	7.3E-04
Ovaries	1.6E-04	2.0E-03	1.4E-04	3.0E-03	3.2E-03	4.9E-03	3.0E-04	1.2E-04	2.5E-05	5.4E-04
Pancreas	2.4E-03	6.2E-05	4.9E-03	5.7E-04	6.2E-04	2.0E-04	1.8E-03	1.1E-03	7.0E-04	4.9E-04
Skin	1.4E-04	1.5E-04	1.2E-04	1.1E-04	1.1E-04	1.3E-04	1.4E-04	1.3E-04	1.4E-04	1.9E-04
Spleen	1.7E-03	1.8E-04	2.7E-03	4.1E-04	3.8E-04	2.2E-04	2.3E-03	2.5E-04	6.2E-04	3.8E-04
Testes	8.6E-06	1.3E-03	1.4E-05	8.4E-05	7.3E-05	4.9E-04	2.4E-05	1.7E-05	2.1E-06	3.0E-04
Thyroid	3.5E-05	5.7E-07	2.4E-05	4.1E-06	4.3E-06	1.5E-06	1.3E-05	4.1E-05	2.5E-04	3.5E-04
Uterus (nongravid)	3.0E-04	4.3E-03	2.1E-02	2.6E-03	1.5E-03	1.9E-03	2.5E-04	1.1E-04	2.2E-05	6.2E-04
Total body	5.9E-04	5.1E-04	5.1E-04	6.5E-04	5.9E-04	6.2E-04	5.9E-04	5.9E-04	5.4E-04	5.1E-04

*** NOTE: the S values for the bone and marrow have been modified to account for the surface distribution of Tc-99m phosphorous radiopharmaceuticals used in bone imaging (Johannson 1981)

MIRD S VALUES FOR TECHNETIUM-99M

S value, or absorbed dose per unit cumulated activity
with units of milligray per megabecquerel-hour
1 mGy/MBq-hr = (37/10000) *rad/μCi-hr

	SOURCE ORGANS									
TARGET ORGANS	Ovaries	Pancreas	Red Marrow	Cortical Bone	Trabecular Bone	Skin	Spleen	Testes	Thyroid	Total body
Adrenals	8.9E-05	2.5E-03	6.2E-04	3.0E-04	3.0E-04	1.8E-04	1.7E-03	8.6E-06	3.5E-05	6.2E-04
Bladder wall	1.9E-03	3.8E-05	2.7E-04	1.4E-04	1.4E-04	1.3E-04	3.2E-05	1.3E-03	5.7E-07	6.2E-04
Bone surface ***	4.1E-04	4.1E-04	1.1E-03	2.2E-02	2.2E-02	2.7E-04	3.0E-04	2.5E-04	2.7E-04	6.8E-04
GI (stom wall)	2.2E-04	4.9E-03	2.6E-04	1.5E-04	1.5E-04	1.5E-04	2.7E-03	8.6E-06	1.2E-05	5.9E-04
GI (small intest)	3.2E-03	4.9E-04	7.0E-04	2.0E-04	2.0E-04	1.2E-04	3.8E-04	9.7E-05	2.5E-06	6.8E-04
GI (ULI wall)	3.0E-03	5.7E-04	5.7E-04	1.9E-04	1.9E-04	1.2E-04	3.8E-04	8.4E-05	3.0E-06	6.5E-04
GI (LLI wall)	4.1E-03	1.5E-04	7.8E-04	2.7E-04	2.7E-04	1.3E-04	1.6E-04	7.3E-04	1.2E-06	6.2E-04
Kidneys	2.5E-04	1.8E-03	5.9E-04	2.2E-04	2.2E-04	1.5E-04	2.5E-03	1.1E-05	9.2E-06	5.9E-04
Liver	1.5E-04	1.2E-03	2.5E-04	1.8E-04	1.8E-04	1.4E-04	2.6E-04	8.4E-06	2.5E-05	5.9E-04
Lungs	1.6E-05	6.8E-04	3.2E-04	2.5E-04	2.5E-04	1.6E-04	6.2E-04	1.8E-06	2.5E-04	5.4E-04
Marrow (red) ***	1.5E-03	7.6E-04	8.4E-03	1.1E-03	4.3E-03	2.6E-04	4.6E-04	2.0E-04	3.0E-04	7.8E-04
Other (muscle)	5.4E-04	4.9E-04	3.2E-04	2.6E-04	2.6E-04	1.9E-04	3.8E-04	3.0E-04	3.5E-04	5.1E-04
Ovaries	1.1E+00	1.1E-04	8.6E-04	1.9E-04	1.9E-04	1.0E-04	1.1E-04	0.0E+00	1.3E-06	6.5E-04
Pancreas	1.4E-04	1.6E-01	4.6E-04	2.3E-04	2.3E-04	1.2E-04	5.1E-03	1.5E-05	1.9E-05	6.5E-04
Skin	1.1E-04	1.1E-04	1.6E-04	1.8E-04	1.8E-04	4.3E-03	1.3E-04	3.8E-04	2.0E-04	3.5E-04
Spleen	1.3E-04	5.1E-03	2.5E-04	1.6E-04	1.6E-04	1.5E-04	8.9E-02	4.6E-06	3.0E-05	5.9E-04
Testes	0.0E+00	1.5E-05	1.2E-04	1.7E-04	1.7E-04	2.5E-04	1.3E-05	3.8E-01	1.4E-07	4.6E-04
Thyroid	1.3E-06	3.2E-05	1.8E-04	2.1E-04	2.1E-04	1.9E-04	2.4E-05	1.4E-07	6.2E-01	4.1E-04
Uterus (nongravid)	5.7E-03	1.4E-04	5.9E-04	1.5E-04	1.5E-04	1.1E-04	1.1E-04	0.0E+00	1.2E-06	7.0E-04
Total body	7.0E-04	7.0E-04	5.9E-04	5.4E-04	5.4E-04	3.5E-04	5.9E-04	5.1E-04	4.9E-04	5.4E-04

*** NOTE: the S values for the bone and marrow have been modified to account for the surface distribution of Tc-99m phosphorous radiopharmaceuticals used in bone imaging (Johannson 1981)

ICRP 26 WEIGHTING FACTORS

ORGAN	WEIGHTING FACTOR
gonads	0.25
breast	0.15
lung	0.12
red bone marrow	0.12
bone surface	0.03
thyroid	0.03
remainder *	5 x 0.06

* five other organs with the next highest absorbed doses

(REF, ICRP 26 1977)

LITERATURE REVIEW OF THE BIODISTRIBUTION OF TC-99M PYROPHOSPHATE

INTRODUCTION

The main problem in internal radiation dosimetry is the lack of biodistribution data on normal and diseased humans (REF, ICRU 32 1979, ICRP 30 1978). The biodistribution of a radiopharmaceutical in humans depends on a variety of physiological and radiopharmaceutical factors. In the absence of human data, animal data are used (REF, Roedler 1981, Lathrop 1981). This requires great care, since there are physiological and anatomical differences between animals and humans.

BIODISTRIBUTION OF TC-99M PHOSPHOROUS BONE IMAGING RADIOPHARMACEUTICALS

Tc-99m pyrophosphate belongs to a family of Tc-99m phosphorous bone imaging radiopharmaceuticals, the first of which was developed in 1971 (REF, Subramanian 1971). At present, there are four such radiopharmaceuticals in routine clinical use: pyrophosphate (PPi), hydroxyethylene diphosphonate (HEDP), methylene diphosphonate (MDP), and hydroxymethylene diphosphonate (HMDP) (REF, Perez 1972, Yano 1973, Subramanian 1975, Bevan 1980).

These Tc-99m phosphorous radiopharmaceuticals are injected intravenously into the body, where they are weakly bound to blood and strongly bound to bone. About 80% of the activity in blood is bound to protein, while the rest is free (non-bound) in plasma (REF, Krishnamurthy 1975). The mechanism of binding to bone is poorly understood, but is known to be related to bone formation and blood flow (REF, Arnold 1982). The radiopharmaceutical is removed from the blood by the kidneys, and excreted in the urine. The kidneys, urinary bladder, skeleton, and some soft tissue are clearly visible in an image of a normal patient (REF, Subramanian 1975, Jones 1976, Davis 1976). In the present study, soft tissue is defined as the whole body less the kidneys, urinary bladder, and skeleton. The soft tissue is also called the "remainder of the body" in other papers. In the rest of the text, the urinary bladder is called the bladder, and the skeleton is called the bone.

FACTORS AFFECTING THE BIODISTRIBUTION

The factors which affect the biodistribution of the radiopharmaceutical fall into two groups: radiopharmaceutical and physiologic. The radiopharmaceutical factors are due to radiochemical impurities which cause increased activity in the soft tissue, thereby increasing the absorbed dose to the soft tissue (see "Quality control of Tc-99m pyrophosphate" section). The physiologic factors are given below.

- BONE FUNCTION

  Abnormal bone function can change the bone uptake and bone blood flow (REF, Alazraki 1984, Rosenthall 1976, Genant 1974).

- RENAL FUNCTION

  Reduced renal function results in reduced renal excretion, and higher blood excretion. Dehydration has the same effect.

- PATIENT AGE

  In general, as the patient age increases, bone uptake decreases and soft tissue uptake increases (REF, Wilson 1981).

- SYSTEMIC THERAPY

  Several drugs affect the biodistribution of bone imaging radiopharmaceuticals (REF, Hladik 1982, Lentle 1979). Chemotherapy and corticosteroids are especially effective in decreasing the bone uptake. Alternatively, they may cause increased lesion radioactivity during the early healing process that follows initiation of chemotherapy.

- OTHER FACTORS

  Uptake in soft tissue is affected by a variety of factors, such as cancer, infection, radiotherapy, etc. (REF, Alazraki 1984).

URINARY EXCRETION

To calculate the activity retained in the body following administration of a radiopharmaceutical, one method is to measure the activity leaving the body (via exhalation, or excretion in the feces and/or urine), and subtract it from the administered activity. For Tc-99m phosphorous radiopharmaceuticals, activity leaves the body mainly in the urine. Urine collections are obtained typically over a period of four physical half lives, which is when there is no more than 6.25% of the injected activity remaining in the body. For Tc-99m, this corresponds to about 24 hours (4 x 6.03 hours). A convenient method of expressing the urine activity is to correct the activity for physical decay, back to the time of administration. The result is called the urinary excretion and is expressed as a percentage of the administered activity. Mathematically, the urinary excretion is given by:

$$UE\ (t_j) = \frac{\sum_{i=1,j} A_{URINE}\ (t_i) \times \exp\ (+\ln(2) \times t_i / T_{1/2})}{\text{injected activity}} \times 100\%$$

$j = 1$ to n	where n is the number of urine collections
$UE\ (t_j)$	urinary excretion at time t_j
$A_{URINE}\ (t_i)$	activity in the urine collection obtained at t_i
$T_{1/2}$	physical halflife of Tc-99m = 6.03 hours

From the urine collections, the time of injections, and the injected activity, one can calculate the activity in the whole body at the time each collection is obtained.

The urinary excretion in humans using Tc-99m pyrophosphate has been measured in three studies (REF, Subramanian 1975, Krishnamurthy 1975, Weber 1974). These results are summarized in (P21, URINARY EXCRETION IN HUMANS USING TC-99M PYROPHOSPHATE (GRAPH AND TABLE)). The urinary excretion increases rapidly, reaching 30% to 40% of the injected activity over the first four hours. At four hours, the urinary excretion curve of Krishnamurthy et al. is significantly lower than that of Subramanian et al., probably due to increased bone lesion uptake.

The dependence of urinary excretion on bone function was studied in normal and diseased humans with other Tc-99m phosphorous bone imaging radiopharmaceuticals. The 24 hour urinary excretion has been measured in three studies using various Tc-99m bone imaging radiopharmaceuticals (REF, Fogelman 1978, Thomsen 1986, Schultz 1987). These results are summarized in (P23, 24 HOUR URINARY EXCRETION IN HUMANS USING VARIOUS TC-99M PHOSPHOROUS BONE IMAGING RADIOPHARMACEUTICALS). Although different radiopharmaceuticals are used, and the definitions of normal and diseased humans differ, there are some similarities among Tc-99m phosphorous bone imaging radiopharmaceuticals:

(1) the range of 24 hour urinary excretion values is large for diseased humans, ranging from about 10% to 80%;

(2) the urinary excretion for normal humans overlaps with the diseased group in the 60% to 80% range; and

(3) the urinary excretion data for the diseased group can be further divided with respect to bone and renal function.

BLOOD

The blood time-activity data in humans using Tc-99m pyrophosphate has been measured in two studies (REF, Subramanian 1975, Krishnamurthy 1975). These results are summarized in (P24, BLOOD TIME-ACTIVITY DATA IN HUMANS USING TC-99M PYROPHOSPHATE, CORRECTED FOR PHYSICAL DECAY, (GRAPH AND TABLE)). These workers did not measure the activity in soft tissue (meaning the whole body less the bone and other source organs). Instead, the activity in soft tissue was assumed to be due to the activity in blood, which was more easily and accurately measured.

In these two studies, the activity in blood was found by measuring the activity in a blood sample and scaling the result by the total blood volume in the body. The total blood volume in an adult body is five litres, based on Reference Man data. The data by Subramanian et al. was based on seven blood samples obtained over a 24 hour period and fitted to a triexponential function. The data by Krishnamurthy et al. was based on five blood samples obtained over a 24 hour period and fitted to a biexponential function. A review of the data by Krishnamurthy et al. showed that they missed the first exponential term by not taking blood samples early enough after injection. Therefore, we will use the data by Subramanian et al. for further discussion.

The constants and half lives of the triexponential function found by Subramanian et al. are compared to those of other Tc-99m

phosphorous bone imaging radiopharmaceuticals (P26, BLOOD TIME-ACTIVITY DATA IN HUMANS USING VARIOUS TC-99M PHOSPHOROUS BONE IMAGING RADIOPHARMACEUTICALS, CORRECTED FOR PHYSICAL DECAY). The values are comparable, except for the half life of the third exponential term. The very wide range of half lives in the third term may reflect the chemical differences of the phosphorous radiopharmaceuticals, such as between the organic phosphonates and inorganic phosphates (REF, Billinghurst 1982). The wide range may also be due to the errors which result from fitting a limited number of points to a triexponential function.

The triexponential time-activity curve of blood is explained in terms of a five compartment model consisting of urine, blood, bone, bone extracellular fluid (ECF), and non-bone ECF (REF, Billinghurst 1982) (P27, FIVE COMPARTMENT MODEL FOR BONE IMAGING RADIOPHARMACEUTICALS). Note that the non-bone ECF and the blood are different. The first exponential is probably due to the distribution of activity throughout the ECF space as well as the blood. The second exponential probably represents bone uptake, via the bone ECF, leading to the re-establishment of the non-bone ECF equilibrium, and results in a drop in both the blood and non-bone ECF activity. The third exponential probably represents the urinary excretion, which seems to be in marked contrast to the fact that 40% to 60% of the activity is excreted in the urine in the first four hours after injection (REF, Subramanian 1975). However, note that:

(1) the urine activity is a direct function of the blood activity, so that the rate at which the urine activity increases is much higher during the early periods when there is a much higher blood activity.

(2) the blood activity remains in equilibrium with the activity in the non-bone ECF which probably returns to the blood as the activity is removed from the blood by the kidneys and is, in turn, excreted by the kidneys.

KIDNEYS

The kidney time-activity data in humans using Tc-99m phosphorous bone imaging radiopharmaceuticals are not available in the literature. Animal studies using Tc-99m pyrophosphate have found that the maximum uptake in the kidneys was 4.3% of the injected activity per 1% body weight [(kidney activity/injected activity)/(kidney weight/body weight)] (REF, Subramanian 1975, Eckelman 1974, Hosain 1973) (P28, KIDNEY TIME-ACTIVITY DATA IN ANIMALS USING TC-99M PYROPHOSPHATE). Assuming that the kidney activity concentration in humans is the same as in animals, then the kidney activity concentration in humans is obtained by multiplying this value by the ratio of the kidney weight to the whole body weight for an adult human, expressed as a percentage. Using Reference Man data, the maximum kidney activity is equal to 1.9% (4.3% x (0.31 kg/70 kg) x 100) of the injected activity. No data is available on the

effective half life of the kidney activity. This data is found in the present study.

BONE

The bone time-activity data in humans using Tc-99m phosphorous bone imaging radiopharmaceuticals are not available in the literature. There are several problems with quantifying the activity in bone (REF, Blau 1976). In a whole body image, a region of interest cannot be drawn that includes only the skeleton. Even if that were possible, it would be very difficult to quantify the activity because the thickness of bone and overlying soft tissue varies over the body. Another method of quantifying the activity involves calculating the activity per unit weight in a sample bone volume where the bone shape and thickness are known, and scaling the result by the total bone weight. However, it has been well documented that the distribution of Tc-99m phosphorous radiopharmaceuticals in bone is non-uniform. A whole body scan of a normal human using Tc-99m pyrophosphate demonstrates that the uptake in the vertebrae and pelvis is higher than in the long bones. Even in different parts of the same bone, such as a rib, the concentration may vary by a factor of three (REF, Subramanian 1975). Also, Tc-99m phosphorous radiopharmaceuticals are distributed on the bone surface, as opposed to being distributed throughout the total bone volume (REF, Arnold 1982). Furthermore, the skeleton consists of cortical bone, trabecular bone, and bone marrow, and the amount of each type of bone varies over the

skeleton (REF, Blau 1976). All these factors make it very difficult to accurately calculate the bone activity directly.

The activity is not taken up instantaneously in bone, but increases over the first two hours (REF, Snow 1975, Citrin 1975, Potsaid 1977, Castronovo 1977). For the purpose of calculating the absorbed doses, Subramanian et al. assumed that 50% of the injected activity was taken up into the bone instantaneously, and only underwent physical decay (REF, Subramanian 1975). Assuming that the skeleton represents 10% of the total body weight in humans, a 50% concentration is equivalent to about 7% of the injected activity per kilogram of bone. Animal studies using Tc-99m pyrophosphate have shown that the uptake in the femur was 8.3% of the injected activity per kilogram of bone in miniature swine, 6.2% in dogs, and 91.4% in rabbits (REF, Eckelman 1974). The 91.4% value for rabbits is much higher than the 7% value, and shows the problem with extrapolating animal data to humans.

Krishnamurthy et al. calculated the activity in the bone and kidneys together by subtracting the blood (= soft tissue) activity from the whole body activity (REF, Krishnamurthy 1975). They calculated the activity in the bone and kidneys to be 59% of the whole body activity at 4 hours (corrected for physical decay). Correcting for the kidney activity, this is comparable to the bone activity estimated by Subramanian et al (REF, Subramanian 1975). In both calculations, it was assumed that there was no uptake in soft tissue.

In summary, due to the non-uniform distribution of activity in bone and the non-uniform composition of bone, the bone activity cannot be accurately calculated directly. In the present study, the bone activity is found by subtracting the activity in the kidneys, bladder, and soft tissue from the whole body activity. As a result, the main problem in the present study was being able to accurately calculate the soft tissue activity.

SOFT TISSUE

The soft tissue time-activity data in humans using Tc-99m phosphorous bone imaging radiopharmaceuticals are not available in the literature. In the present study, the soft tissue is defined as the whole body less the kidneys, bladder, and bone.

URINARY EXCRETION IN HUMANS
USING TC-99M PYROPHOSPHATE

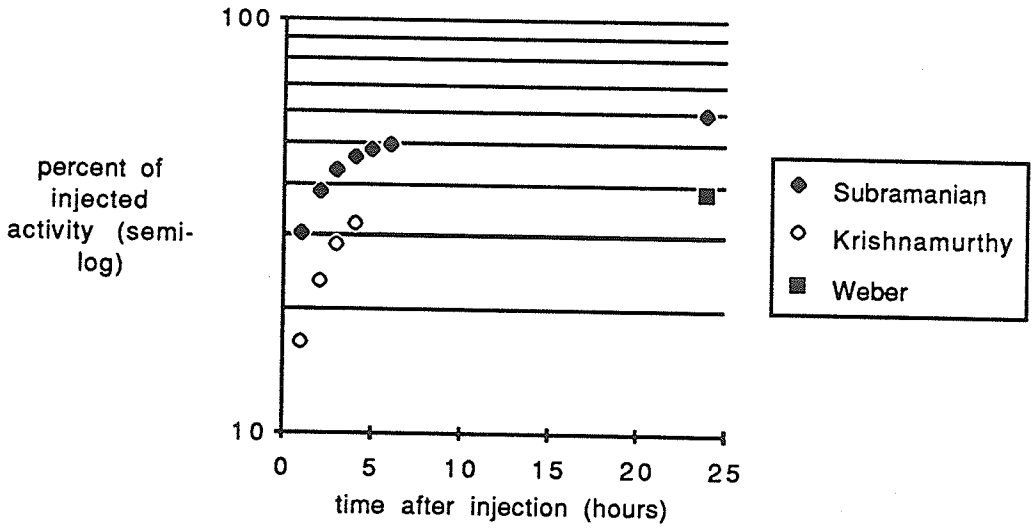

URINARY EXCRETION IN HUMANS USING TC-99m PYROPHOSPHATE

time (hours)	activity (percent of injected activity) A	B	C
0 - 1	29.9 ± 3.9	16.4 ± 3.0	---
0 - 2	38.0 ± 4.3	23.0 ± 3.3	---
0 - 3	42.7 ± 4.1	28.5 ± 3.6	---
0 - 4	45.9 ± 4.3	31.7 ± 4.0	---
0 - 5	48.2 ± 4.5	- - -	---
0 - 6	49.8 ± 4.5	- - -	---
0 - 24	58.9 ± 5.2	- - -	38.2 (28.1 to 56.4)

A - Subramanian, n=6, normal, ±1 standard deviation

B - Krishnamurthy, n=10, abnormal, ±1 standard error

C - Weber, n=5, abnormal

Abnormal refers to patients undergoing bone scans for suspected bone lesions, and "n" is the number of patients in the study.

24 HOUR URINARY EXCRETION IN HUMANS USING
TC-99M PHOSPHOROUS BONE IMAGING RADIOPHARMACEUTICALS

Activity expressed as percentage of the injected activity, ±1 standard deviation or range is specified.

normal	diseased	Tc-99m agent	Reference
59 ± 5	- - -	pyrophosphate	Subramanian, 1975
- - -	32 ± 4	pyrophosphate	Krishnamurthy, 1975
- - -	28 to 56	pyrophosphate	Weber, 1974
81 ± 2	11 to 79	HEDP	Fogelman, 1978
69 ± 5	19 to 60	MDP	Thomsen, 1986
51 ± 5	6 to 54	imidodiphosphate	Schultz, 1987

BLOOD TIME-ACTIVITY DATA IN HUMANS
USING TC-99M PYROPHOSPHATE, CORRECTED
FOR PHYSICAL DECAY

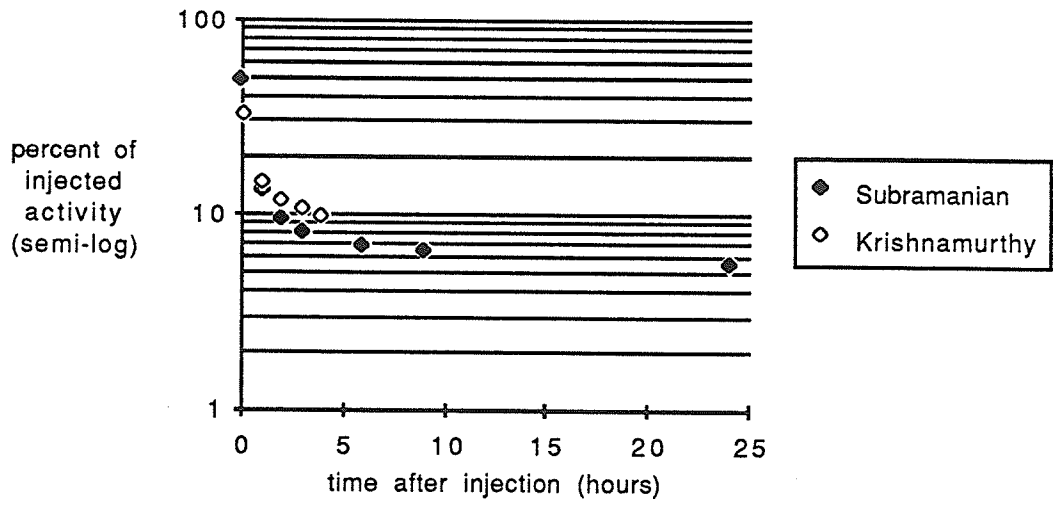

BLOOD TIME-ACTIVITY DATA IN HUMANS USING TC-99M PYROPHOSPHATE, CORRECTED FOR PHYSICAL DECAY

time (hours)	activity (% of the injected activity) A	B
3 min	48.4 ± 8.9	---
5 min	37.9 ± 4.6	---
10 min	- - -	32.0 ± 3.0
0.5 hr	18.1 ± 3.0	20.0 ± 2.0
1	13.0 ± 2.0	14.5 ± 2.0
2	9.35 ± 1.7	11.5 ± 1.5
3	7.95 ± 1.7	10.5 ± 1.5
4	- - -	9.5 ± 1.0
6	6.83 ± 1.4	---
9	6.41 ± 1.3	---
24	5.44 ± 1.0	---

A - Subramanian, n=6, normal, ±1 standard deviation

B - Krishnamurthy, n=10, abnormal, ±1 standard error

Abnormal refers to patients undergoing bone scans for suspected bone lesions, and "n" is the number of patients in the study.

BLOOD TIME-ACTIVITY DATA IN HUMANS USING TC-99M PHOSPHOROUS BONE IMAGING RADIOPHARMACEUTICALS, CORRECTED FOR PHYSICAL DECAY

	Subramanian Tc-99m pyro		Billinghurst other Tc-99m agents	
i	A_i	T_i	A_i	T_i
1	74.0	0.03	70 - 80	0.05 - 0.10
2	18.3	0.64	15 - 20	0.25 - 0.50
3	7.4	53.7	1 - 7	2.50 - 8.33

A_i percentage of the injected activity, corrected for physical decay

T_i half life (hours)

$$\text{activity} = \sum_{i = 1,3} A_i \times \exp\left(-\ln(2) \times t/T_i \right)$$

(ie: Subramanian's blood data is given by

$$A = 74.0\, e^{-\ln(2)\ t/0.03} + 18.3\, e^{-\ln(2)\ t/0.64} + 7.4\, e^{-\ln(2)\ t/53.7})$$

FIVE COMPARTMENT MODEL FOR
BONE IMAGING RADIOPHARMACEUTICALS

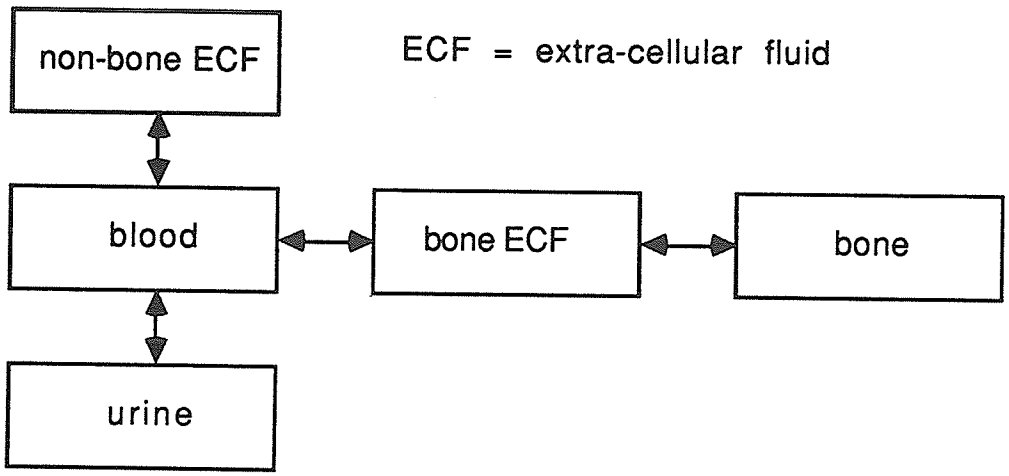

KIDNEY TIME-ACTIVITY DATA IN ANIMALS
USING TC-99M PYROPHOSPHATE

group	A	B	animal
Eckelman	- -	1.3	rabbit
Subramanian	3.0	1.3	rabbit
Krishnamurthy	4.3	1.9	rabbit

A - Percentage of injected activity per 1% (kidney weight/body weight) of the animal.

B - Percentage of the injected activity, extrapolated to a human adult, assuming that the % injected activity per 1% (kidney weight/body weight) is the same in humans as in animals.

PATIENTS

INTRODUCTION

In the present study, 26 patients referred for bone imaging were studied (however, only 25 were used in the dose calculations. The omission of one patient is explained in the "results and discussion; soft tissue" section). Patients were asked to participate, and if they agreed, signed consent was obtained in accordance with the University of Manitoba Committee on the Use of Human Subjects in Research. No attempt was made to select a specific group of patients, but due to patient referral patterns, the patients in the present study were generally old, and had a variety of diseases. The entire study spanned a six month period.

PATIENT DATA

The following data were recorded for each patient: sex, age, weight, height, body thickness over the chest, injected activity, number of scans obtained, time of each scan, bone function (presence of bone lesions), renal function, diagnosis, medical history relevant to the present study, and medication (APPENDIX I, PATIENT DATA). The body thickness over the chest was used to calculate the contribution of counts from soft tissue overlying the kidneys, bladder, and spine. The injected activity was calculated by measuring the activity in the syringe before and after injection. Abnormal bone function was defined as abnormal uptake of activity in any part of the skeleton,

based on the bone scan reports obtained for each patient. Renal function was based on the tests for serum urea, serum creatinine, urine creatinine, and creatinine clearance (REF, Rock 1986). However, these tests are only partial indicators of renal function, and was not availabe on all patients.

The 25 patients (14 male, 11 female) had the following statistics (mean and standard deviation): age (60±19 years), weight (73±19 kg), and height (173±16 cm). The mean weight and height were similar to Reference Man values for adults (70 kg, 170 cm). The patients fell into four groups: possible bone metastases (14), osteomyelitis (7), arthritis (3), and vascular disease (1). Six of the 25 patients were diabetics. Most patients were taking medication such as analgesics to reduce pain, and antibiotics against infection.

PATIENT PROTOCOL

In a clinical bone scan, the patient is injected intravenously with 740 MBq (20 mCi) of Tc-99m pyrophosphate, and scanned two hours later (FIG, CLINICAL WHOLE BODY IMAGES USING TC-99M PYROPHOSPHATE). The two hour time is chosen to maximize the image contrast between bone and soft tissue, while the count rate is still high (REF, Weber 1974). The duration of the scan ranges from 15 to 30 minutes, depending on the area scanned, and results in an image with about 500,000 counts. Care is taken to ensure that the patient does not move during the scan.

In the present study, the patient underwent four whole body scans in addition to the clinical bone scan (P34, SERIAL WHOLE BODY IMAGES OBTAINED IN THE PRESENT STUDY USING TC-99M PYROPHOSPHATE). Note the clarity of the kidneys, bladder, and bone in all the images (some details were lost when the images were transferred from film to paper). The objects adjacent to the legs are calibration sources. The fourth image, taken at about 24 hours after injection, contains much fewer counts than the other three images, thus its statistical quality is compromised. The number and timing of the extra bone scans depend mainly on the cooperation of the patient, and to a lesser extent on the physical half life of the radionuclide and the uptake of radiopharmaceutical. These factors are described below.

- PATIENT COOPERATION

The maximum duration of a scan was about 30 minutes, which was the longest time that one could expect a patient to repeatedly lay on a table without moving, and do so voluntarily. In addition to the extra scans for the present study, patients had their own schedules to follow (ie: eat, sleep, undergo diagnostic tests, etc.).

- PHYSICAL HALF LIFE AND RADIOPHARMACEUTICAL UPTAKE

To obtain images with about 500,000 counts in a 30 minute scan duration, it was important to obtain images early after injection, before too much activity was lost by physical and

biological decay. The biological half life of the bone activity is infinite, so that the effective half life is equal to the 6.03 hour physical half life of Tc-99m.

Patients were scanned four times at about 1.5, 4.5, 7.5, and 25.5 hours after injection, this choice based on the cooperation of the patient, the physical half life of the radionuclide, and the uptake of the radiopharmaceutical. Urine collections were obtained just before each scan, but no blood samples were obtained. The urine collections were cumulative, so that all the urine was collected from the time of injection to the time of the last scan.

In general, a complete patient study consisted of four scans and four urine collections. However, this was not always attainable in practice. Sometimes, a scan was missed because the patient had to undergo other diagnostic tests. Of the 26 patients, 17 patients were scanned four times, and 9 patients were scanned three times. The first urine collection was missed in 9 patients. Missing a scan (usually the third or fourth scan) results in a small increase in the error in the absorbed doses, whereas missing the first urine collection results in a large underestimate in the absorbed doses.

ANTERIOR

POSTERIOR

Clinical whole body images obtained 2 hours after injection using Tc-99m pyrophosphate

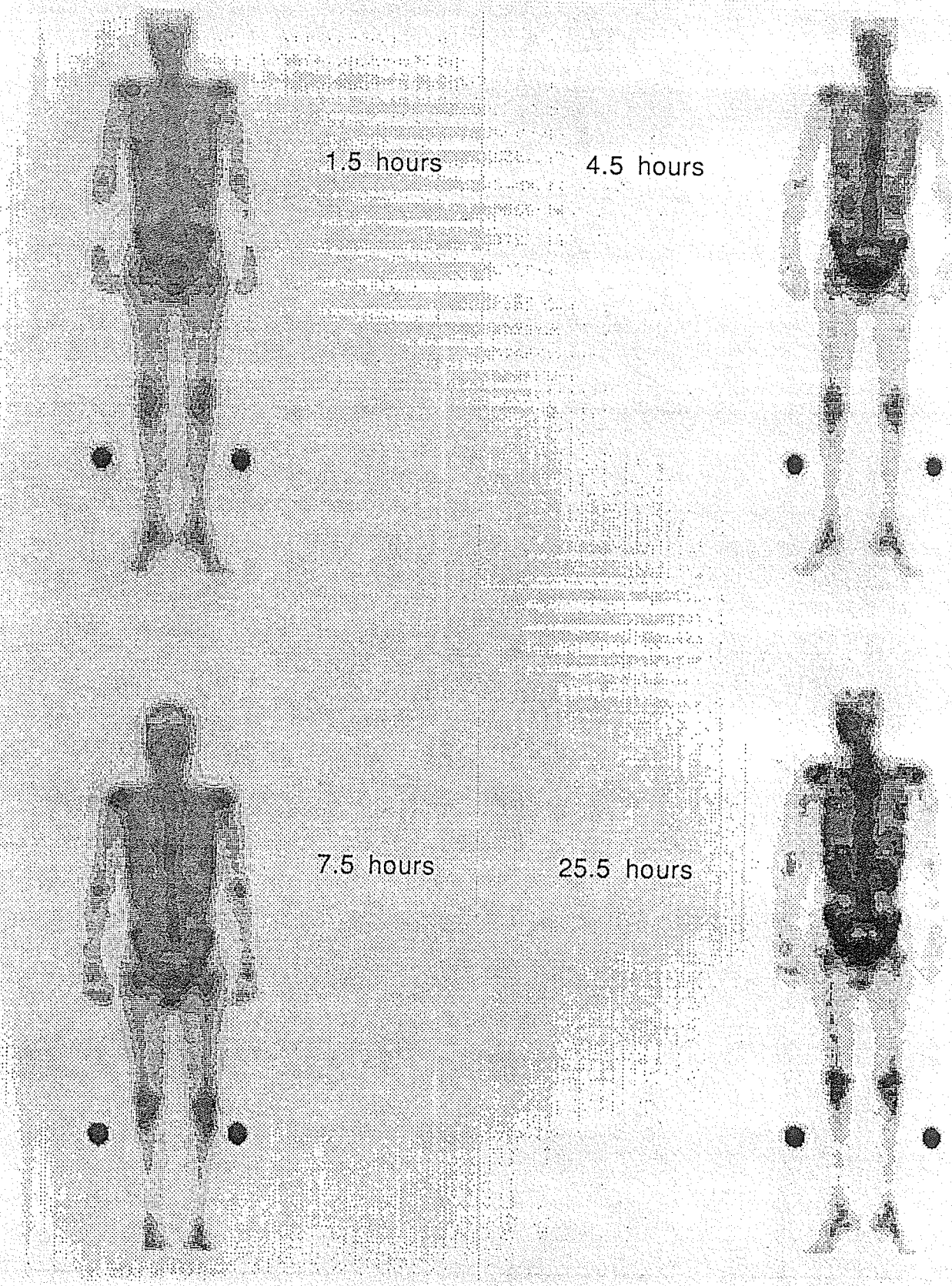

Serial whole body images obtained in the present study using Tc-99m pyrophosphate (ANTERIOR VIEW)

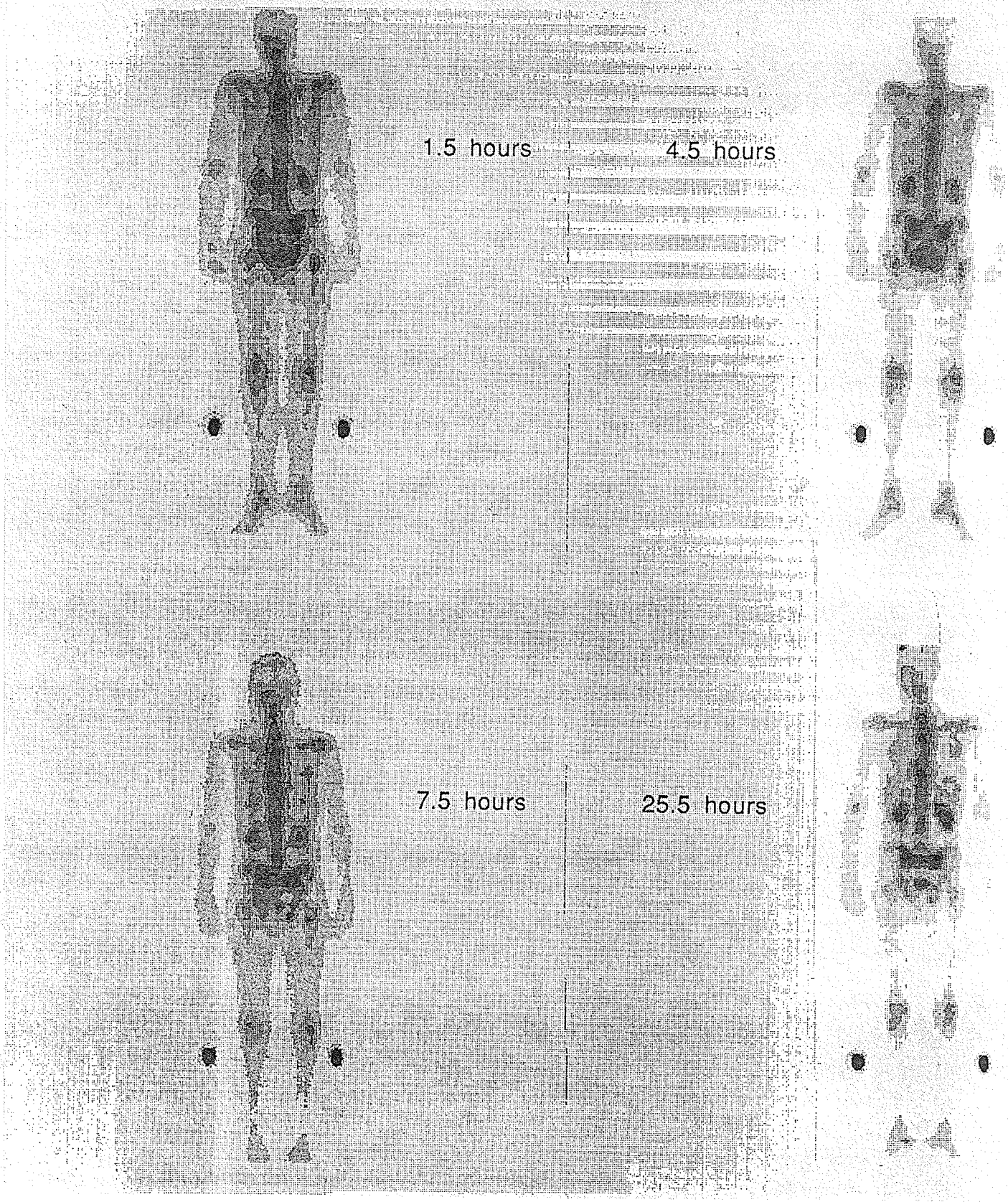

Serial whole body images obtained in the present study using Tc-99m pyrophosphate (POSTERIOR VIEW)

TC-99M PYROPHOSPHATE RADIOPHARMACEUTICAL

PHYSICAL PROPERTIES OF TC-99M

Technetium-99m has excellent physical properties for imaging with a gamma camera (P40, DECAY SCHEME OF TECHNETIUM-99M). The short six hour half life and the absence of beta radiation contributes to low absorbed doses to the organs in the body compared to other radionuclides. The mean energy per unit cumulated activity is 0.303 gram-rad/μCi-hr for Tc-99m. The 140 keV gamma emission has good penetration; 50% is absorbed in 4.6 cm of water, and yet the energy is low enough to be collimated without greatly decreasing the sensitivity.

QUALITY CONTROL OF TC-99M PYROPHOSPHATE

Quality control of the radiopharmaceutical ensures its constant composition, reproducible biologic behavior, and safety for human use. There are a number of chemical, physical, and biologic tests that are done, and are described in detail in the United States Pharmacopeia (REF, USP XX 1975). The main tests are for radioactivity, radiochemical purity, sterility, and pyrogenicity, and are described briefly below. Normally, tests are done prior to the use of the radiopharmaceutical. However, due to the short physical half life of Tc-99m, the results of the tests for sterility and pyrogenicity are only known after the radiopharmaceutical has been

used clinically. Also, these tests take time to do, on the order of several days.

ACTIVITY

In addition to the radioactivity assays on each preparation, the activity in the syringe was measured before and after injection using a dose calibrator, so that the amount injected could be measured accurately. The accuracy of the dose calibrator was estimated to be within ±2%.

RADIOCHEMICAL PURITY

Radiochemical purity is the percentage of the total activity in the specified chemical form. Radiochemical impurities arise from self-radiolysis, heat and light degradation, and the presence of interacting chemical species. Chemical reactions occur in the solvents used because of irradiation of the solvent molecules.

Radiochemical impurities may be taken up into organs that are not under study, causing unnecessary doses to these organs and decreasing the contrast between the organs under study and the surrounding tissue. The two main radiochemical impurities in Tc-99m pyrophosphate are free pertechnetate and colloidal species. The presence of free pertechnetate causes increased activity in the salivary glands, thyroid, stomach, and gastrointestinal tract (REF,

Abdel-dayem 1974). The presence of colloidal species causes increased activity in the liver (REF, Eckelman 1984).

An acceptable and reliable test for the radiochemical purity of Tc-99m pyrophosphate consists of two silica gel thin layer chromatograms, one developed in methyl ethyl ketone to measure the percentage of free pertechnetate and one developed in saline to measure the percentage of colloidal species (REF, Billinghurst 1973). The sum of the percentages of free pertechnetate and colloidal species must be less than 5% for clinical use. This was set somewhat subjectively to maintain a high and consistent image quality while rejecting a minimum number of preparations. For a higher percentage of impurities, say 10%, fewer preparations are failed, but the uptake in non-source organs increases, decreasing the contrast between bone and surrounding tissue.

The tests for radiochemical purity were done on each preparation, prior to its use.

STERILITY

The short six hour half life and the heat sensitivity of Tc-99m pyrophosphate requires it to be sterilized by membrane filtration, as opposed to heat sterilization. Membrane filtration removes organisms and particles greater than 0.22 μm in size, which includes most bacteria. However, this does not include most viruses, which lie in the range of 0.015 to 0.3 μm. The sterility test

consists of incubating the radiopharmaceutical for one to two weeks. The test results are only known after the radiopharmaceutical has been used clinically.

The sterility test was done on each preparation.

PYROGENICITY

Pyrogens are species (chemical or biological) which produce fever in man and animals. Pyrogens ususally result from non-sterile preparations. Pyrogen contamination is prevented by keeping chemicals and equipment sterile. The pyrogenicity test consists of injecting the radiopharmaceutical into three rabbits and measuring the increase in rectal temperature. If none of the rabbits shows an individual temperature rise of greater than 0.6°C, and if the sum of the temperature rise in all three rabbits is less than 1.4°C, then the radiopharmaceutical is considered to be free of pyrogens. The test results are only known after the radiopharmaceutical has been used clinically.

The pyrogenicity test was done on each lot number, from which the preparations were made.

DECAY SCHEME
OF TECHNETIUM-99M

Isomeric level decay
half life = 6.03 hours
(REF, Dillman 1975)

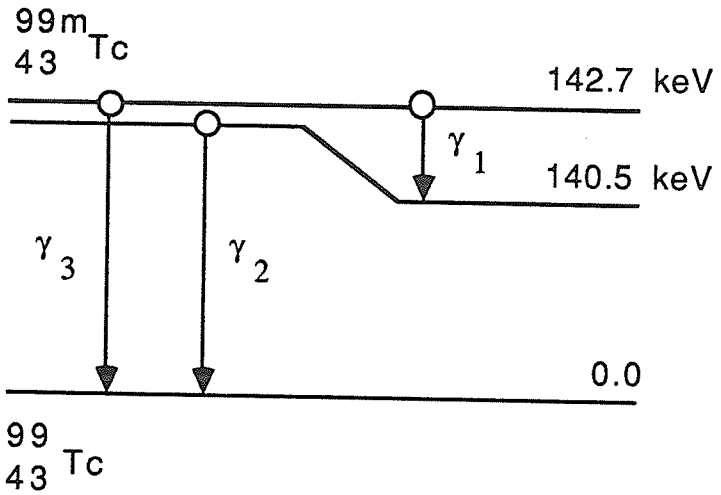

DECAY SCHEME OF TECHNETIUM-99M

isomeric level decay
half life = 6.03 hours
(REF, Dillman 1975)

N mean number per disintegration
E mean energy per particle
Δ equilibrium dose constant

	RADIATION	N	E (MeV)	Δ ($\frac{g\text{-}rad}{\mu Ci\text{-}hr}$)
	GAMMA 1	0.0000	0.0021	0.0000
M	INT CON ELECT	0.9860	0.0016	0.0035
	GAMMA 2	0.8787	0.1405	0.2630
K	INT CON ELECT	0.0913	0.1194	0.0232
L	INT CON ELECT	0.0118	0.1377	0.0034
M	INT CON ELECT	0.0039	0.1400	0.0011
	GAMMA 3	0.0003	0.1426	0.0001
K	INT CON ELECT	0.0088	0.1215	0.0022
L	INT CON ELECT	0.0035	0.1398	0.0010
M	INT CON ELECT	0.0011	0.1422	0.0003
K	ALPHA 1 X-RAY	0.0441	0.0183	0.0017
K	ALPHA 2 X-RAY	0.0221	0.0182	0.0008
K	BETA 1 X-RAY	0.0105	0.0206	0.0004
KLL	AUGER ELECT	0.0152	0.0154	0.0005
KLX	AUGER ELECT	0.0055	0.0178	0.0002
LMM	AUGER ELECT	0.1093	0.0019	0.0004
MXY	AUGER ELECT	1.2359	0.0004	0.0011

WHOLE BODY IMAGING SYSTEM

INTRODUCTION

The whole body imaging system consists of two stationary Picker Dynacamera 3 gamma cameras mounted with one camera above and one below a horizontal scanning table, all interfaced to a Medical Data Systems A^2 minicomputer (P48, WHOLE BODY IMAGING SYSTEM). With the patient lying on the table, the table is motor driven at constant speed between the two gamma cameras such that the entire table is covered in three longitudinal passes. Anterior and posterior images are obtained simultaneously, and stored on a computer disk.

SCANNING TABLE

In scanning mode, the effective scanning area of the gamma camera is a 15.2 cm long by 20.3 cm wide (6" x 8") rectangle. To scan the entire table area of 193 cm long by 61 cm wide (76" x 24"), the table makes three longitudinal passes and two lateral shifts in the shape of an "S" (P50, SCANNING TABLE). The count rate observed at the end of the scan is lower than at the start due to the physical decay of the source and the finite time needed to scan the whole table. The dependence of the count rate on table position was removed by having the table retrace the passes so that the table starts and stops at the same position, making a total of six longitudinal passes and four lateral shifts.

GAMMA CAMERA

The gamma camera obtains a two dimensional image of a three dimensional distribution of radioactivity by a combination of collimation and electronic positioning circuitry. The gamma camera consists of several components including collimator, radiation detector, position and energy determining circuitry, and image display (P51, GAMMA CAMERA). Each component is discussed below.

COLLIMATOR

The resolution of the gamma camera is largely determined by the resolution of the collimator, which in turn, is determined by the type of collimator, number of holes, hole size, hole length, septal thickness, and collimator material. In the present study, a parallel multihole collimator was used. It consists of a lead slab with an array of holes perpendicular to the face of the crystal. Its purpose is to improve the resolution of the gamma camera by only accepting photons which travel approximately parallel to the holes. Photons not travelling parallel to the holes are mostly absorbed by the lead septa.

Using a parallel multihole collimator, the spatial resolution decreases with increasing source-detector distance. The sensitivity in air decreases only slightly with distance, because while the

spatial concentration of photons decreases by the inverse square of the distance, the total area of crystal exposed to the source increases by the square of the distance.

RADIATION DETECTOR

The radiation detector of a gamma camera consists of a single sodium iodide crystal 40.6 cm (16 inch) in diameter and 1.27 cm (0.5 inch) thick. The crystal is viewed by 19 photomultiplier tubes (PMT's) which detect the light produced by photon interactions (photoelectric, Compton) with the crystal. If the energy of an absorbed photon is assumed to be deposited at a single point in the crystal, and if the light is assumed to radiate from this point, then the amount of light sensed by any individual PMT is directly related to its proximity to the point of absorption. In the present study, the PMT's are optically coupled to the crystal by a layer of transparent grease.

POSITION AND ENERGY DETERMINATION

The photomultiplier tubes are connected to an electronic network which is designed such that each tube contributes a fixed portion of its output signal to the generation of a set of four position signals. This is shown schematically in (P52, POSITION DETERMINING CIRCUITRY OF THE GAMMA CAMERA). Each PMT is connected through capacitors to four output leads called x+, x-, y+, and y-. The amount of signal that each PMT contributes to these four leads is directly

proportional to the capacitance values shown in the diagram. For example, tube 7 contributes an equal amount to each of the four coordinate signals, while tube 1 contributes three times as much to x- as to x+. In this manner, the position coordinates (x,y) of an interaction in the crystal is found by taking the difference of the x+ and x- signals to give x, and taking the difference of the y+ and y- signals to give y.

The four signals x+, x-, y+, and y- from each photomultiplier are fed into a summation circuit, which determines the total amount of light produced and hence the total amount of energy deposited in the crystal. The output of the summation circuit, the z pulse, is used for energy discrimination by the pulse height analyzer (PHA). The PHA allows only those pulses that have amplitudes falling within a preselected energy range to pass on for further processing. The PHA thereby excludes pulses created by scattered photons and by radioisotopes other than that being imaged.

IMAGE DISPLAY

If the z pulse meets the energy window requirements, the (x,y) position signals are applied to the deflection plates of a cathode ray oscilloscope. Accepted pulses from the PHA are used to unblank the oscilloscope, which results in a flash of light on the screen at a position directly related to the position of the interaction in the crystal.

GAMMA CAMERA - COMPUTER INTERFACE

In a single gamma camera system, the position signals (x,y) for each valid photon interaction, together with the position signals of the table (x',y'), are fed to the offset control and gate circuitry to generate a new photon signal (X,Y) in the reference frame of the table. This is shown schematically in (P53, CAMERA DATA PATHWAY PRIOR TO MODIFICATION). These analog signals are digitized into a matrix for each detector and stored in the computer. In the present study, two gamma cameras are used to obtain anterior and posterior images simultaneously. The digital signal resulting from the addition of the position and table signals of camera B (anterior camera) are fed to the multiplexer unit inserted in the data pathway of camera A (posterior camera). This is shown schematically in (P54, CAMERA DATA PATHWAY AFTER MODIFICATION). The multiplexer contains pulse shaping and delay circuitry to minimize dead time losses, which result when signals from camera B are sent to the multiplexer while it is processing signals from camera A.

IMAGE ACQUISITION

The computer acquires images from the gamma camera in a variety of modes. In the present study, anterior and posterior images are acquired simultaneously in "list mode". In this mode, the computer records in sequence the position coordinates (X,Y) and time of each photon accepted by the PHA. The data are stored in a buffer, and then written onto the removable disk. Later, when the image

acquisition is complete, this sequential list of data is sorted into the anterior and posterior images. Each count generates one 16 bit word. Since the storage capacity of a removable disk is 1.2 million 16 bit words, then the maximum number of counts in each of the anterior and posterior images must be less than 600,000 counts, since the timing marks occupy some space as well. The rate at which data is written onto the disk must be compatible with the maximum count rate of the gamma camera. In the present study, images are stored as 128 x 128 word matrices, which correspond to a spatial resolution of 1.755 cm. A higher resolution can be achieved by using 256 x 256 word matrices, but one would require four times the number of disks to store the images.

WHOLE BODY IMAGING SYSTEM

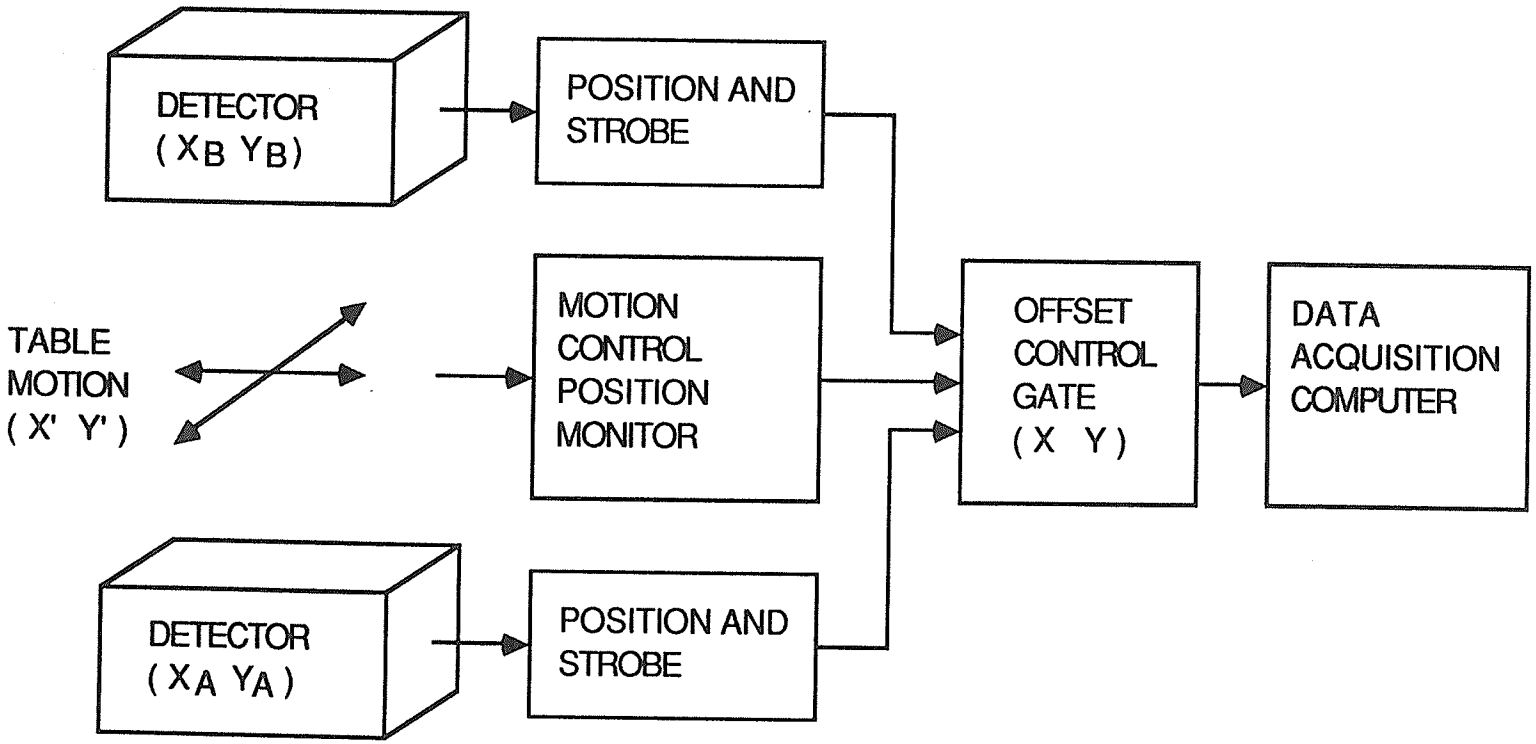

WHOLE BODY IMAGING SYSTEM

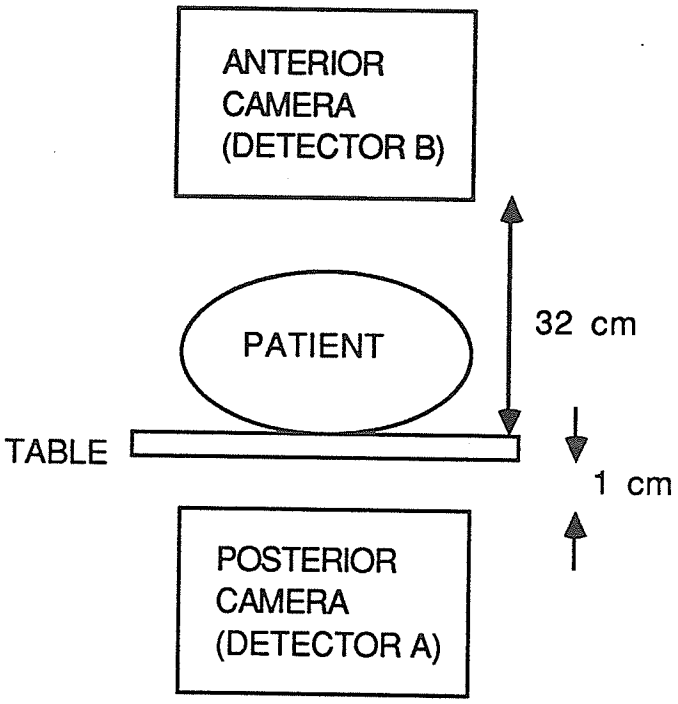

SCANNING TABLE

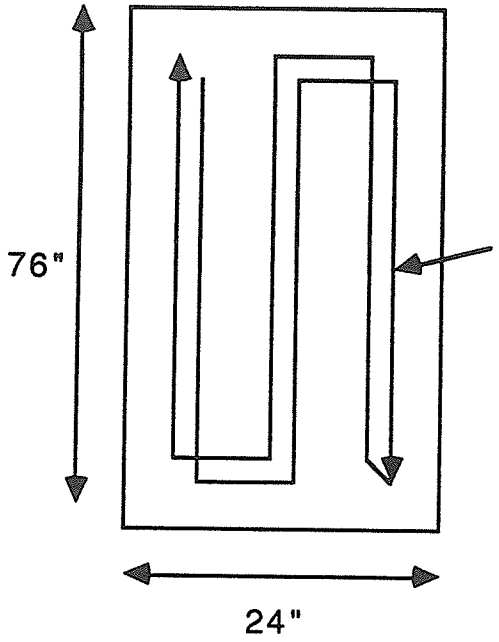

Motion of the table with respect to the gamma camera.

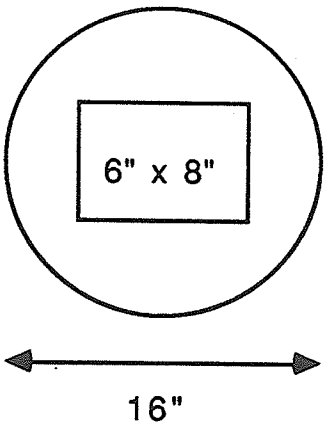

The effective scanning area of the gamma camera is a 6" by 8" rectangle even though the crystal diameter is 16". Since the width of the rectangle is 8", three longitudinal passes are required to scan the 24" wide table.

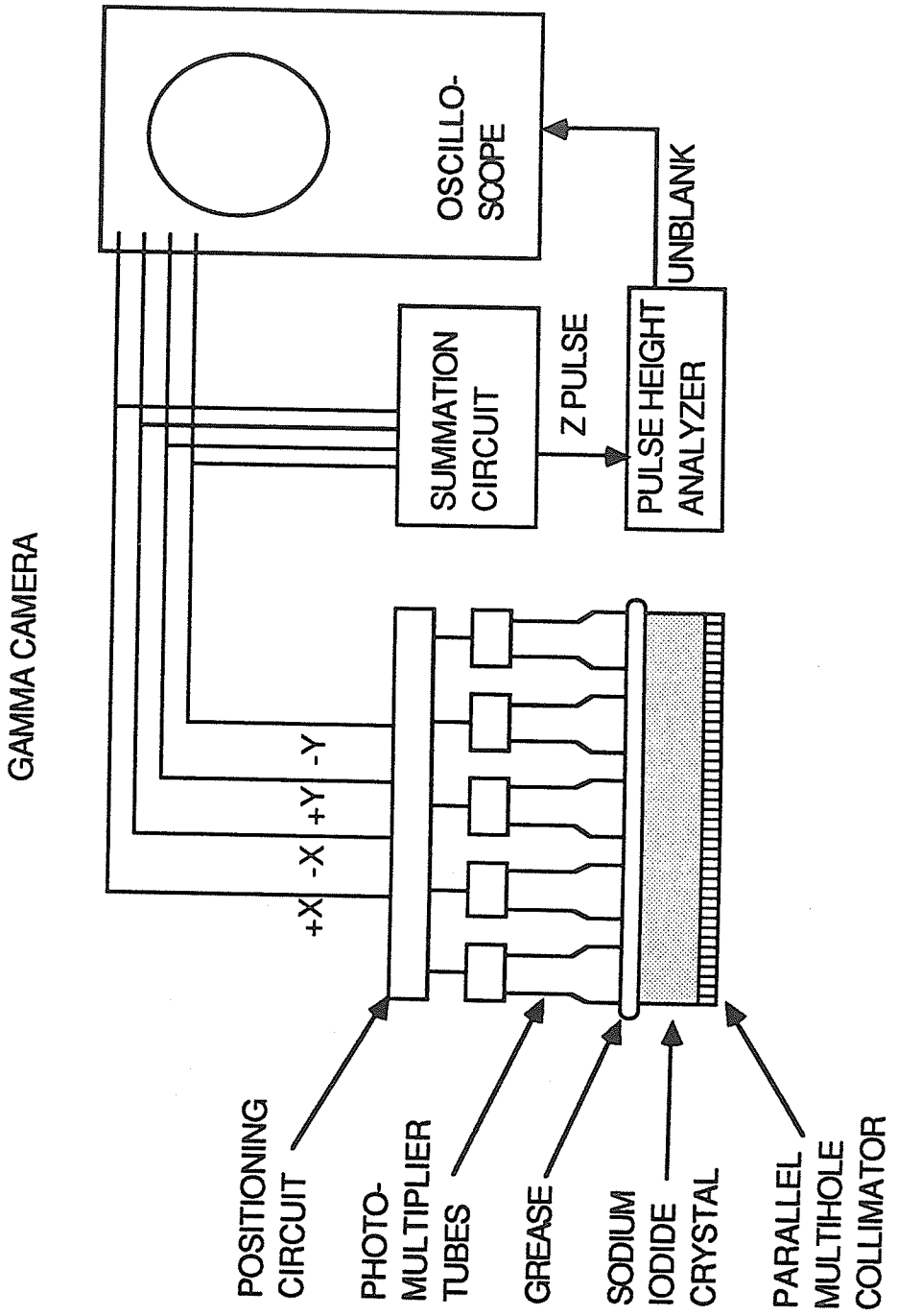
GAMMA CAMERA
OSCILLO-
SCOPE
SUMMATION
CIRCUIT
Z PULSE
PULSE HEIGHT
ANALYZER
UNBLANK
+X
-X
+Y
-Y
POSITIONING
CIRCUIT
PHOTO-
MULTIPLIER
TUBES
GREASE
SODIUM
IODIDE
CRYSTAL
PARALLEL
MULTIHOLE
COLLIMATOR

POSITION DETERMINING CIRCUITRY
OF THE GAMMA CAMERA

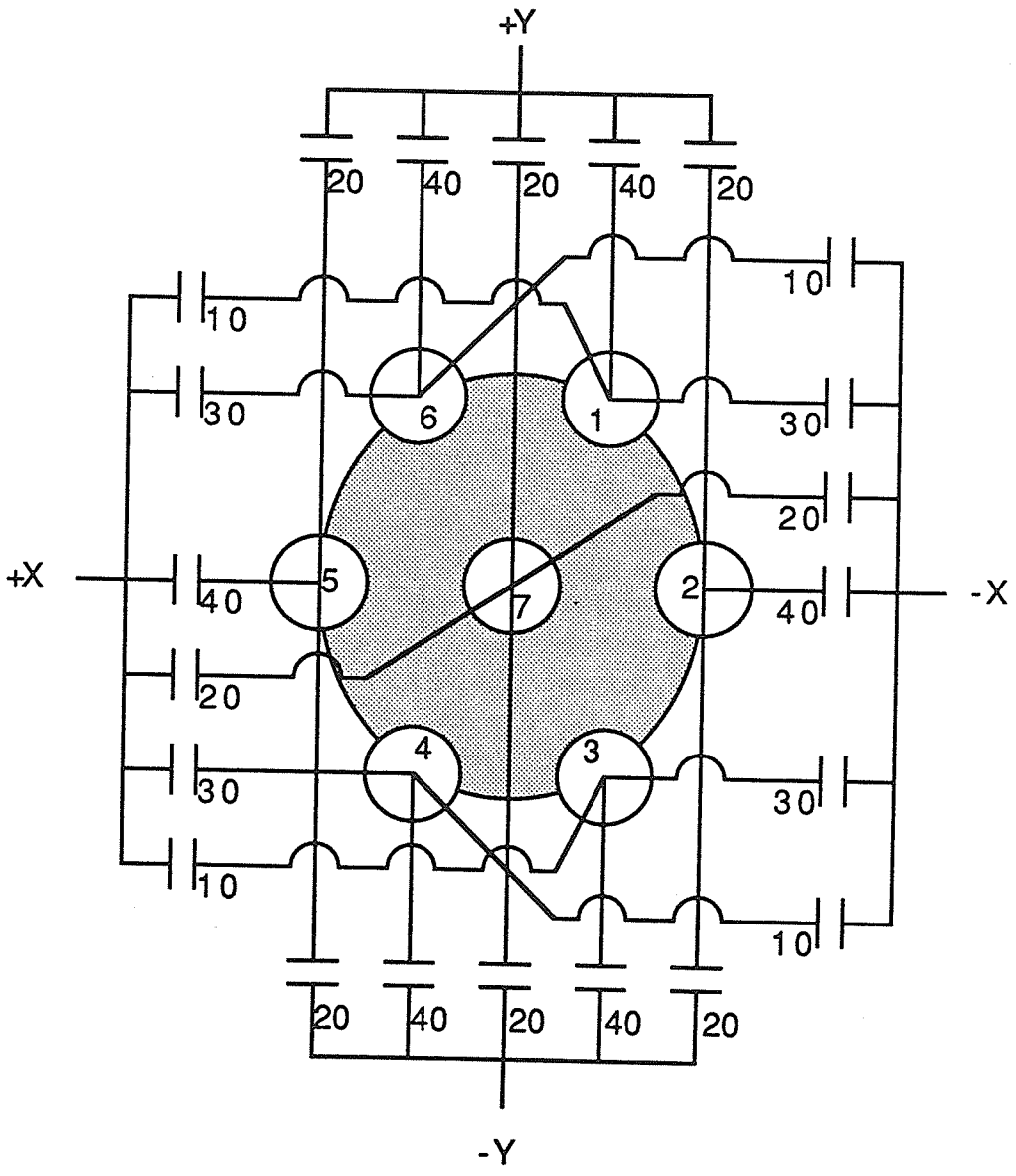

CAMERA DATA PATHWAY
PRIOR TO MODIFICATION

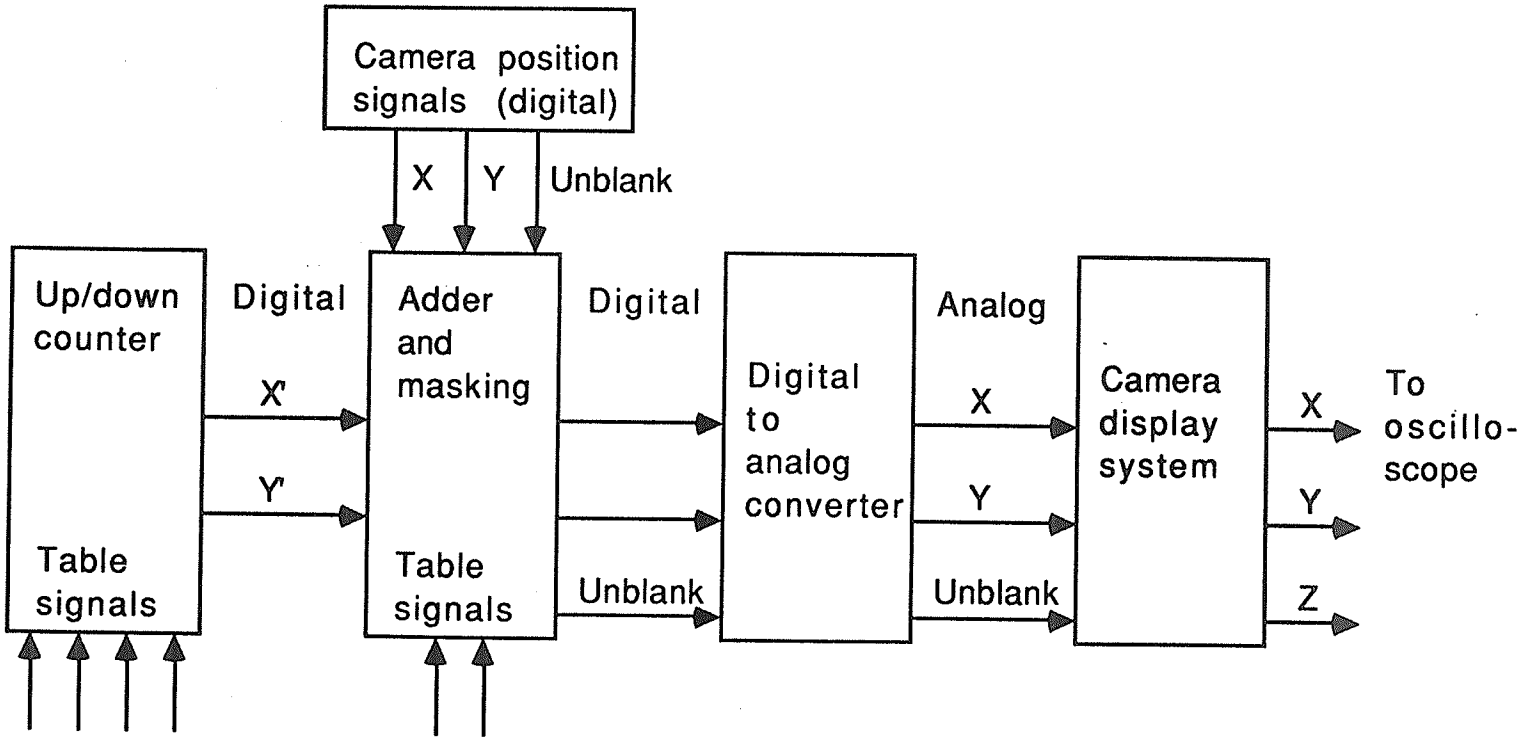

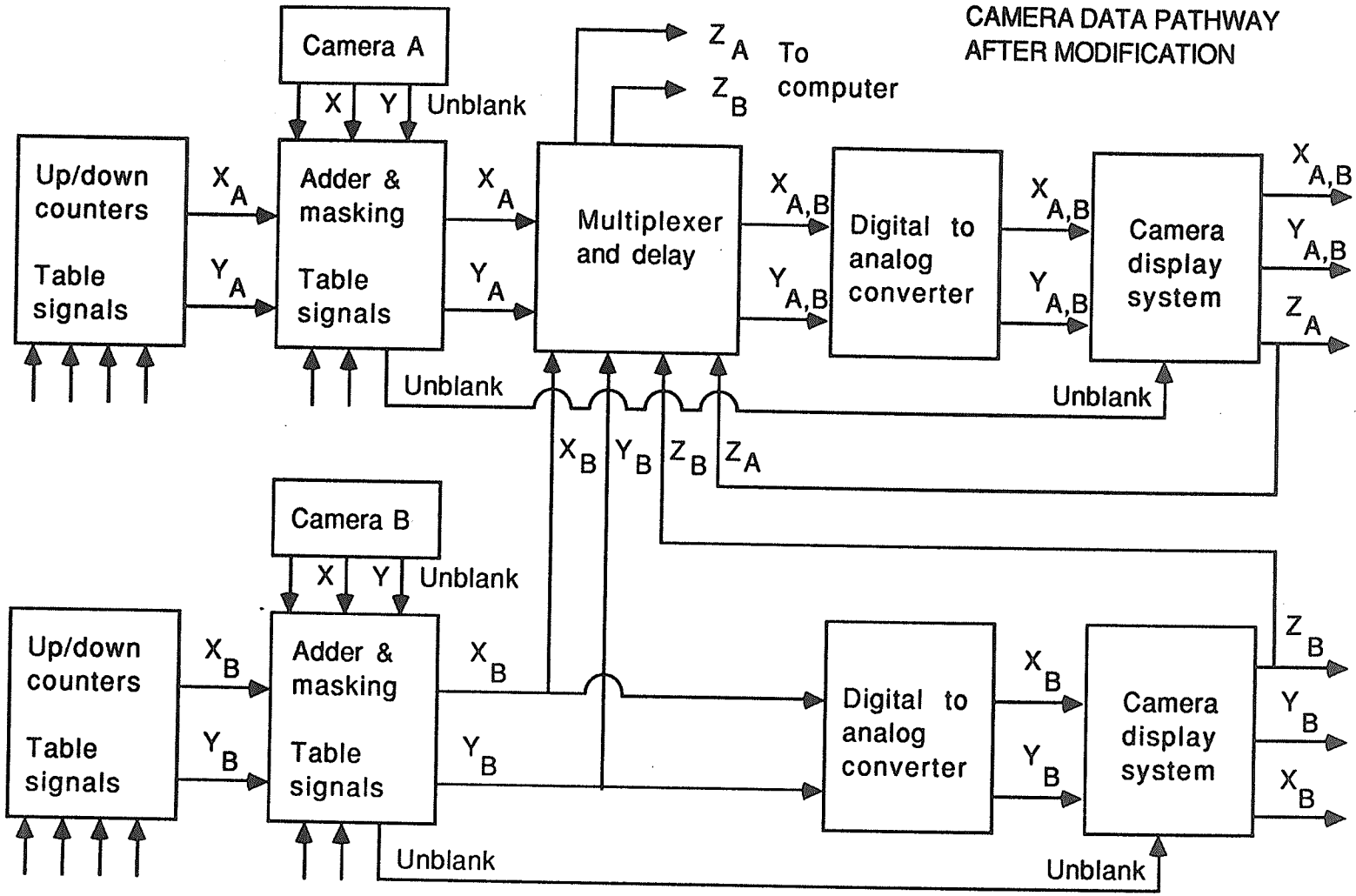
CAMERA DATA PATHWAY
AFTER MODIFICATION
Camera A
X
Y
Unblank
Z A
Z B
To
computer
Up/down
counters
Table
signals
X A
Y A
Adder &
masking
Table
signals
X A
Y A
Multiplexer
and delay
X A,B
Y A,B
Digital to
analog
converter
X A,B
Y A,B
Camera
display
system
X A,B
Y A,B
Z A
Unblank
Unblank
X B
Y B
Z B
Z A
Camera B
X
Y
Unblank
Up/down
counters
Table
signals
X B
Y B
Adder &
masking
Table
signals
X B
Y B
Digital to
analog
converter
X B
Y B
Camera
display
system
Z B
Y B
X B
Unblank
Unblank

QUALITY CONTROL OF THE IMAGING SYSTEM

INTRODUCTION

Quality control of the imaging system ensures that the images are reproducible and of high quality. Quality control consists of several qualitative and quantitative tests. In the present study, the scanning table was tested for uniform motion. The two gamma cameras were tested for spatial resolution, uniformity, linearity, sensitivity, deadtime, and reproduciblilty of energy window setting. All tests were done under typical patient scanning conditions with the collimators attached to the gamma cameras.

RADIATION SOURCES

All quality control tests involved the use of radioactive sources. In the present study, three types of sources were used: point, line, and flood. The point source consisted of a 10 ml syringe. The line source consisted of a 3 mm diameter plastic tube 30 cm long. The tube was held straight by a plastic sheath. The flood source consisted of a 40 cm x 40 cm x 2.5 cm plastic container. These sources were filled with a uniform mixture of water and Tc-99m activity. For measurements in water, sources were placed in a rectangular aquarium, whose dimensions were 50 cm x 25 cm x 30 cm (height).

To obtain a flood image of the entire table, a scan was obtained with the flood source placed on the posterior gamma camera (the one under the table), covering the effective viewing area of the two gamma cameras. The flood source was stationary with respect to the gamma cameras. The result was a flood image which looked the same as if a flood source the size of the table area was used.

SCANNING TABLE

To ensure that the table speed was uniform, a flood source was scanned for each patient. A uniform table speed should produce a constant count (within statistical error) for count profiles obtained parallel to the length of the table (P62, FLOOD PROFILE). The variation in the longitudinal count profile for the flood images was typically under 10%, indicating that the table speed was approximately uniform. The absorption of counts by the table was assumed to be small and uniform over the entire table.

SPATIAL RESOLUTION

The spatial resolution was measured by scanning a line source in air and in water. At the mid-plane between the two detectors, the full width at half maximum (FWHM) of the two detectors was (2.3±0.9) cm in air and (3.5±0.9) cm in 25 cm of water (P63, SPATIAL RESOLUTION IN AIR AND WATER). The error in the FWHM, 0.9 cm, was set equal to one half of the pixel dimension (0.5 x 1.755 cm). The

spatial resolution in water does not increase smoothly with distance because of the large pixel size in the image. In the present study, the smallest organ of interest was the kidney, whose width is about 6 cm. Over the course of the entire study, for all patients, the resolution of the posterior camera remained constant, while the resolution of the anterior camera became steadily worse, increasing by about 0.5 cm. This may have been due to the drying of the grease which couples the photomultiplier tubes with the crystal.

DETECTOR UNIFORMITY

An ideal gamma camera has a uniform detection efficiency across its field of view, such that an image of a uniform flood source would also be uniform and a profile of a flood image of a uniform detector would be of uniform amplitude. In practice, the detection efficiency varies across the field of view, such that an image of a uniform flood source is non-uniform. A profile of a flood image of a non-uniform detector is shown in (P62, FLOOD PROFILE). Thus, any phantom or patient image requires correction for the non-uniform detector response. The patient and phantom images were corrected for the detector non-uniformity by dividing the patient image by the flood image, and scaling the result by some constant. This method of uniformity correction preserves the relative difference in counts among different pixels, allowing quantitative information to be obtained. This method is explained in more detail in the "Data analysis, Detector uniformity" section. The variation in

the latitudinal count profile for the flood images was typically 15% to 40%.

LINEARITY

Linearity is the ability of the gamma camera to produce an image of a line source without spatial distortion. A scan was made with the line source placed diagonally across the table, and the linearity was checked visually in the image. The linearity was checked twice, once at the beginning and once at the end of the entire study. No distortion was observed in the images at either time.

SYSTEM SENSITIVITY

The sensitivity of the imaging system is defined as the count rate per unit activity. In the present study, the counts per unit activity for a given scan duration was measured in each patient scan by placing a point source, filled with a known amount of Tc-99m activity, on the table beside the patient. The counts over the point source were obtained from the image by drawing a region of interest around the source, and the counts were normalized to the 9.6 minute scan duration. The counts per unit activity at the normalized scan duration varied by less than 10% over the course of the entire study, for all patients (P64, SYSTEM SENSITIVITY). The sensitiviity seems to decrease over time, probably due to the drying of the grease which couples the crystal to the photomultiplier tubes.

DEADTIME

While the gamma camera processes the positional and energy information from each pulse, it is unable to begin processing a second pulse, so that some interaction events are lost. In the present study, the deadtime was measured by the paired source method, where the counting rates of two sources were counted, separately as R_1 and R_2, and together as R_{12}. Assuming that the imaging system was paralyzable, then the deadtime T is given by (REF, Harbert 1984):

$$T = \frac{2\, R_{12}\ \ln\left[\,(R_1 + R_2)/R_{12}\,\right]}{(R_1 + R_2)^2}$$

The sources were counted separately and simultaneously under constant conditions of geometry, scatter, and absorption. The deadtime of the gamma camera was measured once at the start of the entire study, and was found to be about 3 μsec.

Data is not written directly on the computer disk, because of the relatively long time (70 msec) needed to move the read-write head to the correct location on the disk. Instead, the computer memory is used as a buffer to allow data acquisition at high count rates, so that when the buffer is filled, the data is then transferred in a block to the disk. The data transfer rate for a 16 bit word is 11

μsec for the computer disks used in the present study. With the buffer, the deadtime of the imaging system is limited by the gamma camera, and not by the computer.

To see if the images in the present study needed correction for deadtime, the counts were measured from several point sources (10 ml volumes of water) with activities ranging up to 35 MBq using a typical patient scan duration (P65, DEADTIME). The counts start to increase non-linearly at about 30 MBq. Typical concentrations of activity in the body fall below 5 MBq per 10 ml of tissue (eg: for a 700 MBq injection into a 70 kg body, and assuming a uniform distribution, then the activity per 10 ml volume is approximately given by 700 MBq/70000 ml = 0.7 MBq/10 ml). The maximum concentration of activity in the body, usually found in the bladder, is about 25 MBq per 10 ml, based on the urine collections. Therefore, since the typical activity concentrations observed in the patients of the present study fell in the linear part of the deadtime curve, no deadtime corrections were necessary.

ENERGY WINDOW SETTING

The choice of energy window setting is a trade off between sensitivity to the primary gamma rays versus the ability to discriminate against scattered photons. If a relatively wide energy window is used to increase the sensitivity, then a proportionately larger number of scattered photons are accepted as valid events, which decreases the spatial resolution. In the present study, an

asymmetric, 15% window was used, ranging from 135 keV to 156 keV. This setting was used to decrease the counts due to scattered photons. The energy window setting was checked once per month, and readjusted to the above range if necessary.

FLOOD PROFILE

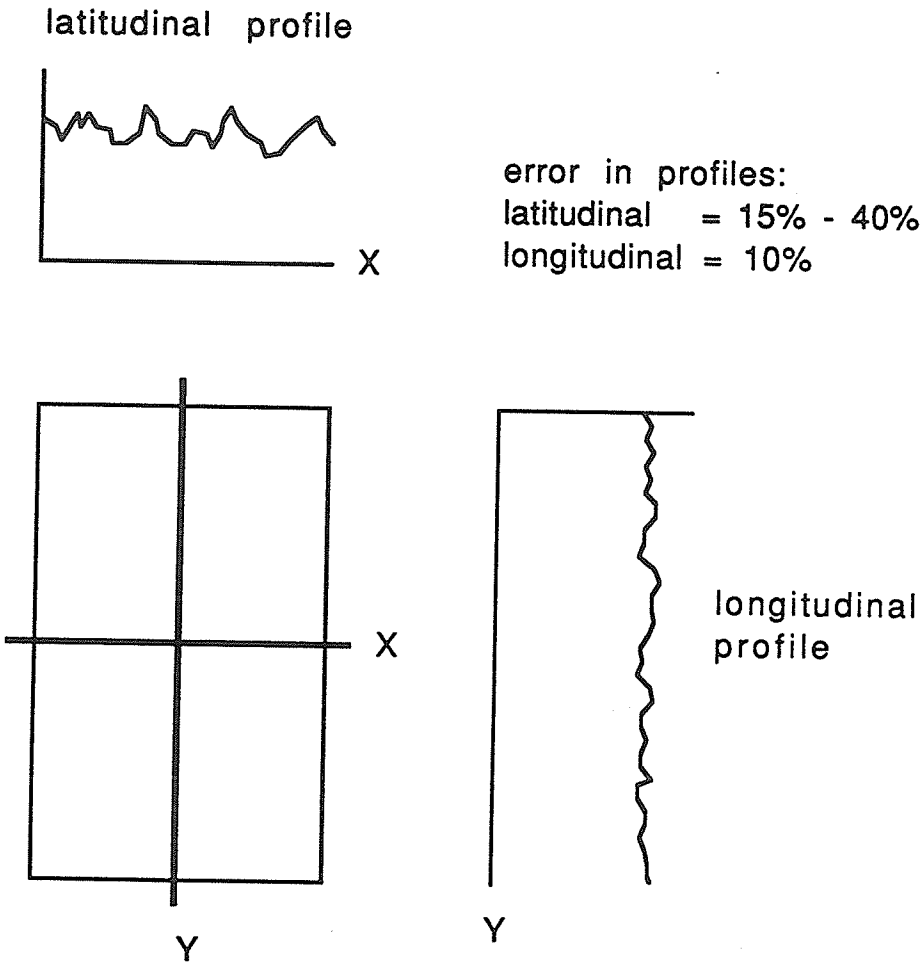

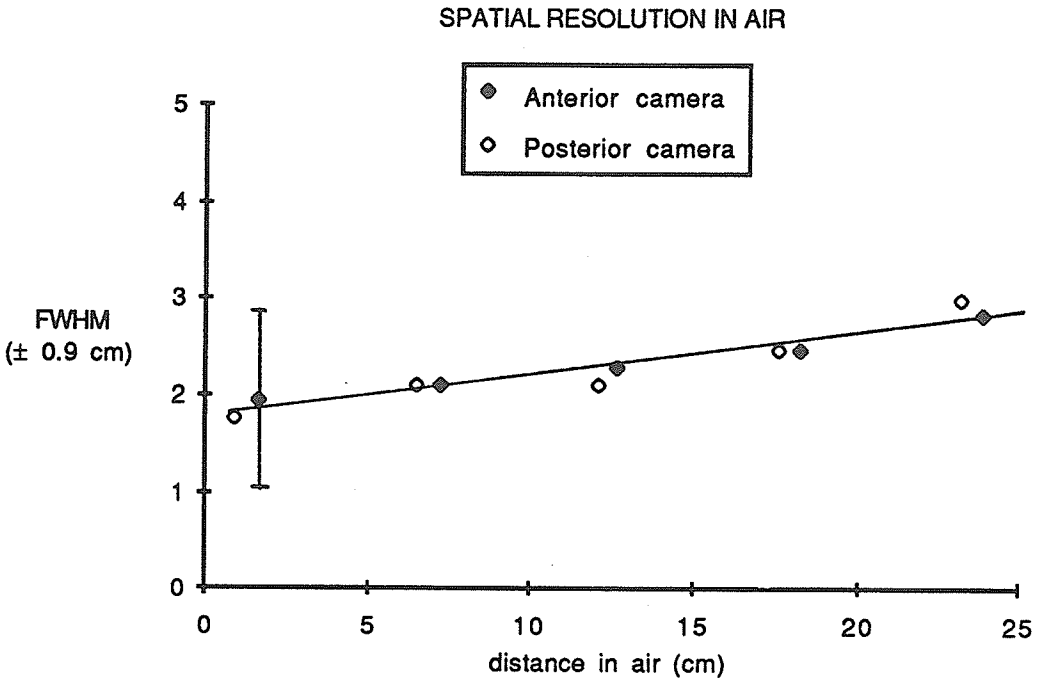
SPATIAL RESOLUTION IN AIR
Anterior camera
Posterior camera
FWHM
(± 0.9 cm)
0
1
2
3
4
5
0
5
10
15
20
25
distance in air (cm)

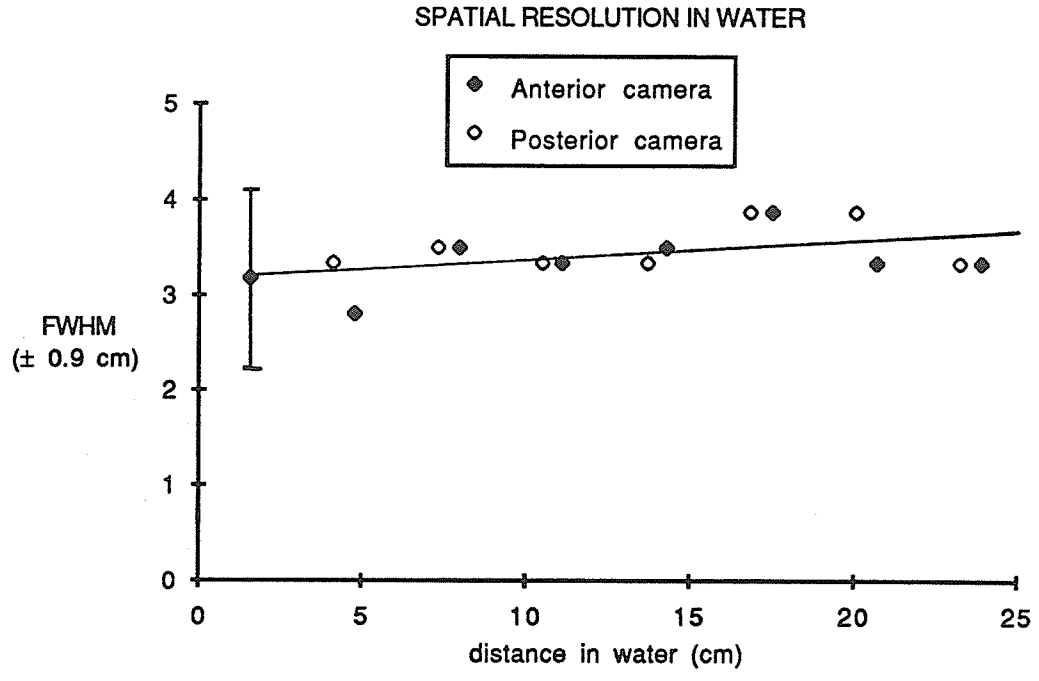
SPATIAL RESOLUTION IN WATER
Anterior camera
Posterior camera
FWHM
(± 0.9 cm)
0
1
2
3
4
5
0
5
10
15
20
25
distance in water (cm)

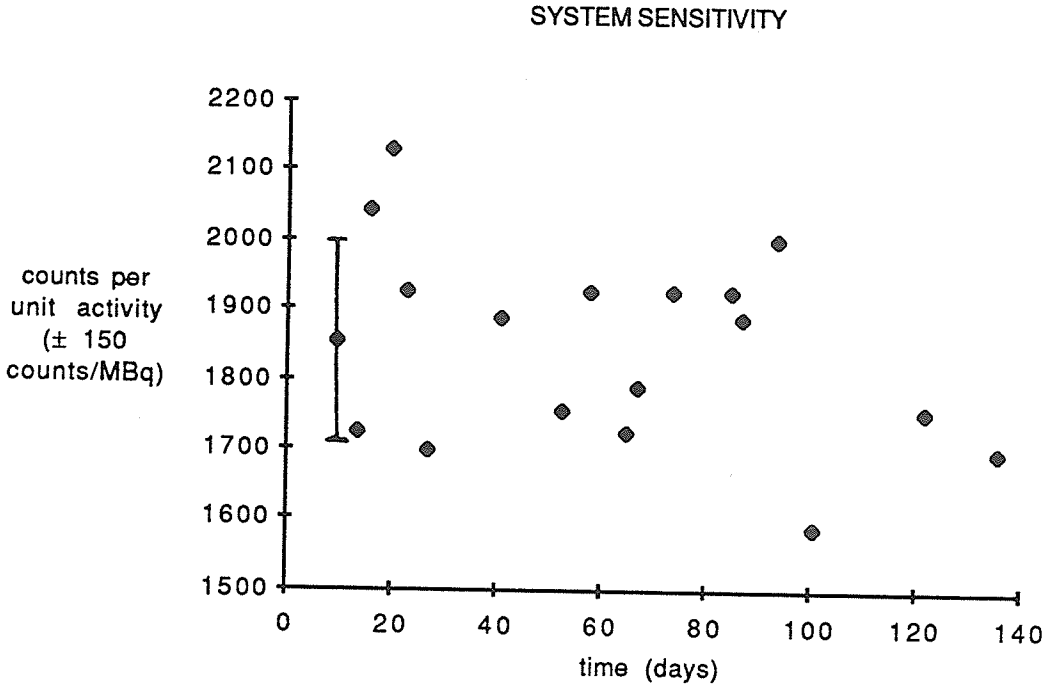
SYSTEM SENSITIVITY
counts per unit activity (± 150 counts/MBq)
2200
2100
2000
1900
1800
1700
1600
1500
0
20
40
60
80
100
120
140
time (days)

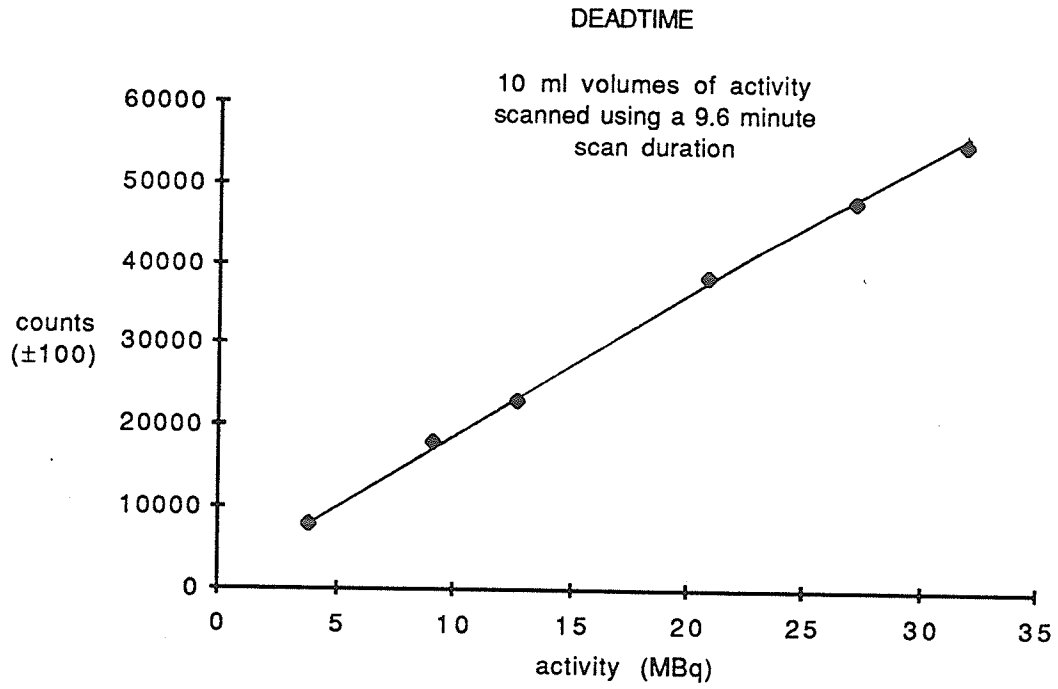
DEADTIME
10 ml volumes of activity scanned using a 9.6 minute scan duration
counts (±100)
60000
50000
40000
30000
20000
10000
0
0
5
10
15
20
25
30
35
activity (MBq)

BASIC DATA

Patients were scanned four times at 1.5, 4.5, 7.5, and 25.5 hours after injection of 740 MBq of Tc-99m pyrophosphate. Urine collections were obtained just before each scan, so that they spanned the periods from 0 to 1.5 hours, 1.5 to 4.5 hours, 4.5 to 7.5 hours, and 7.5 to 25.5 hours. Patients were not asked to urinate before injection.

To correct the non-uniformity of the gamma cameras, a flood source was scanned for each patient. With the dual gamma camera imaging system, each scan generated anterior and posterior views simultaneously, which were stored as 128 x 128 word matrices. Thus, a complete study consisted of four urine collections, four anterior and four posterior whole body images, and one anterior and one posterior flood image, for a total of ten images.

The count statistics for typical patient and flood images are shown in (P68, COUNT STATISTICS OF PATIENT AND FLOOD IMAGES). The area of the table was about 4000 pixels. The area of the body was about 2000 pixels, found by including only pixels with counts greater than some threshold value (the delineation of areas in the patient image is described in the "Regions of interest" section). The total count in each of the first three patient images was maintained at about 400000 counts by increasing the scan duration to compensate for the physical and biological decay of the activity. Typical scan durations and scan times are shown in (P69, SCAN DURATIONS AND SCAN

TIMES). The fourth image was limited to about 60000 counts by the maximum scan duration of 30 minutes. The mean count is equal to the total count divided by the area over which the total count is obtained. The maximum count in the patient image was usually located over the bladder.

The background count was measured for each patient study by doing a scan using a 9.6 minute scan duration, with all radioactive sources including the patient, removed from the vicinity of the imaging system. The contribution of the background counts to the patient counts was less than one percent, which was small compared to other errors in the present study, so that no correction was made for background counts. The variation of the background counts over the five months of the present study was about 10% (P70, BACKGROUND COUNTS AS A FUNCTION OF TIME). The anterior gamma camera was about 30% more sensitive than the posterior gamma camera.

COUNT STATISTICS OF PATIENT AND FLOOD IMAGES

image	area (pixels)	---------- counts ---------- total	mean	maximum
patient (1-3)	2000	400000	200	5500
patient (4)	2000	60000	30	825
flood	4000	2000000	500	800
background	4000	1000	0.25	4

1 pixel = 1.755 cm x 1.755 cm = 3.080 cm^2

"patient (1-3)" refers to the first three scans obtained over the first eight hours after injection, while "patient (4)" refers to the fourth scan obtained at about 25.5 hours after injection.

TYPICAL SCAN DURATIONS AND SCAN TIMES

scan time (hours)	scan duration (minutes)	patient image counts
1.5	10	400000
4.5	16	400000
7.5	23	400000
25.5	30	60000

Scan time refers to the length of time after injection that the scan was performed.

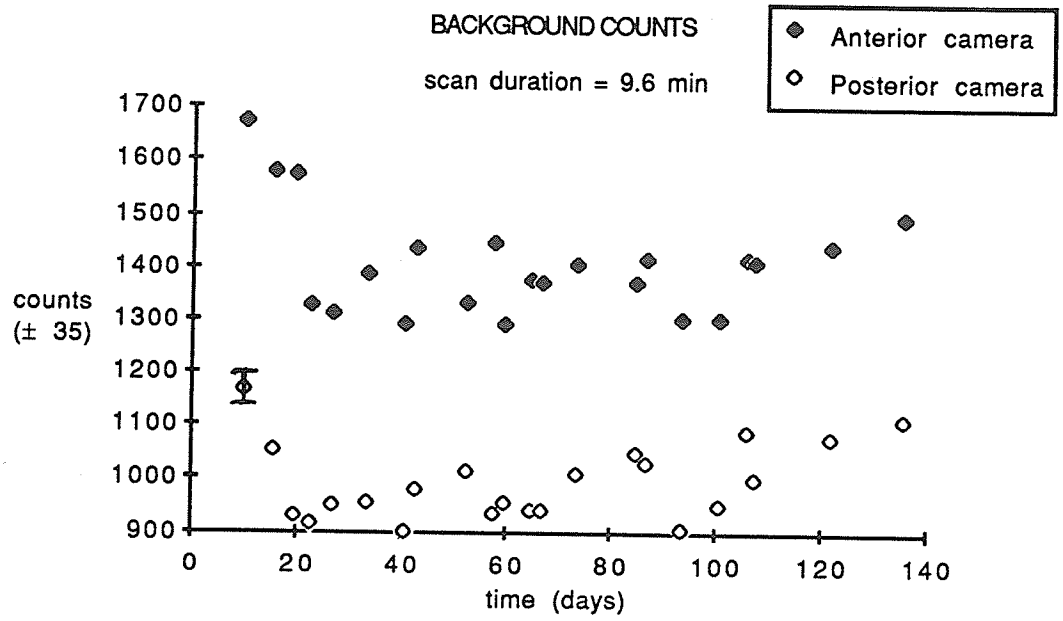
BACKGROUND COUNTS
scan duration = 9.6 min
Anterior camera
Posterior camera
counts
(± 35)
1700
1600
1500
1400
1300
1200
1100
1000
900
0
20
40
60
80
100
120
140
time (days)

SCAN DURATION CORRECTION

To quantify the activity in the body, it was convenient to normalize the counts in the images to the 9.6 minute scan duration, which was the shortest duration used to scan patients. This allowed us to compare the counts from image to image for a given patient, since different scan durations were used to obtain each image. The scan duration was measured by the computer. Recall that the table made three longitudinal passes and two lateral shifts in an "S" shape in one direction, and then retraced the "S" shape in the opposite direction to complete the scan. During the time which the table made the lateral shifts, the gamma camera did not accept data. Therefore, the time of the lateral shifts, totalling one minute, was subtracted from the scan duration to obtain the actual time during which data was accepted. The error in the scan duration was less than 1%. Given that the table speed was constant for a given scan duration, and that all images were obtained over the same area, then the normalized count is given by:

$$C_T = C_t \times (T-1)/(t-1)$$

C_T normalized count using scan duration T,
where T = 9.6 minutes

C_t measured count using scan duration t, where t is in minutes. The scan duration t was measured by the computer.

DETECTOR UNIFORMITY CORRECTION

To correct the 15% to 40% variation in the uniformity of the two gamma cameras used in the present study, a flood source was scanned for each patient studied. The non-uniformity in a patient image was removed by dividing the patient image by a flood image, with appropriate scaling of the two images. The anterior flood image was used to correct the anterior patient images, and the posterior flood image was used to correct the posterior patient images.

The problem with performing division and multiplication operations on an image was that the computer software only allows integer values to be stored in a pixel. Therefore, fractional numbers were truncated to the next lower integer value, resulting in an underestimate of the number. One can define a truncation error as the fraction truncated divided by the integer value (example: 21/5 = 4.2, truncation error = 0.2/4 = 0.05 or 5%). In practice, the truncated value was unknown, and since the maximum truncated value was 0.99, then it was convenient to define a maximum truncation error, given by 0.99 divided by the integer value (using the previous example, the maximum truncation error is equal to 0.99/4 = 0.25 or 25%).

In the present study, the mean counts per pixel in the flood image was large compared to the mean counts per pixel in the patient image, so that the division of the patient image by the flood

image would produce a large truncation error in the counts of the resulting image. The error was minimized by scaling up the patient image and scaling down the flood image before the division operation.

The uniformity correction featured three types of image operations: multiplication by a constant, division by a constant, and division by an image. To multiply or divide an image by a constant, the user selected the image and entered the constant into the computer. The constant was specified up to two decimal places. The value in each pixel of the image was then multiplied or divided by the constant. The result was truncated, and replaced the original pixel value. To divide one image by another, the user selected the two images. The value in each pixel in the first image was divided by the pixel value in the second image with the same coordinates. The result was truncated, and replaced the original pixel value in the first image. Division by zero resulted in a zero value being assigned to the resulting pixel.

The uniformity correction consisted of four operations, given below, and was performed on each pixel in the image.

$$Q = \{ [(P \times F1)_1 / (R / F2)_2]_3 \times F3 \}_4$$

$_{1,2,3,4}$	order of operations
P	uncorrected patient image
Q	corrected patient image

R	flood image
F1	scaling factor for uncorrected patient image = $32767/P_{max}$
32767	maximum pixel value in a word mode image
P_{max}	maximum pixel value in the patient image
F2	scaling factor for flood image, chosen to minimize the truncation error
F3	normalization factor

In the first operation, the uncorrected patient image P was multiplied by a constant F1. The constant was chosen such that the maximum pixel value in the uncorrected patient image was scaled up to 32767, which is the maximum value of a signed 16 bit integer. The maximum pixel value in the uncorrected patient image was determined by the computer, and the constant was calculated by hand. The muliplication operation was then performed.

In the second operation, the flood image R was divided by a constant F2. The constant was chosen such that the net effect of the maximum truncation errors due to each operation was minimized. This is explained in greater detail later.

In the third operation, the scaled up patient image (P x F1) was divided by the scaled down flood image (R / F2), resulting in an un-normalized and corrected patient image.

In the fourth operation, the un-normalized, corrected patient image was multiplied by a constant F3. The constant was chosen such that the total count in the corrected patient image, Q, equaled the total count in the uncorrected patient image, P.

Consider the effect of the flood scaling factor on the maximum truncation errors, using typical patient and flood image counts (see "Basic data" section):

P_{max} = maximum pixel value in uncorrected patient image
= 5500

P_{ave} = mean pixel value (over body) in uncorrected patient image
= 200

R_{ave} = mean pixel value in flood image
= 500

F1 = scaling factor for patient image
= $32767/P_{max}$
= 32767/5500
= 6

Q_{ave} = mean pixel value (over body) in corrected patient image
= 200

FLOOD SCALING FACTOR

TABLE 1

Calculation of corrected patient image as a function of flood scaling factor (F2):

F2	P_{ave} x F1	R_{ave} / F2	$\frac{P_{ave} \times F1}{R_{ave} / F2}$	Q_{ave}	F3
3	1200	167	7.2	200	27.8
15	1200	33.3	36	200	5.56
70	1200	7.14	168	200	1.19

TABLE 2

Maximum truncation error (expressed as a percentage) in each operation as a function of the scaling factor for the flood image, F2, obtained by dividing 0.99 by the count in columns 2, 3, 4 & 5 in the table above.

F2	$\frac{0.99}{P_{ave} \times F1}$	$\frac{0.99}{R_{ave} / F2}$	$\frac{0.99}{\frac{P_{ave} \times F1}{R_{ave} / F2}}$	$\frac{0.99}{Q_{ave}}$	sum of max truncation errors
3	-0.1%	+0.6	-14	-0.5	-14
15	-0.1	+3.0	-2.8	-0.5	-0.4
70	-0.1	+14	-0.6	-0.5	+13

In (P76, FLOOD SCALING FACTOR, TABLE 1), the corrected patient images are calculated for different flood scaling factors, showing the counts after each operation. In (P76, FLOOD SCALING FACTOR, TABLE 2), the maximum truncation errors are calculated for each operation. The sign of the error indicates whether the error causes the corrected patient image, Q_{ave}, to be over or under estimated (corresponding to + and - respectively). The truncation error in scaling the flood image competes against the truncation errors in the other operations. The sum of these maximum truncation errors is given in the last column and is shown graphically in (P78, SUM OF THE MAXIMUM TRUNCATION ERRORS VERSUS THE FLOOD SCALING FACTOR). The sum is zero when the flood scaling factor is equal to about 15 for patient images with a mean count per pixel of 200. For patient images with a lower mean count, the flood scaling factor is correspondingly higher. This calculation is also performed for the whole range of counts in the patient images (P79, SUM OF THE MAXIMUM TRUNCATION ERRORS VERSUS THE PIXEL VALUE), and the sum of the maximum truncation errors is found to lie within ±5% of zero for counts greater than about one third of the mean count per pixel in the patient image. Over 70% of the pixels over the body have counts greater than one third of the mean count per pixel (P80, PIXEL VALUE DISTRIBUTION IN THE PATIENT IMAGES). Shown in the diagram is the count distribution in two patient images, one with good contrast and one with poor contrast.

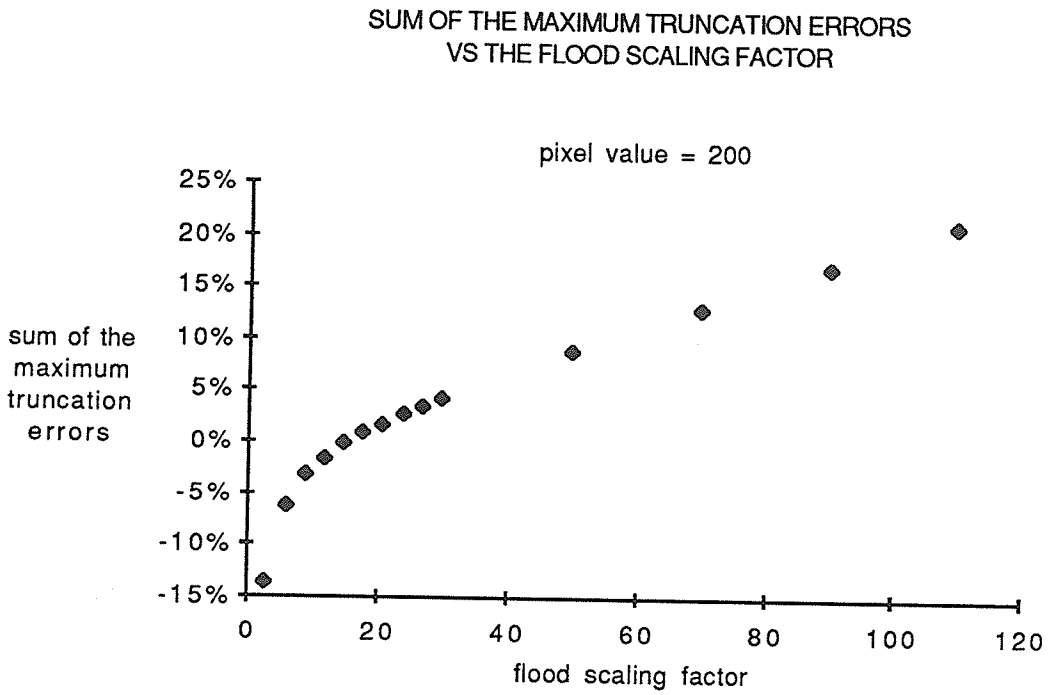
SUM OF THE MAXIMUM TRUNCATION ERRORS
VS THE FLOOD SCALING FACTOR
pixel value = 200
sum of the maximum truncation errors
25%
20%
15%
10%
5%
0%
-5%
-10%
-15%
0
20
40
60
80
100
120
flood scaling factor

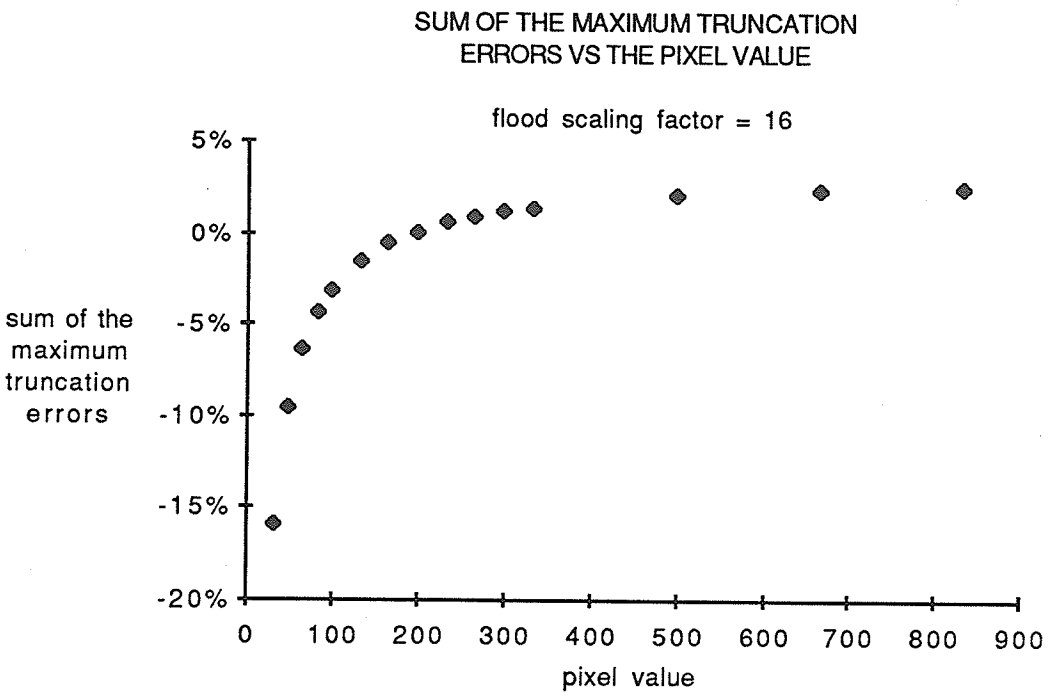
SUM OF THE MAXIMUM TRUNCATION ERRORS VS THE PIXEL VALUE
flood scaling factor = 16
sum of the maximum truncation errors
5%
0%
-5%
-10%
-15%
-20%
0
100
200
300
400
500
600
700
800
900
pixel value

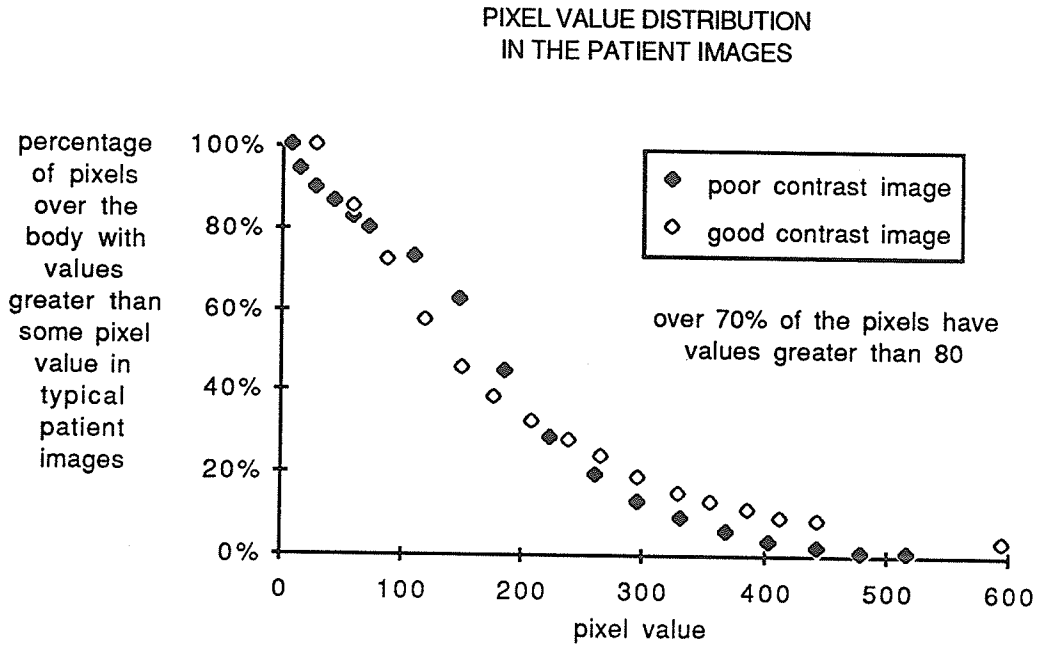
PIXEL VALUE DISTRIBUTION
IN THE PATIENT IMAGES
percentage of pixels over the body with values greater than some pixel value in typical patient images
100%
80%
60%
40%
20%
0%
0
100
200
300
400
500
600
pixel value
poor contrast image
good contrast image
over 70% of the pixels have values greater than 80

REGIONS OF INTEREST

The computer software allows one to draw regions of interest (ROI's) in an image to obtain count statistics on those regions. In the present study, anterior and posterior images were obtained simultaneously in each scan, so that it was only necessary to construct ROI's for the images of one view. The drawing of the ROI's was based on the posterior images, because the posterior camera was closer to the patient, and hence the resolution of the posterior images was slightly better than that of the anterior images. An exception was the bladder, which appeared more clearly in the anterior image due to its proximity to the front of the body and due to the presence of bone (lower pelvis) behind the bladder.

In the patient images, both rectangular and irregular shaped ROI's were drawn to obtain count statistics. These statistics included the maximum, minimum, average and total counts, together with the number of pixels in the region. The construction of the rectangular and irregular ROI's is described below.

The keyboard and joystick were used to enter the coordinates and dimensions of the rectangular ROI's into the computer. Rectangular ROI's were drawn around the following regions: table, calibration sources, left thigh, right thigh, left intestine, right intestine, upper spine, and lower spine (P83, REGIONS OF INTEREST). The dimensions of the rectangular ROI's were constant over all images of all patients.

The location of some of these rectangular regions are not self evident from the names given to these regions. The thigh ROI's were defined by an area on the inside of the upper legs, excluding the bone. The intestine ROI's were defined by the soft tissue below the kidneys, above the pelvis, and to the left and right of the spine. The upper and lower spine ROI's were defined approximately by the areas between the first and seventh thoracic and the first and fifth lumbar vertebrae respectively.

Irregular ROI's were constructed by first enclosing the region with a rectangular ROI, and then drawing a second ROI within the rectangular ROI such that only pixels above some threshold count were included. The threshold count was selected such that the area was approximately constant over all images of a given patient. Irregular ROI's were drawn around the kidneys, bladder, and whole body.

REGIONS OF INTEREST

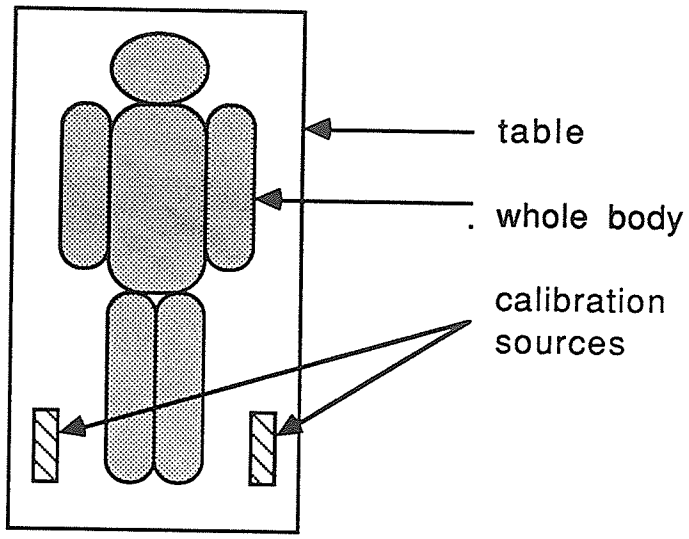

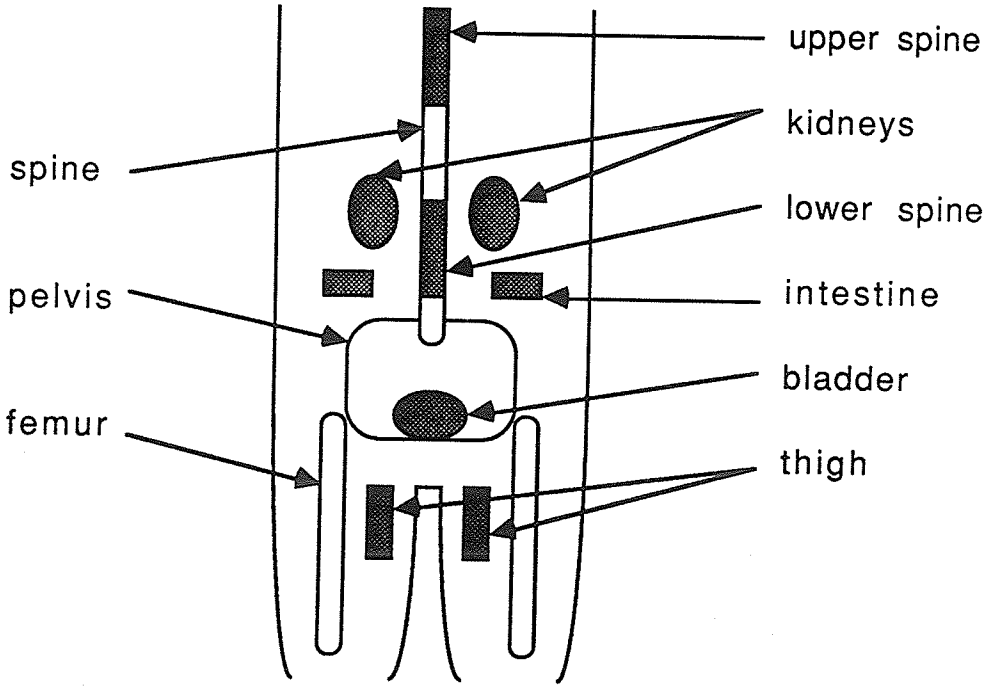

URINE AND WHOLE BODY ACTIVITY

URINE ACTIVITY

The activity in a urine collection was calculated by comparing the count rate from a 10 ml urine sample to the count rate from a 10 ml volume of water containing a known amount of Tc-99m activity. The count rates were measured using a well counter. The urine sample was usually diluted to make the count rate low enough so that count losses due to the dead time of the well counter were negligible. At least 10000 counts were obtained from each sample so that the error from counting statistics was less than 1%. Each urine collection was sampled twice, from which an average activity per 10 ml urine sample was obtained. The activity per unit volume in the sample was scaled up by the dilution factor and by the total urine volume in that collection, and corrected for physical decay, to give the activity in the urine collection at the time the collection was obtained.

WHOLE BODY ACTIVITY

There are two methods for calculating the whole body activity:

(1) using only the urine collections; and
(2) using the whole body counts from the four scans and the first urine collection.

In the present study, the second method was used becasue it was probably more accurate. This is explained below.

- URINE COLLECTIONS

The whole body activity at the time of each scan is given by:

$$A_{BODY}(t_i) = A_{BODY}(t_{i-1}) \times \exp[-\ln(2) \times (t_i - t_{i-1})/T_{1/2}] - A_{URINE}(t_i)$$

t_i time of the i'th scan, i = 1, 2, 3, 4

$T_{1/2}$ physical half life of Tc-99m, 6.03 hours

$A_{URINE}(t_i)$ activity in the i'th urine collection, or activity in the urine collected between t_i and t_{i-1} (MBq)

$A_{BODY}(t_i)$ whole body activity at the time of i'th scan (MBq)

$A_{BODY}(t_0)$ whole body activity at the time of injection and equal to the injected activity (MBq) (defined only for i=1)

The whole body activity at the time of a scan can be calculated given the whole body activity at the time of the previous scan, the activities in the urine collections, and the time of each scan. The injected activity was measured using a dose calibrator with an accuracy of ±2%. A typical time-activity curve for the whole body is shown in (P89, WHOLE BODY TIME-ACTIVITY CURVE). In the diagram, the regions of constant slope correspond to the decay of Tc-99m, with a physical half life of 6 hours. They are separated by regions with a sharp decrease in activity, corresponding to the excreted urine. The

accuracy of the whole body activity calculations depend mainly on the completeness of the urine collections. If urine was missed in a collection, the activity in the body was overestimated. Urine collections were prone to being incomplete due to patients forgetting or being unable to urinate into the containers provided. As a result, this method of calculating the whole body activity was not used in the present study, and instead, a method using the whole body counts and the first urine collection was used.

A convenient method of accounting for all the activity is to correct the activities for physical decay and express the result as a percentage of that injected. One can define the whole body retention (WBR) and urinary excretion (UE) as follows:

$$WBR\ (t_i) = \frac{A_{BODY}\ (t_i) \times \exp\ [+\ln(2) \times (t_i - t_0)/T_{1/2}]}{A_{BODY}\ (t_0)} \times 100\%$$

where i = 1, 2, 3, 4

$$UE\ (t_j) = \frac{\sum_{i=1,j} A_{URINE}\ (t_i) \times \exp\ [+\ln(2) \times (t_i - t_0)/T_{1/2}\ ]}{A_{BODY}\ (t_0)} \times 100\%$$

where j = 1, 2, 3, 4

The sum of the whole body retention and the urinary excretion should equal 100% at all times. If a urine collection was incomplete, the sum would be less than 100%.

- WHOLE BODY COUNTS

A more accurate method of calculating the whole body activity, employed in the present study, used the whole body counts and the first urine collection. This method assumes that the activity per unit count for the whole body is constant with time:

$$A_{BODY}(t) / C_{BODY}(t) = \text{constant}$$

$A_{BODY}(t)$ whole body activity as a function of time (MBq)

$C_{BODY}(t)$ geometric mean of the anterior and posterior whole body counts as a function of time (see "Geometric mean method" section)

The whole body activity at the time of each scan is given by:

$$A_{BODY}(t_i) = C_{BODY}(t_i) \times A_{BODY}(t_1) / C_{BODY}(t_1)$$

where i = 1, 2, 3, 4

$C_{BODY}(t_i)$ whole body counts at the time of the i'th scan (count)

$A_{BODY}(t_i)$ whole body activity at the time of the i'th scan (MBq)

$A_{BODY}(t_1)$ whole body activity at the time of the first scan (MBq)

$= A_{BODY}(t_0) \times \exp[-\ln(2) \times (t_1-t_0)/T_{1/2}] - A_{URINE}(t_1)$

The whole body activity at the time of the first scan was calculated as in the previous method, using the activity in the first urine collection. The urine activity at the time of the second, third, and fourth urine collections was then calculated from the corresponding whole body activity:

$$A_{URINE}\ (t_i) = A_{BODY}\ (t_{i-1}) \times \exp\ [-\ln(2) \times (t_i - t_{i-1})/T_{1/2}] - A_{BODY}\ (t_i)$$

where $i = 2, 3, 4$

If all the urine collections were complete, then the urine activities as calculated from the whole body counts should equal the urine activities as calculated from the urine collections. This comparison is shown later in the "Results and discussion" section.

WHOLE BODY TIME-ACTIVITY CURVE

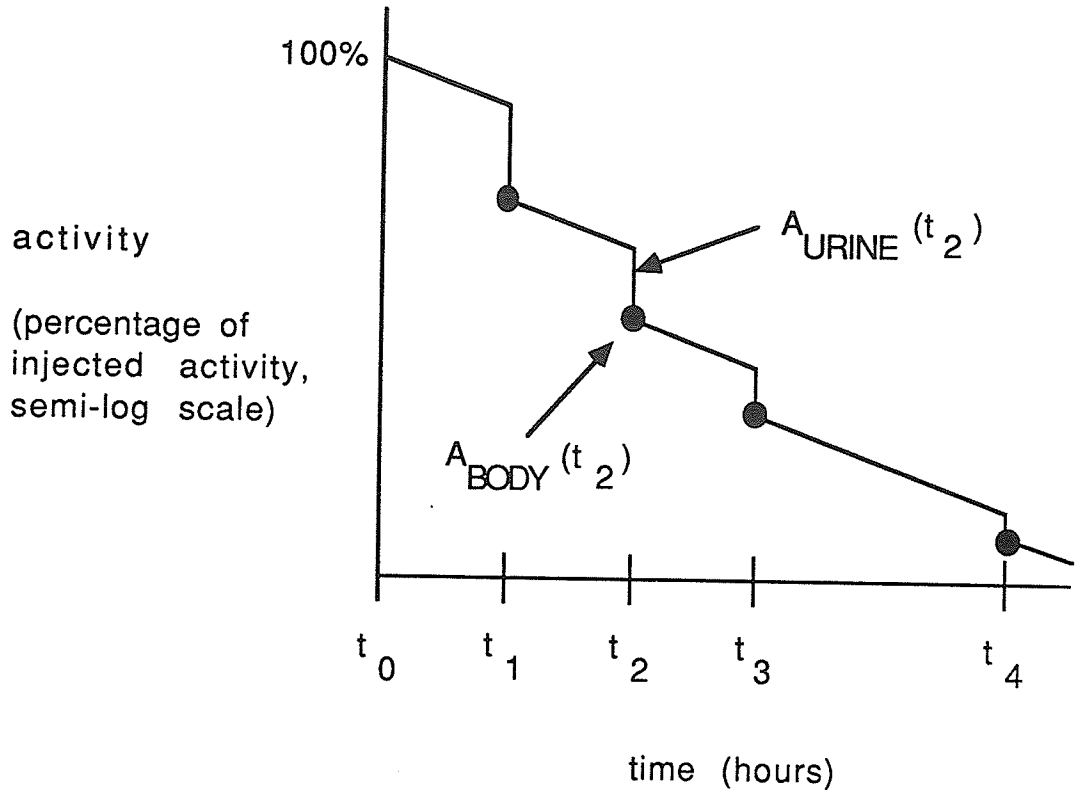

Shown is a typical whole body time-activity curve.
Vertical lines represent voided urine activity at each scan time.
The dots represent whole body activity at each scan time.
Slope of the curve corresponds to the 6 hour half life of Tc-99m.

SOFT TISSUE, KIDNEY, BLADDER, AND BONE ACTIVITY

INTRODUCTION

The gamma camera image consists of a two dimensional count map of a three dimensional distribution of activity. To quantify the activity in an organ from the image, a region of interest is drawn around the organ to obtain the counts over the organ. For some organs, it is necessary to subtract the counts due to activity in overlying soft tissue. The organ counts are then multiplied by an activity per unit count conversion factor, which is obtained from phantom studies. This conversion factor requires a knowledge of the organ thickness and the body thickness over the organ. In this section, it is shown how to quantify the activity in the four source organs: soft tissue, kidneys, bladder, and bone.

There were several problems in calculating the organ activity:

- DEPENDENCE OF COUNT RATE ON SOURCE DEPTH

The count rate detected by a single gamma camera decreases exponentially with organ depth due to attenuation by overlying soft tissue. The depths of the various organs could not be easily and accurately measured for all patients. This problem was solved by using the geometric mean method, the details of which are discussed later in the "Geometric mean section".

- COUNTS DUE TO OVERLYING SOFT TISSUE

The counts over an organ such as the kidneys or bladder were mixed with counts from overlying soft tissue. This problem was solved by subtracting some fraction of the intestine counts, which is discussed later.

- CALCULATION OF THE SOFT TISSUE ACTIVITY

A region of interest could not be drawn around the whole soft tissue volume without including the kidneys, bladder, and bone. Also, the soft tissue thickness varied over the whole body. This problem was solved by calculating the activity in a sample soft tissue volume, such as the thigh, and scaling the result by the total soft tissue volume. The total soft tissue volume was found using the sex and weight of the patient, as well as Reference Man data. This method assumed that the distribution of activity in soft tissue was uniform.

- CALCULATION OF THE BONE ACTIVITY

The calculation of the bone activity had the same problems as in the calculation of the soft tissue activity, with the additional problem that the distribution of activity in bone was highly non-uniform, so that one could not calculate the bone activity from a sample bone volume. This bone activity was obtained by subtracting

the activity in the kidneys, bladder, and soft tissue from the activity in the whole body.

GEOMETRIC MEAN METHOD

In the present study, the activities in the soft tissue, kidneys, and bladder were calculated using the geometric mean method. Using this method, the calculated activity was approximately independent of the organ depth.

Consider the counts measured by the anterior and posterior gamma cameras due to a rod of uniform activity perpendicular to the camera faces, lying within a tank of water (P97, GEOMETRIC MEAN METHOD). In terms of the patient, the rod corresponds to an organ and the water tank corresponds to the body. The anterior and posterior counts (C_{ANT} and C_{POST} respectively) are given by:

$$C_{ANT} = E\ A \exp(-\mu_1 a) \int_0^l \exp(-\mu_2 x)\, dx$$

$$= E\ A\ [\exp(-\mu_1 a)]\ [1 - \exp(-\mu_2 l)] / \mu_2$$

$$C_{POST} = E\ A\ [\exp(-\mu_1 b)]\ [1 - \exp(-\mu_2 l)] / \mu_2$$

E	counts per unit activity in air	(counts/MBq)
A	activity per unit length	(MBq/cm)
μ_1	linear attenuation coefficient of water	(cm^{-1})
μ_2	linear attenuation coefficient of the rod	(cm^{-1})
L	depth of water = a + b + l	(cm)

l	anteroposterior length of rod, $l \leq L$	(cm)
a, b	water depth separating the rod from the anterior and posterior cameras, respectively	(cm)

The geometric mean count C is given by:

$$C = (C_{ANT}\, C_{POST})^{1/2}$$
$$= E\, A\, [\exp(-\mu_1(a + b)/2)]\, [1 - \exp(-\mu_2 l)] / \mu_2$$
$$= E\, A\, l \exp(-\mu_1 L/2) \exp((\mu_1 - \mu_2)\, l/2)\, (2/\mu_2 l) \sinh(\mu_2 l/2)$$

where $L = a + b + l$, and $\sinh(z) = [\exp(z) - \exp(-z)] / 2$.

The geometric mean count is theoretically independent of the source depth, that is, independent of a and b. The activity in the rod is given by:

$$A_l = \frac{C}{E \exp(-\mu_1 L/2) \exp((\mu_1 - \mu_2)\, l/2)\, (2/\mu_2 l) \sinh(\mu_2 l/2)}$$

$\exp(-\mu_1 L/2)$	attenuation due to water of depth L
$\exp((\mu_1 - \mu_2)\, l/2)$	replace rod of μ_1 with rod of μ_2
$(2/\mu_2 l) \sinh(\mu_2 l/2)$	dependence on rod length
	= 1, for $l = 0$ (point source)
	> 1, for $L \geq l > 0$ (line source)
A_l	activity in rod
E	counts per unit activity in air

C geometric mean of the anterior and posterior counts

In practice, the geometric mean is slightly dependent on the source depth. A phantom study was done with spherical flasks ranging from 50 ml to 1000 ml, filled with known activities of Tc-99m, and placed at various depths in 25 cm of water (P98, GEOMETRIC MEAN AND ARITHMETIC MEAN). The geometric mean count was plotted against the source depth for the various source volumes. For graphical purposes, lines are used to connect the points even though the curves should be smooth. At the midplane (12.5 cm depth in water), the geometric mean and arithmetic mean counts were equal for all source volumes. However, at 10 cm above or below the midplane, the deviation of the geometric mean counts from the midplane counts was within ±10% of the midplane counts while the arithmetic mean counts increased by over 50%. The deviation in the arithmetic mean counts increased with decreasing source size. These results are consistent with those of other workers (REF, Tothill 1971, Fleming 1979). Organs such as the kidneys and bladder are typically within 10 cm of the midplane of the body, so that the error in the geometric mean counts would be within ±10%. Therefore, to a first approximation, the geometric mean counts were independent of source depth.

ACTIVITY PER UNIT COUNT

For a rod whose length l is equal to the water depth L, and assuming that the attenuation coefficient of the rod is equal to that of water (ie: $\mu_1 = \mu_2 = \mu$), then the activity in the rod is given by:

$$AL = \frac{C}{E \exp(-\mu L/2)\ (2/\mu L)\ \sinh(\mu L/2)}$$

The term:

$$\frac{1}{E \exp(-\mu L/2)\ (2/\mu L)\ \sinh(\mu L/2)}$$

represents the activity per unit count. It takes into account the self absorption of the source. This term was measured in a phantom study using a water tank filled with various depths of water and a known activity of Tc-99m uniformly mixed in the water. The study was performed using a 9.6 minute scan duration. The activity per unit count was plotted against the water depth, and using a least squares fit method, the graph was found to be linear over a large range of patient depths (10 to 30 cm) (P101, ACTIVITY PER UNIT COUNT). The activity per unit count R is a function of the water depth L, and is given by:

$$R = (0.887 + 0.059 \times L)\ /1000, \qquad L = \text{water depth (cm)}$$

This result is independent of the area of the region of interest selected, as long as the region of interest lies within the area defined by the water tank.

In the present study, the attenuation coefficient of water was measured in a phantom study with a point source placed at various depths in a tank filled with water to a depth of 25 cm. Using a least squares fit method, the attenuation coefficient of water was found to be 0.115 cm^{-1} (P102, ATTENUATION COEFFICIENT OF WATER). The graph is not perfectly linear due to scatter. For comparison, the attenuation coefficient under narrow beam geometry conditions is 0.15 cm^{-1}.

GEOMETRIC MEAN METHOD

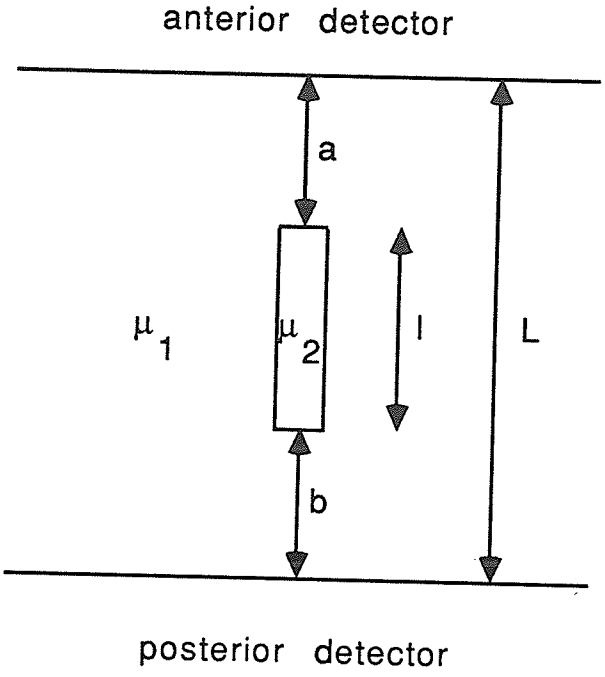

$\mu 1$ = linear attenuation coefficient of water
$\mu 2$ = linear attenuation coefficient of rod
L = depth of water = a + b + l
l = anteroposterior length of rod, $l \leq L$
a, b = water depth separating rod from the anterior and posterior cameras, respectively

50 ML FLASK

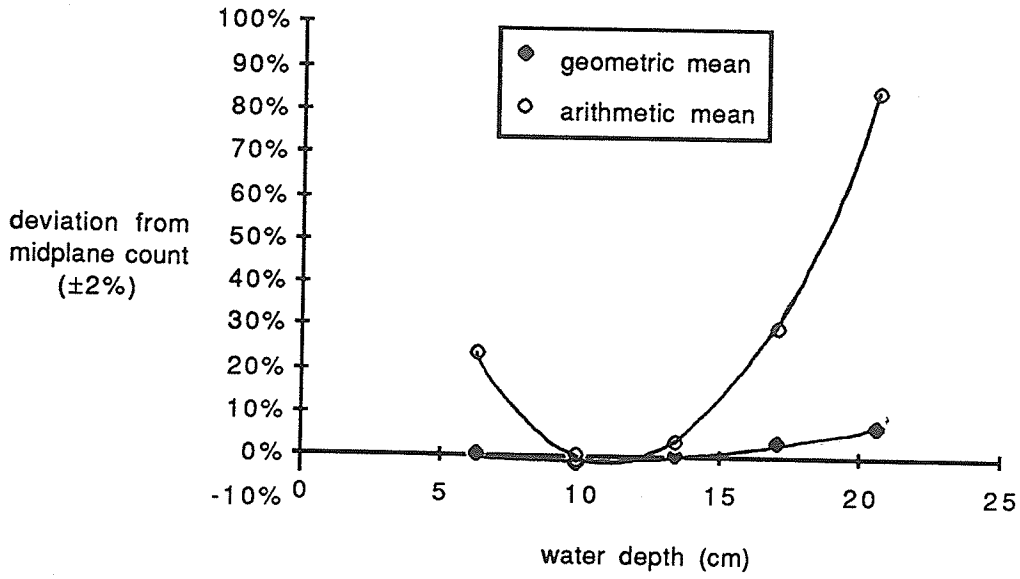

100 ML FLASK

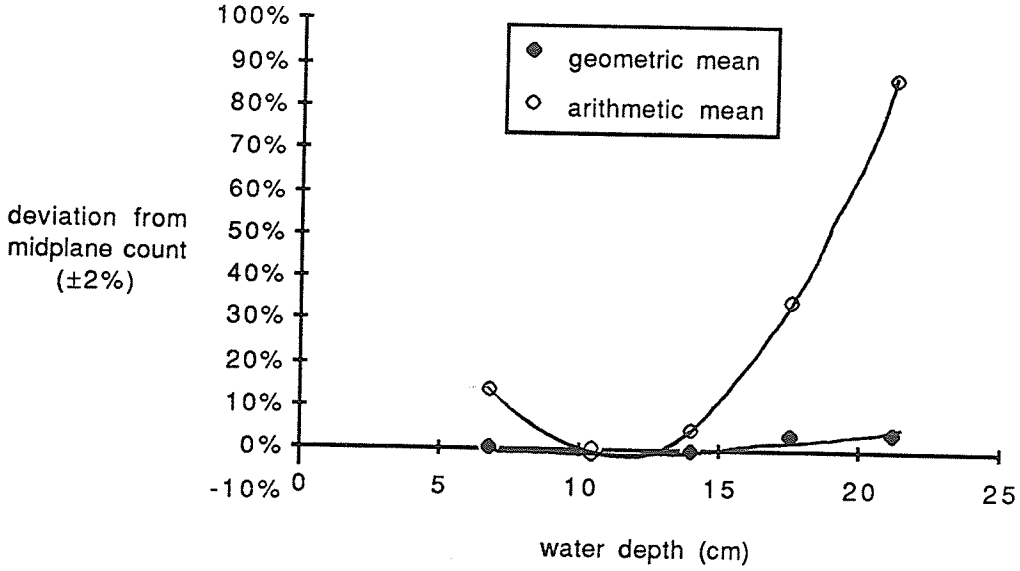

250 ML VOLUME

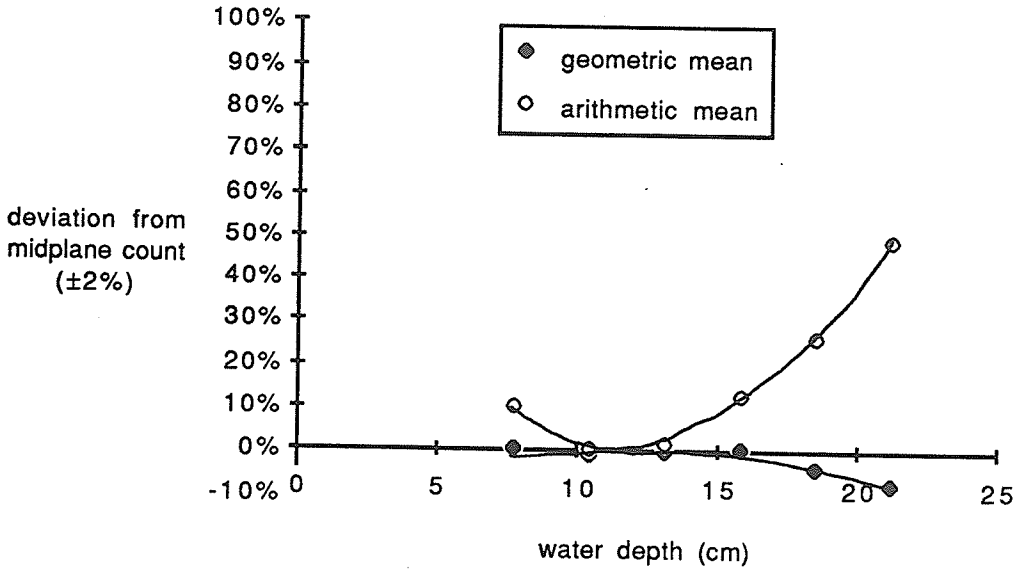

500 ML FLASK

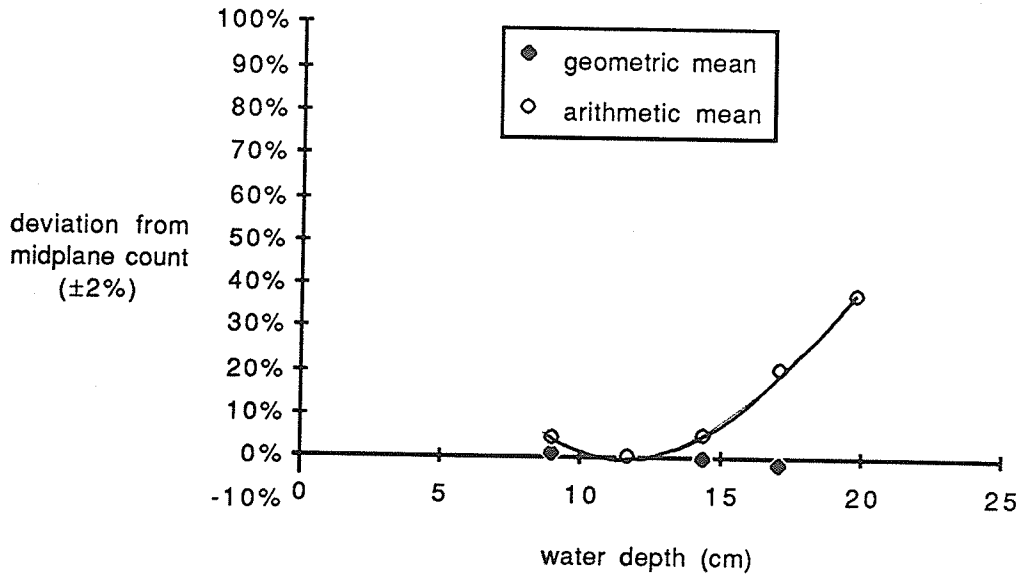

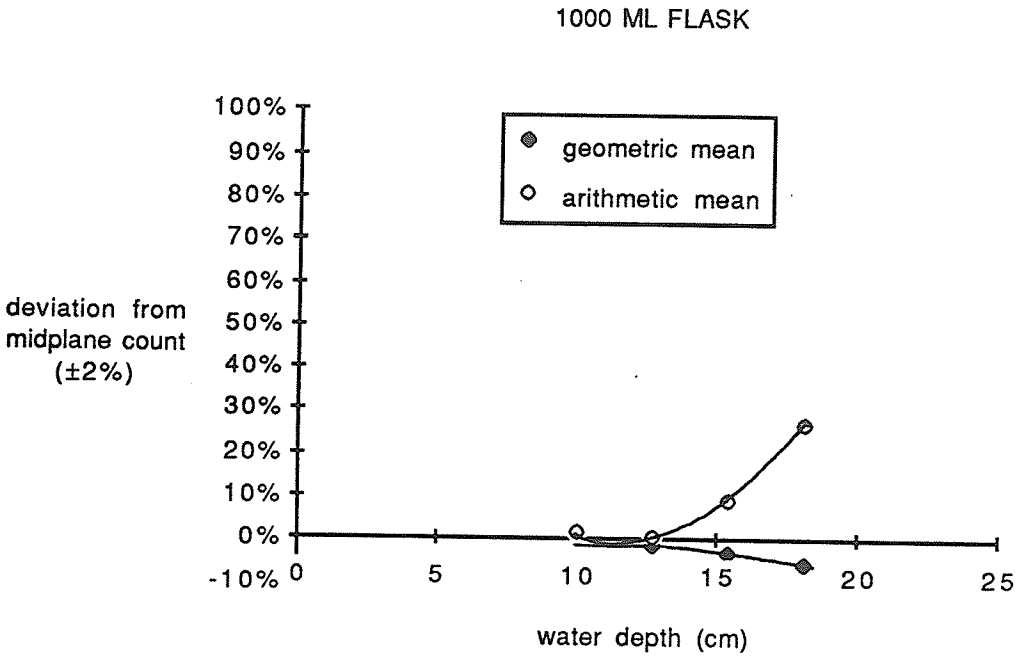
1000 ML FLASK
100%
90%
80%
70%
60%
50%
40%
30%
20%
10%
0%
-10%
0
5
10
15
20
25
geometric mean
arithmetic mean
deviation from midplane count (±2%)
water depth (cm)

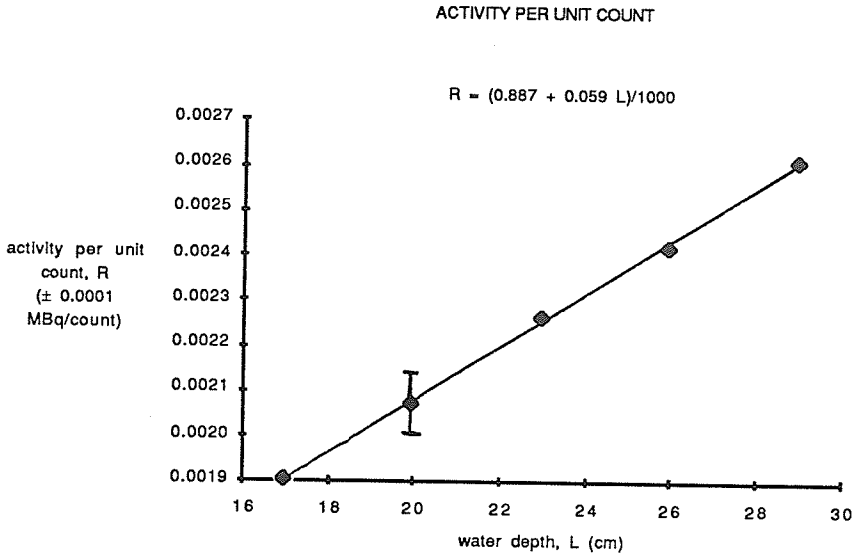
ACTIVITY PER UNIT COUNT
R = (0.887 + 0.059 L)/1000
activity per unit count, R (± 0.0001 MBq/count)
0.0027
0.0026
0.0025
0.0024
0.0023
0.0022
0.0021
0.0020
0.0019
16
18
20
22
24
26
28
30
water depth, L (cm)

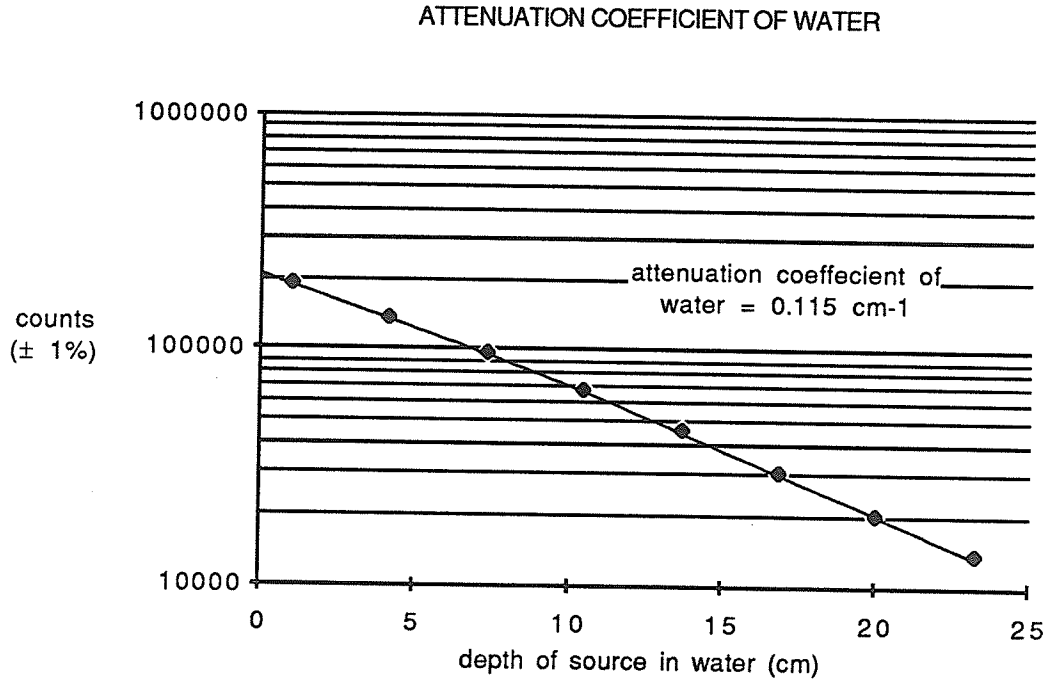
ATTENUATION COEFFICIENT OF WATER
1000000
100000
10000
counts
(± 1%)
attenuation coeffecient of
water = 0.115 cm-1
0
5
10
15
20
25
depth of source in water (cm)

SOFT TISSUE ACTIVITY

To calculate the soft tissue activity, the geometric mean method was used to calculate the activity in the thigh, and the result was scaled up by the total soft tissue volume in the body. The method assumed that the activity per unit volume in the thigh was the same as the rest of the soft tissue.

The activity in the thigh and soft tissue is given by:

$$A_{THI} = C_{THI} \times R_L$$

$$A_{ST} = A_{THI} \times V_{ST} / V_{THI}$$

R_L	activity per unit count,	(MBq/count)

which in this case is a function of the thickness over the thigh, L

C_{THI}	thigh counts over one pixel	(count)
A_{THI}	thigh activity	(MBq)
V_{THI}	thigh volume	(cm^3)

= thickness over the thigh x area of one pixel

= 0.6 x thickness over chest x $(1.755\ cm)^2$

A_{ST}	soft tissue activity	(MBq)
V_{ST}	soft tissue volume	(cm^3)

The activity in the thigh volume delineated by one pixel is given by the product of the mean count per pixel over the thigh and the activity per unit count factor, which is a function of the thigh thickness. The thigh thickness is assumed to be equal to 0.6 times

the thickness over the chest, based on an anatomical atlas with cross sectional views (REF, Rohen 1983). The body thickness over the chest was measured for each patient. The thigh volume delineated by one pixel is given by the product of the thigh thickness and the pixel area.

The total soft tissue volume was estimated using the sex and mass of the patient together with Standard Man data. Standard Man data gives the bone mass as a fraction of the body mass for normal adults (ICRP 23, 1974), as well as the mass and dimensions of the kidneys and bladder. The soft tissue mass was calculated by subtracting the mass of the kidneys, bladder, and bone from the mass of the body. Assuming that the soft tissue density was the same as that of water, then the soft tissue volume is given by:

$$\text{volume}_{ST} = \text{mass}_{ST} / \text{density}_{ST}$$

$$\text{density}_{ST} = 1.0 \text{ E-03 kg/cm}^3$$

$$\text{mass}_{ST} = M_{BODY} - (M_{KIDNEYS} + M_{BLADDER} + M_{BONE})$$

M_{BONE} = 13.5% M_{BODY} (male), 11.5% M_{BODY} (female)

$M_{KIDNEYS}$ = 0.310 kg (male), 0.275 kg (female)

$M_{BLADDER}$ = 0.245 kg (male and female)

M = mass

ST = soft tissue

The bone mass used in the above calculation did not take into account the age dependence. After the age of 30, the bone mass

decreases by 5% to 10% per decade. The mean age of the patients in the present study was about 60, which corresponds to a 15% to 30% decrease in bone mass. However, because the soft tissue mass is about six times greater than the bone mass, the decrease in bone mass corresponds to at most a 5% (30%/6) increase in the soft tissue mass, and hence soft tissue activity. As a result, no correction was made to the bone mass for age dependence.

KIDNEY AND BLADDER ACTIVITY

The activities in the kidneys and bladder were obtained by measuring the counts over these organs, subtracting the counts due to overlying soft tissue, and applying the geometric mean method. To calculate the soft tissue contribution to the counts over the kidneys and bladder, it was convenient to express the contribution as a fraction of the counts over the intestine. It was assumed that the body thickness over the intestine was the same over the kidneys and bladder, and that the activity per unit volume in the intestine was the same as in the soft tissue overlying the kidneys and bladder. Based on Reference Man data, the anteroposterior dimensions of the kidneys and bladder are about 4 cm for all patients. The attenuation coefficients of soft tissue, kidneys and bladder were assumed to be the same as water.

Recall that for a rod of length l in water of depth L, the activity in the rod is given by:

$$C_l = E\ A\ l \exp(-\mu_1 L/2)\ [\exp((\mu_1-\mu_2)\ l/2)]\ (2/\mu_2 l)\ \sinh(\mu_2 l/2)$$

E	counts per unit activity in air	(counts/MBq)
A	activity per unit length	(MBq/cm)
μ_1	linear attenuation coefficient of water	(cm^{-1})
μ_2	linear attenuation coefficient of the rod	(cm^{-1})
L	depth of water = a + b + l	(cm)
l	anteroposterior dimension of rod, $l \leq L$	(cm)

Assuming that the attenuation coefficient of the rod is equal to that of water ($\mu_1 = \mu_2 = \mu$), then the count is given by:

$$C_l = E\ A\ l\ [\exp\ (-\mu L/2)]\ [(2/\mu l)\ \sinh\ (\mu l/2)]$$

For a rod whose length l equals the body thickness L, the count is given by:

$$C_L = E\ A\ L\ [\exp\ (-\mu L/2)]\ [(2/\mu L)\ \sinh\ (\mu L/2)]$$

Therefore, for a rod of length l, the fractional contribution to the counts from the overlying soft tissue, is given by:

$$1 - C_l / C_L = 1 - \sinh\ (\mu l/2) / \sinh\ (\mu L/2)$$

Given that $\mu = 0.115\ cm^{-1}$ and l = 4 cm, then for body thicknesses ranging from 20 cm to 30 cm, $(1 - C_l / C_L)$ varies from 0.80 to 0.87. Since this variation is small, 0.85 was used as the fraction of intestine counts overlying the kidneys and bladder for all patients.

To calculate the activity per unit count for the kidneys and bladder, one could do phantom studies using sources of various sizes in water. However, a more convenient method was to use the activity per unit count calculated for a source with anteroposterior

dimension equal to the body thickness. For the kidneys and bladder, the activity is given by:

$$A_I = \frac{C_I}{E\ [\exp\ (-\mu L/2)]\ [(2/\mu l)\ \sinh\ (\mu l/2)]}$$

and the activity per unit count is now given by:

$$R_I = \frac{1}{E\ [\exp\ (-\mu L/2)]\ [(2/\mu l)\ \sinh\ (\mu l/2)]}$$

l anteroposterior dimension of kidney or bladder (cm)

L body thickness over chest (cm)

However, R_L is given by:

$$R_L = \frac{1}{E\ [\exp\ (-\mu L/2)]\ [(2/\mu L)\ \sinh\ (\mu L/2)]}$$

so that:

$$R_I = \frac{R_L\ [(2/\mu L)\ \sinh\ (\mu L/2)]}{[(2/\mu l)\ \sinh\ (\mu l/2)]}$$

Therefore, the activity in the kidneys or bladder is given by:

$$A_{KI/BL} = (C_{KI/BL} - 0.85\ C_{INT}) \times area_{KI/BL} \times R_I$$

$A_{KI/BL}$	activity in the kidneys or bladder (MBq)
$C_{KI/BL}$	counts per pixel over the kidneys or bladder
C_{INT}	counts per pixel over the intestine
$area_{KI/BL}$	number of pixels over kidneys or bladder
R_I	activity per unit count for kidneys or bladder (MBq/count)

BONE ACTIVITY

The activity in bone was found by subtracting the activity in the kidneys, bladder, and soft tissue from the activity in the body:

$$A_{BONE} = A_{BODY} - (A_{SOFT\ TISSUE} + A_{KIDNEYS} + A_{BLADDER})$$

CUMULATED ACTIVITY

INTRODUCTION

In the present study, the cumulated activity was calculated for the kidneys, bladder, bone, and soft tissue. For a given organ, the cumulated activity is given by the integral of the time-activity curve:

$$\tilde{A} = \int_0^\infty A(t)\ dt$$

$\tilde{A}$ cumulated activity (MBq-hours)
$A(t)$ activity in an organ as a function of time (MBq)
t time (hours)

TIME-ACTIVITY CURVES OF THE SOURCE ORGANS

In the present study, the time-activity curve for an organ of a given patient consisted of four points, corresponding to the four scans obtained at about 1.5, 4.5, 7.5, and 25.5 hours after injection. Assuming that the activity in an organ followed an exponential decay, the logarithms of the activities were calculated, and the four points were fitted to a line using a least squares fit method. This was equivalent to fitting the points to a single exponential function. The method generated three parameters describing the line: the initial activity, the effective half life, and the correlation

coefficient. The initial activity is the activity in the organ at the time of injection, and was found by extrapolating the line back to the injection time. The effective half life is the slope of the line, and takes into account the biological and physical half lives. The correlation coefficient describes how well the data fits the line. A correlation coefficient approaching either +1 or -1 means that the fit is good, while a value approaching zero means that the fit is poor.

The cumulated activty is found by integrating the single exponential function:

$$\tilde{A} = \int_0^\infty A(t_0) \times \exp(-\ln(2) \times t/T_{1/2})\, dt$$
$$= A(t_0) \times T_{1/2} / \ln(2)$$
$$= A(t_0) \times T_{1/2} \times 1.443$$

$\tilde{A}$	cumulated activity	(MBq-hours)
$A(t_0)$	initial activity	(MBq)
$T_{1/2}$	effective half life	(hours)
t	time after injection	(hours)

Calculation of the cumulated activity in this way assumes that the activity is taken up instantaneously into the organ, and follows a single exponential decay. In practice, the assumption of instantaneous uptake does not hold, especially for the bladder and bone, and the assumption of a single exponential decay does not hold

for the soft tissue. Modifications to the calculation of the cumulated activities were made depending on how applicable the modifications were to all patients. In the present study, the calculation of the cumulated activities for only the bladder and soft tissue were changed, while those for the kidneys and bone were unchanged. This was based on the published time-activity data and on a patient study (done in the present study) where one patient was scanned six times over the first two hours after injection (P117, SIX SCAN STUDY). This is explained as follows.

- KIDNEYS

There is no published data on the time-activity curve of the kidneys in humans using Tc-99m phosphorous radiopharmaceuticals. The time-count curve for the kidneys obtained from the six scan study shows that the uptake reaches a maximum before the first scan was obtained (at about ten minutes), so that the uptake can be considered to be instantaneous. However, this curve is only for one patient, and the initial uptake is strongly dependent on the kidney function. Since the kidney function varied greatly among the patients in the present study, it was difficult to modify the calculation of the cumulated activity for the kidneys in a way that was applicable to all patients. Therefore, no modification was made to the time-activity curve of the kidneys.

- BONE

Published data on the time-activity curve of bone using Tc-99m phosphorous radiopharmaceuticals indicate that the maximum uptake occurs about one to two hours after injection, and that the initial uptake over that time period is strongly dependent on the bone function (REF, Snow 1975, Citrin 1975, Potsaid 1977, Castronovo 1977). The six scan study is consistent with the first observation, as seen from the time-count curve for the upper spine region. The spine counts were corrected for the counts due to overlying soft tissue. Since the bone function varied greatly among the patients in the present study, it was difficult to modify the calculation of the cumulated activity for the bone in a way that was applicable to all patients. Therefore, no modification was made to the time-activity curve of the bone.

- SOFT TISSUE

There is no published data on the time-activity curve of the soft tissue in humans using Tc-99m phosphorous radiopharmaceuticals. However, data is available on the blood activity component of soft tissue. The blood activity reaches a maximum value instantaneously (within 2 or 3 circulations), since the activity is injected directly into the vein. This observation is consistent with the six scan study, where the soft tissue counts is seen to be highest in the first scan. However, the effective half life of the blood activity over the first hour was shorter than the half life after one hour. Assuming that the blood activity was representative of the soft tissue activity, then the cumulated

activity for soft tissue was underestimated if a single exponential decay was assumed. Therefore, a better method of calculating the cumulated activity for the soft tissue is to set the initial soft tissue activity equal to the initial whole body activity minus the initial activities in the kidneys, bladder, and bone. The soft tissue activity is assumed to decrease linearly with time until the line intercepts the original soft tissue curve at one hour (P118, TIME-ACTIVITY CURVES FOR THE KIDNEYS, BLADDER, BONE, SOFT TISSUE AND VOIDED URINE). The cumulated activity for the soft tissue is now given by:

$$\tilde{A} = [\ A(t_0)^* + A(1hr)\ ] \times 1hr/2 + A(1hr) \times T_{1/2} / \ln(2)$$

$$A(1hr) = A(t_0) \times \exp(-\ln(2) \times 1hr / T_{1/2})$$

$\tilde{A}$	cumulated activity	(MBq-hours)
$T_{1/2}$	effective half life	(hours)
$A(t_0)$	initial activity	(MBq)
	(calculated from the least squares fit method)	
$A(t_0)^*$	modified initial activity, where	(MBq)

$$A(t_0)^*_{\text{SOFT TISSUE}} = A(t_0)_{\text{BODY}} - [A(t_0)_{\text{KIDNEYS}} + A(t_0)_{\text{BONE}}]$$

$$A(t_0)^*_{\text{BLADDER}} = 0$$

The choice of one hour is somewhat arbitrary, but is based on the fact that at one to two hours after injection, the exchange of activity between the various organs in the body reach equilibrium. Also, all the first scans in the present study were obtained after one hour postinjection.

- BLADDER

There is no published data on the time-activity curve of the bladder in humans using Tc-99m phosphorous radiopharmaceuticals. The time-count curve for the bladder obtained from the six scan study shows that the bladder count starts at zero and increases gradually as activity is removed from the blood by the kidneys and is transferred in the urine to the bladder. The present method of calculating the cumulated activity for the bladder would result in an overestimate. Therefore, a better method of calculating the bladder cumulated activity is to set the initial bladder activity to zero, and assume that it increases linearly with time until the line intercepts the original bladder curve at one hour (P118, TIME-ACTIVITY CURVES FOR THE KIDNEYS, BLADDER, BONE, SOFT TISSUE AND VOIDED URINE). The choice of one hour is based on the reasons given previously in the calculation of the cumulated activity of the soft tissue. The equation used to calculate the cumulated activity for the bladder is the same as for the soft tissue, except that the modified initial activity is set to zero.

- VOIDED URINE

There is a contribution to the cumulated activity of the bladder from the voided urine. Since the patients were asked to void just before each scan, the time-activity curve for the bladder only represents the activity retained in the bladder. The contribution from the voided urine was calculated by assuming that the urine

activity in the bladder increased linearly with time (P119, TIME-ACTIVITY CURVES FOR THE KIDNEYS, BLADDER, BONE, SOFT TISSUE AND VOIDED URINE), so that the cumulated activity of the voided urine is given:

$$\tilde{A}_{URINE} = \Sigma_{i=1,4} (t_i - t_{i-1}) \times A_{URINE}(t_i) / 2$$

$\tilde{A}_{URINE}$ bladder cumulated activity due to voided urine (MBq-hours)

$A_{URINE}(t_i)$ activity in the i'th urine collection, or activity in the urine collected between t_i and t_{i-1} (MBq)

t_i time of the i'th scan (hours)

The method assumed that the urine in each collection was all excreted at the time the collection was obtained. The fact that there is a large time difference of about 18 hours between the third and fourth scans does not significantly affect the results. Therefore, the total bladder cumulated activity is given by the sum of the cumulated activity due to the bladder and the cumulated activity due to voided urine.

$$\tilde{A}_{URINE+BL} = \tilde{A}_{URINE} + \tilde{A}_{BL}$$

$\tilde{A}_{URINE}$ = cumulated activity due to voided urine

$= \Sigma_{i=1,4} (t_i - t_{i-1}) \times A_{URINE}(t_i) / 2$

$\tilde{A}_{BL}$ = cumulated activity due to the bladder

$= A(1hr)_{BL} \times 1hr/2 + A(1hr)_{BL} \times T_{1/2} / \ln(2)$

$A(1hr)_{BL} = A(t_0)_{BL} \times \exp[-\ln(2) \times 1hr / T_{1/2}]$

SIX SCAN STUDY

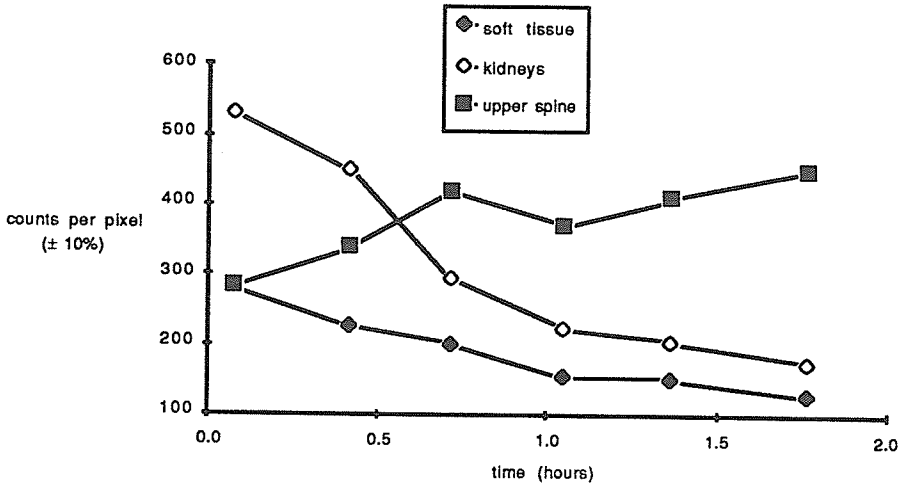

SIX SCAN STUDY

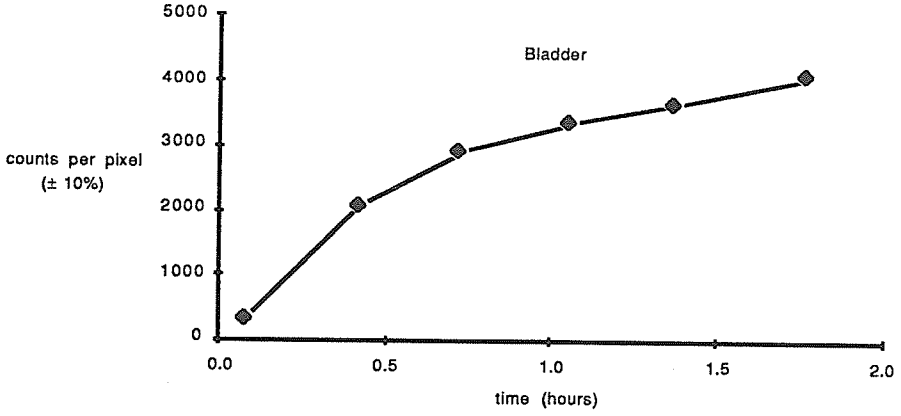

TIME-ACTIVITY CURVES FOR THE KIDNEYS, BLADDER, BONE, SOFT TISSUE AND VOIDED URINE

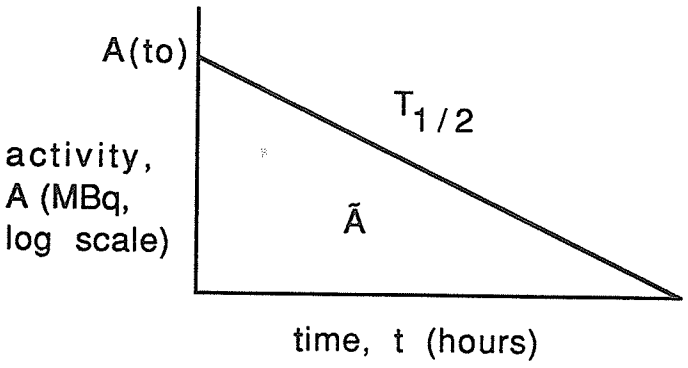

$A(to)$ = initial activity (MBq)

$T_{1/2}$ = effective half life (hours)

$\tilde{A}$ = cumulated activity (MBq-hours)

$= A(to) \times T_{1/2} / \ln(2)$

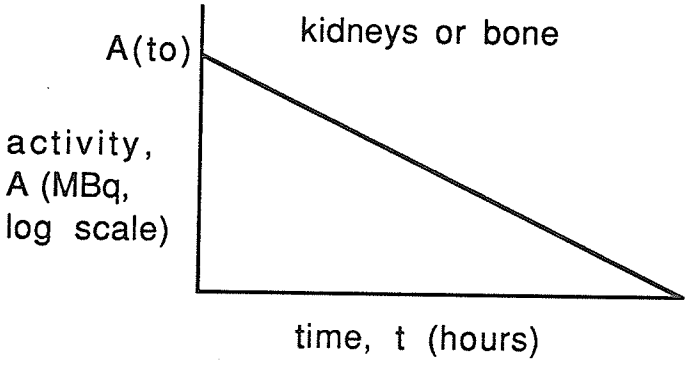

TIME-ACTIVITY CURVES FOR THE KIDNEYS, BLADDER, BONE, SOFT TISSUE AND VOIDED URINE

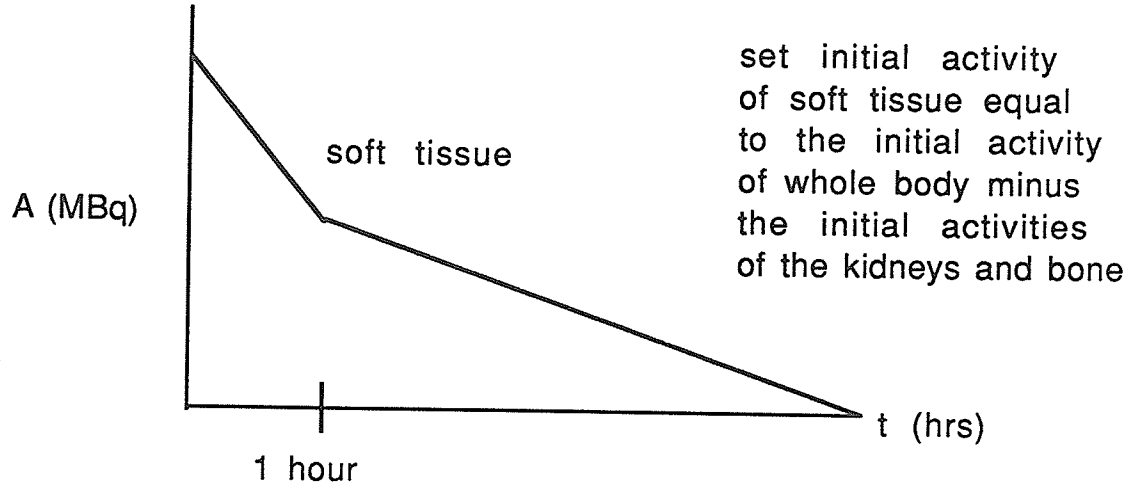

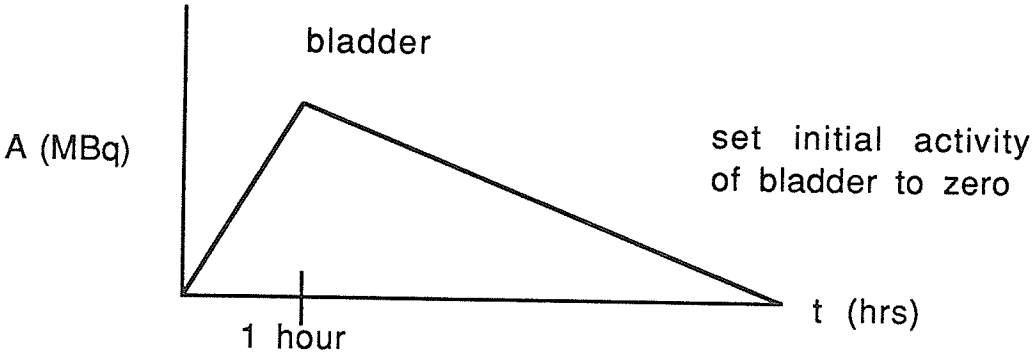

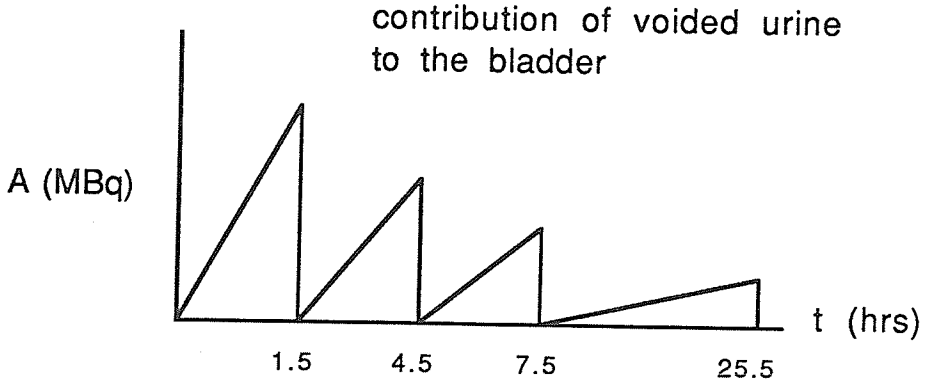

DOSE CALCULATIONS

ABSORBED DOSE

The absorbed doses to the various target organs were calculated from the cumulated activities of the source organs and the MIRD S values (absorbed dose per unit cumulated activity) for Tc-99m. In the present study, the kidneys, bladder, bone (skeleton), and soft tissue were chosen as source organs. In the table of S values, the kidneys and bladder contents are listed as source organs. However, the soft tissue is not listed as a source organ, while the skeleton is not listed as a single organ, but is composed of three different types of bone. The soft tissue and bone are dealt with below.

- SOFT TISSUE

To a first approximation, the "soft tissue" as defined in the present study was assumed to be equivalent to the "total body" as defined in the table of S values. This is because the soft tissue weight represents about 85% of the total body weight. The 85% value is found by subtracting the weight of the kidneys, bladder, and bone from the whole body weight [ie: 70 kg - (0.31+0.245+10) kg = 59.4 kg, 59.4/70 = 85% using Reference Man data].

- BONE

In the MIRD model, the skeleton is divided into three types of bone: red marrow, cortical bone, and trabecular bone. The distribution of activity among these three types of bone depends on whether the radiopharmaceutical is distributed throughout the total bone volume or on the bone surface. The model further assumes that the activity in bone is uniformly distributed in the cortical and trabecular bone. The ratio of the weights of the cortical bone and trabecular bone is four to one for a volume distribution, and one to one for a surface distribution (REF, Johannson 1981). Tc-99m bone imaging radiopharmaceuticals have been shown to have a surface distribution (REF, Arnold 1982), so that the activity in bone is equally divided between cortical and trabecular bone. The standard table of MIRD S values assumes a volume distribution.

The S values for a surface distribution have been calculated (REF, Johannson 1981), and are given in (P123, S VALUES FOR Tc-99M FOR SURFACE AND VOLUME DISTRIBUTIONS OF ACTIVITY IN BONE). The S values for a surface distribution are used in the present study. Using the surface distribution model, activity in the trabecular bone causes a larger absorbed dose to the red marrow. The absorbed dose received by the bone surface from the cortical and trabecular bone is higher than that received by the total bone. This is due not only to the different mass distribution but also to the relatively small mass of the bone surfaces, 120 g, compared to the total mineral bone, 5000 g.

EFFECTIVE DOSE EQUIVALENT

The effective dose equivalent was calculated using the absorbed doses to the various organs and the ICRP 26 weighting factors. This calculation required the absorbed doses to the gonads, breast, lung, bone marrow, bone surface, thyroid, and five other organs with the next highest doses. These five organs were chosen to be the kidneys, bladder, upper large intestine, lower large intestine, and small intestine. The choice of the last three of the five organs was somewhat arbitrary, since the absorbed doses to these three organs and the remaining target organs were less than 4 mSv, which was small compared to the absorbed doses to the kidneys (about 10 mSv) and the bladder (10 to 40 mSv). The breast is not a target organ listed in the table of S values, but it was assumed to be equivalent to the "others (muscle)" organ for the purpose of absorbed dose calculations.

S VALUES FOR TC-99M FOR SURFACE AND VOLUME DISTRIBUTIONS OF ACTIVITY IN BONE

Units are in mGy/MBq-hr

1 mGy/MBq-hr = (37/10000) x rad/μCi-hr

SURFACE DISTRIBUTION

target organs	source organs	
	cortical	trabecular
bone surface	2.2E-02	2.2E-02
RBM	1.1E-03	4.3E-03

VOLUME DISTRIBUTION

target organs	source organs	
	cortical	trabecular
total bone	3.2E-03	2.7E-03
RBM	1.1E-03	2.5E-03

SAMPLE CALCULATIONS AND ERROR ANALYSIS

DETECTOR UNIFORMITY CORRECTION

The detector uniformity correction is achieved by dividing the uncorrected patient image by the flood image (with appropriate scaling of these images).

$$Q(x,y) = P(x,y) \,/\, R(x,y)$$

$P(x,y)$	counts in pixel (x,y) in the uncorrected patient image
$Q(x,y)$	counts in pixel (x,y) in the corrected patient image
$R(x,y)$	counts in pixel (x,y) in the flood image

The statistical error in the counts of the corrected patient image is given by:

$$\partial Q(x,y)/Q(x,y) = [\ (\partial P(x,y)/P(x,y))^2 + (\partial R(x,y)/R(x,y))^2\ ]^{1/2}$$
$$= [\ 1/P(x,y) + 1/R(x,y)\ ]^{1/2}$$

For example, the mean counts per pixel over the kidneys is typically 400 counts, while the mean counts in the flood image is 500 counts, so that the statistical error is given by $[\ 1/400 + 1/500\ ]^{1/2} = 6.7\%$. This calculation was done for other regions in the patient image, and is summarized in (P136, ERROR ANALYSIS).

AREA OF REGION OF INTEREST

For a region with n pixels, each with Q counts, then the error in the total counts C (= n x Q) is given by:

$$\partial C/C = n^{-1/2} \times (\partial Q/Q)$$

As the number of pixels in an area of interest increases, the error decreases. For example, the area of the kidneys is typically 25 pixels, and each pixel typically has 400 counts, so that the error in the total counts over the kidneys is $6.7\%/\sqrt{25} = 1.3\%$.

GEOMETRIC MEAN COUNTS

The geometric mean counts C is given by:

$$C = (C_A \times C_P)^{1/2}$$

C_A anterior counts

C_P posterior counts

The error in the geometric mean counts is given by:

$$\partial C/C = (1/2) \left[(\partial C_A / C_A)^2 + (\partial C_P / C_P)^2 \right]^{1/2}$$
$$= (1/\sqrt{2}) (\partial C_A / C_A)$$

assuming that $\partial C_A / C_A = \partial C_P / C_P$, which means that the fractional error in the anterior and posterior counts are approximately the same. This assumption is valid since the sensitivity of the detectors were similar. For example, the error in the kidney counts is $1.3\%/\sqrt{2} = 0.92\%$. There is an additional 10% systematic error due to the fact that the geometric mean correction was not absolutely independent of the source depth, so that the error becomes 10% + 0.92% = 10.9%. This additional 10% error only applies to organs such as the kidneys, bladder, and spine, and not to the thigh or intestine, since the activity in the thigh and intestine is assumed to be uniformly distributed.

CORRECTION FOR OVERLYING SOFT TISSUE

The counts over organs such as the kidneys, bladder, and spine must be corrected for the counts due to overlying soft tissue. This contribution is estimated to be 0.85 of the intestine counts, assuming that:

(1) body thickness over the chest (measured) is the same as over the intestine, kidneys, bladder, and spine;
(2) concentration of activity in the intestine is the same as in the soft tissue overlying these other organs; and
(3) anteroposterior thicknesses of kidneys and bladder are 4 cm.

The true counts over an organ such as the kidneys or bladder is given by:

$$C^*_{ORG} = C_{ORG} - 0.85\ C_{INT}$$

C^*_{ORG} mean counts per pixel over organ, corrected for overlying soft tissue

C_{ORG} mean counts per pixel over organ

C_{INT} mean counts per pixel over intestine

The error in the corrected counts is given by:

$$\partial C^*_{ORG} / C^*_{ORG} = [\ (\partial C_{ORG})^2 + (0.85)^2\ (\partial C_{INT})^2\ ]^{1/2} / C^*_{ORG}$$

For example, the corrected counts over the kidneys is given by:

$$C^*_{KI} = 400 - 0.85 \times 200 = 230$$

$$\partial C_{KI} = 0.109 \times 400$$

$$\partial C_{INT} = 0.013 \times 200$$

Therefore, the error in the corrected kidney counts is 19%.

ACTIVITY PER COUNT RATIO

The activity in the kidneys or bladder is given by:

$$A_{KI/BL} = C^*_{KI/BL} \times area_{KI/BL} \times R_l$$

$A_{KI/BL}$ activity in the kidneys or bladder

$C^*_{KI/BL}$ counts per pixel over the kidneys or bladder, corrected for overlying soft tissue

$area_{KI/BL}$ number of pixels over the kidneys or bladder

$$R_l = \frac{R_L \ (2/\mu L) \ \sinh \ (\mu L/2)}{(2/\mu l) \ \sinh \ (\mu l/2)}$$

R_l activity per unit count for activity uniformly distributed in an organ of thickness l

R_L activity per unit count for activity uniformly distributed in a body of thickness L

$= [0.887 + 0.059 \times L(cm)] / 1000$

μ attenuation coefficient of water, measured to be 0.115 cm^{-1}

l anteroposterior thickness of organ (kidneys or bladder), assumed to be 4 cm.

The term R_L was measured from phantom studies for various values of L, and fitted to a line using a least squares fit method. The error in R_L was about 3.5% for values of L ranging from 20 to 30 cm. The error in measuring L was about 5%. The error in μ was under 1%. Therefore, the error in R_l was about 6.2%.

For example, assuming that there is no error in the organ area, the error in the kidney activity is given by:

$$\partial A_{KI} / A_{KI} = [(\partial C^*_{KI} / C^*_{KI})^2 + (\partial R_l / R_l)^2]^{1/2}$$
$$= [(0.19)^2 + (0.062)^2]^{1/2}$$
$$= 0.20$$

ACTIVITY IN THE WHOLE BODY AND URINE

The whole body activity is given by:

$$A_{BODY}(t_i) = C_{BODY}(t_i) \times A_{BODY}(t_1) / C_{BODY}(t_1)$$

where i = 1, 2, 3, 4

$C_{BODY}(t_i)$ whole body counts at the time of the i'th scan (count)

$A_{BODY}(t_i)$ whole body activity at the time of the i'th scan (MBq)

$A_{BODY}(t_1)$ whole body activity at the time of the first scan (MBq)

$= A_{BODY}(t_0) \times \exp [-\ln(2) \times (t_1 - t_0)/T_{1/2}] - A_{URINE}(t_1)$

The error in the whole body activity is given by:

$$\partial A_{BODY}(t_i) / A_{BODY}(t_i) = [\,(\partial C_{BODY}(t_i) / C_{BODY}(t_i))^2 + (\partial A_{BODY}(t_1) / A_{BODY}(t_1))^2 + (\partial C_{BODY}(t_1) / C_{BODY}(t_1))^2\,]^{1/2}$$

The error in the whole body counts is 0.13%. The error in the whole body activity at the time of the first scan depends on the accuracy with which the injected activity and the activity in the first urine collection are measured. The injected activity was measured using a dose calibrator with an accuracy of 2%. The urine activity was measured with an accuracy of about 5%. However, the injected activity was typically much greater than the urine activity, so that the error in the whole body activity at the time of the first scan was about 2%. Therefore, the error in the whole body activity is about 2%.

SOFT TISSUE ACTIVITY

The activity in the soft tissue is given by:

$$A_{ST} = C_{THI} \times R_L \times V_{ST} / V_{THI}$$

A_{ST}	soft tissue activity	(MBq)
C_{THI}	mean counts per pixel over thigh	(count)
R_L	activity per unit count for activity uniformly distributed in organ of thickness L	(MBq/count)
L	body thickness over thigh	(cm)

V_{THI} thigh volume (cm^3)

= thickness over thigh x area of one pixel

= 0.6 x thickness over chest x $(1.755\ cm)^2$

V_{ST} soft tissue volume (cm^3)

The error in the soft tissue activity is given by:

$$\partial A_{ST}/A_{ST} = [\ (\partial C_{THI}/C_{THI})^2 + (\partial R_L/R_L)^2 + (\partial V_{ST}/V_{ST})^2 + (\partial V_{THI}/V_{THI})^2\ ]^{1/2}$$

$\partial C_{THI}/C_{THI}$ = 1.4%

$\partial R_L/R_L$ = 3.5%

$\partial V_{THI}/V_{THI}$ = 5%

$\partial V_{ST}/V_{ST}$ = 5%, based on Reference Man data

Therefore, the error in the soft tissue activity is about 8%.

BONE ACTIVITY

The bone activity is given by:

$$A_{BONE} = A_{BODY} - (A_{ST} + A_{KI} + A_{BL})$$

Using typical organ activities at the time of the first scan, the bone activity is equal to:

$$A_{BONE} = 482 - (303 + 13 + 22)$$
$$= 145 \text{ MBq}$$

The error in the bone activity is given by:

$$\partial A_{BONE} / A_{BONE} = [(\partial A_{BODY})^2 + (\partial A_{ST})^2 + (\partial A_{KI})^2 + (\partial A_{BL})^2]^{1/2} / A_{BONE}$$

∂A_{BODY} = 2% x 482

∂A_{ST} = 8% x 303

∂A_{KI} = 20% x 13

∂A_{BL} = 15% x 22

Therefore, the error in the bone activity is about 18%, and depends mainly on the error in the soft tissue activity.

CUMULATED ACTIVITY

The cumulated activity is given by:

$$\tilde{A} = A(t_0) \times T_{1/2} / \ln(2)$$

$\tilde{A}$	cumulated activity	(MBq-hours)
$A(t_0)$	initial activity	(MBq)
	or activity at the time of injection	
$T_{1/2}$	effective half life	(hours)
t	time after injection	(hours)

The error in the cumulated activity is given by:

$$\partial\tilde{A}/\tilde{A} = [\ (\partial A(t_0)\ /A(t_0)\ )^2 + (\partial T_{1/2}\ /T_{1/2}\ )^2\ ]^{1/2}$$

The errors in the initial activities and the half lives are calculated from the least squares fit method. The errors in the cumulated activities are typically 15% for the kidneys, 10% for the bladder, and 2% for the soft tissue and bone. It is difficult to estimate the errors in assuming that the uptake were instantaneous for the kidneys and bone.

ORGAN DOSE AND EFFECTIVE DOSE EQUIVALENT

The organ dose is given by:

$$D_t = \Sigma_s \tilde{A}_s \times S(t, s)$$

D_t absorbed dose to target organ "t" (mGy)

$\tilde{A}_s$ cumulated activity in source organ "s" (MBq-hr)

$S(t, s)$ absorbed dose per unit cumulated activity to target organ "t" from source organ "s" (mGy/MBq-hr)

The error in the organ dose is given by:

$$\partial D_t / D_t = [\, \Sigma_s \, (\partial \tilde{A}_s)^2 \times (S(t, s))^2 \,]^{1/2} / D_t$$

The errors in the abosrbed doses are typically 15% for the kidneys, 10% for the bladder, and 2% for the rest of the organs.

The effective dose equivalent is given by:

$$H_e = \Sigma_i w_i \times H_i$$

H_e effective dose equivalent (mSv)

w_i weighting factor (no units)

H_i dose equivalent to organ "i" (mSv)

The error in the effective dose equivalent is given by:

$$\partial H_e/H_e = [\ \Sigma_i (\partial D_i)^2 \times (w_i)^2\ ]^{1/2} / H_e$$

The error in the effective dose equivalent is typically 3%.

ERROR ANALYSIS

ROI	patient image	mean count per pixel	pixel area	count error	area error	geom mean error	dev'n from midplane	soft tissue subtract	counts to activity	cumu-lated activity
kidneys	1-3	400	25	6.7%	1.3%	0.9%	11%	19%	20%	20%
	4	100	25	11.0%	2.2%	1.5%	12%	16%	17%	
bladder	1-3	1000	10	5.5%	1.7%	1.2%	11%	14%	15%	10%
	4	100	10	11.0%	3.5%	2.4%	12%	17%	18%	
thigh	1-3	100	30	11.0%	2.0%	1.4%			8%	2%
	4	10	30	31.9%	5.8%	4.1%			9%	
intestine	1-3	200	24	8.4%	1.7%	1.2%				
	4	30	24	18.8%	3.8%	2.7%				
body	1-3	200	2000	8.4%	0.2%	0.1%			2%	5%
	4	30	2000	18.8%	0.4%	0.3%			2%	
spine	1-3	400	12	6.7%	1.9%	1.4%	11%	20%		
	4	100	12	11.0%	3.2%	2.2%	12%	16%		
bone									18%	5%

The error in the effective dose equivalent is about 3%

RESULTS

The time-activity data and dose data for the 25 patients (14 male, 11 female) are given in (APPENDIX II, TIME-ACTIVITY DATA AND DOSE DATA OF 25 PATIENTS) and are summarized in (P139, TIME-ACTIVITY DATA, DOSE DATA) in terms of the mean and standard deviation. For comparison, typical errors in the time-activity data and dose data for a single patient are also shown. The initial activities are expressed as a percentage of the injected activity. The effective half lives are expressed in hours. The absorbed doses and effective dose equivalents are expressed in mGy and mSv respectively, and are normalized to a 740 MBq injection of Tc-99m pyrophosphate. Note that one patient (patient number 2 in Appendix I) was not used to generate results (see "Soft tissue" section for reason).

- TIME-ACTIVITY DATA

The time-activity curve of an organ is characterized by three parameters: the initial activity, the effective half life, and the correlation coefficient. These parameters were calculated for the kidneys, bladder, bone, soft tissue, and whole body, and the latter two parameters were calculated for the upper spine, lower spine, and intestine. These parameters were calculated by fitting the logarithm of the activities to a line using a least squares fit method. The activities were not corrected for physical decay. The sum of the mean initial activities of the kidneys, bladder, bone, and soft tissue was 98% of the injected activity. Except for the

effective half life of the kidneys, the errors in the time-activity data of a single patient were relatively small compared to the standard deviation among all patients. The correlation coefficients for these organs ranged from -0.93 to -1.00, which indicated that the fits were good and that the number of points were small.

- DOSE DATA

The absorbed dose to a target organ was calculated from the cumulated activities of the source organs and from the MIRD S values for Tc-99m. The effective dose equivalent was calculated from the absorbed doses to the target organs and from the ICRP 26 weighting factors. The absorbed doses to the testes were based on 14 male patients, and the absorbed doses to the ovaries and uterus (nongravid) were based on 11 female patients. The dose data were divided according to the sex of the patients, and the difference in the means are calculated. The errors in the dose data for a single patient were relatively small compared to the standard deviation of the group. For comparison, the dose data published by Subramanian et al. (1975) are given in the last column.

TIME-ACTIVITY DATA

organ	initial activity (% injected activity)		single patient error	effective half life (hours)		single patient error	correlation coefficient	
	mean	stdev		mean	stdev		mean	stdev
kidneys	2.7%	1.8%	0.2%	6.7	2.5	1.9	-0.95	0.06
bladder	10%	11%	0.3%	3.7	1.4	0.2	-0.96	0.04
bone	35%	15%	1.0%	7.0	1.3	0.2	-0.95	0.06
soft tissue	50%	16%	0.8%	4.6	0.5	0.1	-0.99	0.01
whole body	95%	7%	0.2%	5.7	0.3	0.0	-1.00	0.00
upper spine	---	---	---	5.9	0.5	0.1	-0.99	0.02
lower spine	---	---	---	6.1	0.6	0.2	-0.98	0.03
intestine	---	---	---	5.7	0.7	0.0	-0.99	0.01

The time-activity data consists of three parameters for each organ of interest:
the initial activity (expressed as a percentage of the injected activity),
the effective half life (expressed in hours), and the correlation coefficient.
The mean and standard deviation for the 25 patients (11 female, 14 male) are calculated for each parameter.
For comparison, the typical errors in the time-activity data of a single patient is given for each organ.

organ	present study all patients		stdev/ mean % error	single patient error	n=11 female mean	n=14 male mean	male-female diff	publish Subra-manian
	mean	stdev						
Adrenals	2.8	0.3	12%	5%	2.7	2.9	0.3	---
Bladder wall	21	11	53%	8%	20	21	0.8	64
Bone surface	56	17	30%	2%	61	53	-8.3	78
GI (stom wall)	2.1	0.4	19%	2%	1.8	2.2	0.4	---
GI (small intest)	2.7	0.4	17%	2%	2.4	2.9	0.4	---
GI (ULI wall)	2.5	0.4	17%	2%	2.2	2.7	0.4	---
GI (LLI wall)	3.1	0.6	18%	2%	2.9	3.3	0.4	---
Kidneys	10.7	3.2	30%	18%	11.7	9.9	-1.8	9.4
Liver	2.1	0.4	17%	2%	1.9	2.3	0.4	2.8
Lungs	2.0	0.3	15%	1%	1.8	2.2	0.3	---
Marrow (red)	9.0	1.6	18%	1%	9.3	8.9	-0.5	11.5
Other (muscle)	2.2	0.3	12%	1%	2.0	2.3	0.3	---
Ovaries	2.8	0.5	17%	0%	2.8	---	---	4.0
Pancreas	2.5	0.4	15%	3%	2.3	2.7	0.4	---
Skin	1.4	0.2	13%	1%	1.3	1.5	0.2	---
Spleen	2.4	0.4	16%	4%	2.2	2.5	0.3	---
Testes	2.3	0.4	17%	2%	---	2.3	---	2.8
Thyroid	1.5	0.2	15%	1%	1.4	1.7	0.2	---
Uterus (nongrav)	3.8	1.0	26%	0%	3.8	---	---	---
Total body	3.0	0.2	7%	2%	2.9	3.1	0.2	2.0
effective dose (mSv) equivalent	6.1	0.8	12%	3%	6.3	5.9	-0.4	9.1

Results are normalized to a 740 MBq injection of Tc-99m pyrophosphate
Absorbed doses are expressed in mGy and the effective dose equivalents are expressed in mSv.
In the first column are the 20 target organs.
In columns 2 and 3, the mean and standard deviation for the 25 patients
(11 female, 14 male) are calculated for each parameter.
In column 4, the standard deviation is expressed as a percentage (100% x stdev/mean).
In column 5, the typical error in the organs doses for a single patient are shown.
In columns 6 and 7, the dose data is grouped according to the patient sex.
The mean female doses are based on 11 patients, and the mean male doses are based on 14 patients
In column 8, the difference in the mean male and female doses are shown (male - female).
In the last column, dose data published by Subramanian (1975) are shown.

DISCUSSION

TIME-ACTIVITY DATA

The time-activity data for Tc-99m pyrophosphate in humans and animals is discussed in the "Literature review" section, and are referred to in this section. The present study was restricted to diseased humans.

URINARY EXCRETION

In the present study, the 24 hour urinary excretion was calculated from the whole body time-activity data as follows:

$$UE\ (t=24hrs) = 100\% - A(t_0)_{BODY} \times \exp\left[-\ln(2) \times t \times \left(1/T_{1/2,\ BODY} - 1/T_{1/2,\ PHYS}\right)\right]$$

$$= 100\% - 93.3\% \times \exp\left[-\ln(2) \times 24 \times (1/5.68 - 1/6.03)\right]$$

$$= 21\%$$

$T_{1/2,\ BODY}$ effective half life of activity in body

$T_{1/2,\ PHYS}$ physical half life of radionuclide, 6.03 hours

t time after injection (hours)

$A(t_0)_{BODY}$ initial activity in the whole body, calculated from the least squares fit method, and expressed as a percentage of the injected activity

This 24 hour urinary excretion of (21±7)% is less than that measured by other workers: 38% (Weber), (32±4)% (Krishnamurthy), and (59±5)% (Subramanian) (see "Literature review" section). It is not possible to correlate the low 24 hour urinary excretion found in the present study to a specific patient characteristic, because of the small number of patients and the large variety of diseases present in the patients.

The accuracy of the urinary excretion, as calculated from the whole body counts, mainly depends on the accuracy with which the first urine collection is obtained. Recall that the activities in the second, third, and fourth urine collections are calculated from the whole body activities, which in turn, are calculated from the whole body counts and the first urine collection. If urine was missed in the first urine collection, it would be impossible to determine the amount of urine missing. However, the accuracy of the second, third and fourth urine collections can be checked by comparing urine activities in these urine collections to their corresponding urine activities calculated from the whole body counts. This provides an indirect check on the accuracy with which the first urine collection was obtained.

A convenient method of checking the accuracy with which the second, third, and fourth urine collections were obtained is to plot the whole body retention (ie: whole body activity, corrected for physical decay), as calculated from the whole body counts, versus the urinary excretion (ie: cumulative urine activity, corrected for

physical decay), as calculated from the urine collections (P147, WHOLE BODY RETENTION VERSUS URINARY EXCRETION). The sum of the whole body retention and the urinary excretion should equal 100% of the injected activity, which would appear as a diagonal line (100% line) going from (UE=0%, WBR=100%) to (UE=100%, WBR=0%). If urine was missed in a collection, the point would fall below the 100% line. The points corresponding to the second, third, and fourth urine collections are shown. The statistical error in the points is about ±5%. The points corresponding to the first urine collections are not shown because they are assumed to be complete. The points lie in two groups. In one group, most of the points lie on the 100% line, indicating that the urine collections corresponding to these points were efficiently obtained. In the other group, most of the points lie well below the 100% line, or even along the whole body retention axis, suggesting that the urine collections corresponding to these points were not obtained.

The mean whole body retention and urinary excretion corresponding to the four scans are shown in (P148, WHOLE BODY RETENTION AND URINARY EXCRETION), and the individual data are shown in Appendix II. The urinary excretion is calculated from the urine collections. Note that the time of a given urine collection is generally not the same among all patients. For example, the first collections were obtained between 1.3 and 2.7 hours after injection. Also, in some patients, only three urine collections were obtained. The sum of the whole body retention and the urinary excretion is

less than 100% after the first scan, as a result of incomplete collections.

Based on these results, complete urine collections are very difficult to obtain over a 24 hour period, so that use of the whole body counts to calculate the whole body activity is probably more accurate than using only the urine collections. Also, since the accuracy of calculating the whole body activity is dependent on the accuracy with which the first urine collection is obtained, it is important to ensure that the first urine collection is complete.

KIDNEYS

In the present study, the mean initial activity in the kidneys is (2.7±1.8)% of the injected activity, which is greater than the 1.9% value obtained by other workers, based on animal studies (see "Literature review" section). The mean effective half life of the kidney activity is (6.7±2.5) hours. The fact that the effective half life of the kidney activity is greater than the physical half life of Tc-99m presumably means that the kidney uptake is not instantaneous in some patients. As a result, inclusion of the first point in the least squares fit method increases the effective half life. The standard deviations in the initial activity and effective half life are large (68% and 38% respectively), due to the large variation in the urinary excretion among the patients.

BONE

In the present study, the mean initial activity in bone was (35±15)% of the injected activity, which is lower than the 50% value obtained by other workers based on animal and human studies (see "Literature review" section). The mean effective half life of the bone activity was (7.0±1.3) hours. The probable reason that the effective half life of the bone is longer than the physical half life of Tc-99m is that the first points on the time-activity curves were obtained at 1.5 to 2 hours after injection, which was when the bone uptake reached a maximum. As a result, inclusion of the first point in the least squares fit method increases the effective half life. Based on the patient images, the activity in bone was observed to be very non-uniform. Qualitatively, the activity is highest in the sacro-iliac and spine, followed by the rest of the pelvis and bone joints, and least visible are the long bones. The ribs are not consistently visible in the patient images.

SOFT TISSUE

The mean effective half life of the soft tissue (thigh) activity is (4.6±0.5) hours, which is significantly ($p = 0.01$) lower than the (5.7±0.7) hours measured over the intestine. The difference in the half lives suggests that the distribution of activity in soft tissue is non-uniform. However, the assumption of a uniform distribution of activity in soft tissue is used to calculate the soft tissue activity from the thigh counts, and used to calculate the contribution of

counts from soft tissue overlying the kidneys, bladder, and spine. A possible explanation for this inconsistency is that the intestine count is overestimated due to its proximity to regions of high activity, which include the kidneys, spine, and pelvis. Another possibility is that there is increased activity in the intestines.

In calculating the soft tissue activity, we had the choice of using either the intestine counts and/or the thigh counts. Use of the intestine counts results in the soft tissue activity being greater than the whole body activity in over half of the patients, which is not possible. However, use of the thigh counts results in this problem occuring in only 1 of 26 patients (patient number 2 in Appendix I). As a result, the thigh counts were used to calculate the soft tissue activity. Use of the thigh counts failed for the one patient probably because the patient was tall and obese (height of 230 cm, weight of 107 kg), so that the assumption of the thigh thickness being equal to 0.6 times the body thickness over the chest was not valid. The thigh thickness was probably underestimated, resulting in an overestimate of the thigh counts, and hence overestimating the soft tissue activity.

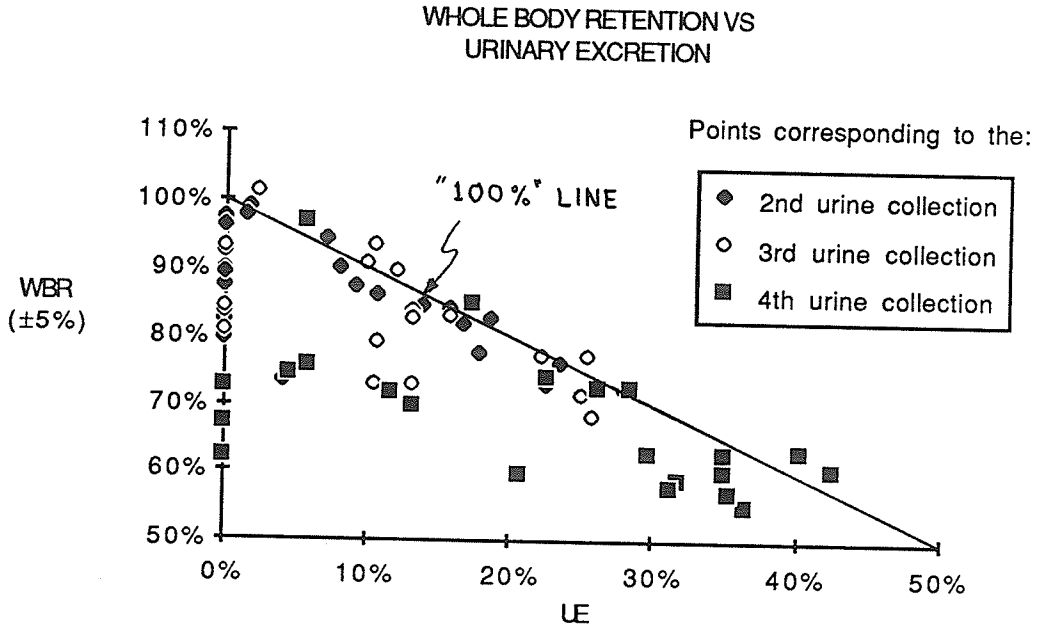
WHOLE BODY RETENTION VS
URINARY EXCRETION
WBR
(±5%)
110%
100%
90%
80%
70%
60%
50%
"100%" LINE
Points corresponding to the:
2nd urine collection
3rd urine collection
4th urine collection
0%
10%
20%
30%
40%
50%
UE

WHOLE BODY RETENTION AND URINARY EXCRETION DATA

scan	WBR		UE		WBR+UE	number
	mean	stdev	mean	stdev	mean	of patients
1	94%	7%	6%	7%	100%	25
2	85%	8%	9%	9%	94%	25
3	83%	9%	12%	10%	95%	19
4	68%	10%	21%	15%	88%	23

The mean and standard deviation of the whole body retention (WBR) and urinary excretion (UE) were calculated for 25 patients (11 female, 14 male). Results expressed as a percentage of the injected activity For most patients, four urine collections were obtained at about 1.5, 4.5, 7.5, and 25.5 hours after injection. In patient studies where only three urine collections were obtained, either the third or fourth collection was missed.

ABSORBED DOSE

The highest mean absorbed dose is received by the bone surface (56 mGy), followed by the bladder wall (21 mGy), kidneys (11 mGy), and red marrow (9.0 mGy) (P140, DOSE DATA). All other organs received less than 4 mGy. These results reflect the fact that Tc-99m pyrophosphate is taken up mainly by bone and is excreted by the renal system. Except for the bladder wall, bone surface, kidneys, and red marrow, the absorbed doses for the male patients are typically about one standard deviation (0.2 to 0.4 mGy) greater than the absorbed doses for the female patients. This is due to the higher activity in bone compared to soft tissue in males as a result of assuming that the bone mass is 13.5% for males and only 11.5 % in females (see "Soft tissue activity" section).

The highest percentage errors in the absorbed doses are in the bladder wall (53%), kidneys (30%), bone surface (30%), and uterus (26%). The errors in the absorbed doses to the other organs range from 7% to 19%. These results reflect the large variation in the urinary excretion among the patients.

The absorbed doses calculated in the present study are consistent with the published data (P140, DOSE DATA). The only large difference is in the dose to the bladder wall; 64 mGy in the published data versus 21 mGy in the present study. This reflects the low activity in the urinary excretion of the patients in the present study. The published data originally assumes that the bone activity

is uniformly distributed throughout the bone volume. For comparison purposes, the published data is recalculated assuming that the bone activity is uniformly distributed on the bone surface, as is done in the present study. This increased the published bone dose by about a factor of 7 and increased the bone marrow dose by about a factor of 1.5. The absorbed dose to the bone is very dependent on the model used.

EFFECTIVE DOSE EQUIVALENT

The effective dose equivalent of (6.1±0.8) mSv is less than the 9.1 mSv calculated from the published data, because of the lower absorbed dose to the bladder wall in the present study. For comparison, a proposal from the ICRP would limit the dose equivalent for non-medical exposure to members of the public to 1 mSv per year (REF, ICRP 45, 1985). The effective dose equivalent calculated in the present study is comparable to that of other diagnostic studies in nuclear medicine (REF, Johannson 1984, Huda 1986).

The effective dose equivalent calculated in the present study depends mainly on the distribution of activity among the bladder, bone, and soft tissue. Let us assume that the effective half lives in all organs is 6.0 hours and that there is no urinary excretion.

Consider two cases:

(1) $A_{BONE} + A_{ST} = \text{constant}$

$A_{KIDNEYS} = 3\%$

$A_{BLADDER} = 7\%$

(2) $A_{BLADDER} + A_{BONE} + A_{ST} = \text{constant}$

$A_{KIDNEYS} = 3\%$

$A_{ST} / A_{BONE} = 1.7$

In case (1), the sum of the activities in bone and soft tissue is constant, as may be the situation in patients with some type of bone disease, where the bone activity increases at the expense of the soft tissue activity. Let us assume that the initial activity is 3% in the kidneys and 7% in the bladder. The effective dose equivalent ranges from 5.7 mSv ($A_{BONE} = 0\%$, $A_{ST} = 90\%$) to 9.0 mSv ($A_{BONE} = 90\%$, $A_{ST} = 0\%$).

In case (2), the sum of the activities in the bladder, bone, and soft tissue is constant, as may be the situation in patients with abnormal renal function, so that a decrease in the bladder activity corresponds to an increase in the activities in the soft tissue and possibly bone. Let us assume that the initial activity is 3% in the kidneys, and that the ratio of the soft tissue activity to the bone activity is 1.7, which was what is found in the present study. The effective dose equivalent ranges from 5.7 mSv ($A_{BLADDER} = 0\%$) to 14 mSv ($A_{BLADDER} = 50\%$).

Therefore, the effective dose equivalent for a Tc-99m bone imaging radiopharmaceutical can fall in the range of 5 to 15 mSv, depending largely on the relative uptake between bladder and bone.

SOURCES OF ERROR

The accuracy of the time-activity data and dose data for an individual patient are mainly limited by the following assumptions:

(1) the patient anatomy is assumed to conform to Reference Man;
(2) the activity in a source organ (kidneys, bladder, bone surface, soft tissue) is assumed to be uniformly distributed; and
(3) the thigh thickness is assumed to be equal to 0.6 times the body thickness over the chest.

The first two assumptions are inherent to the MIRD method of calculating the absorbed doses. The last assumption is used in the present study to calculate the soft tissue activity, which in turn, is used to calculate the bone activity. To further improve the accuracy with which the absorbed doses are calculated, one could use the actual patient anatomy to calculate the S values. The patient anatomy could be obtained using single photon emission computed tomography (SPECT). SPECT could also be used to quantify the activity in the source organs more accurately. However, the long time needed to obtain SPECT images would make these methods impractical. A possibly more practical method of improving the

accuracy of dose calculations may be to use a higher resolution imaging system, so that more accurate regions of interest could be drawn. However, it is doubtful if this would lead to a significant improvement since the statistical error in the counts per pixel is already large, typically 10%.

CONCLUSION

The highest mean absorbed dose is received by the bone surface (56 mGy), followed by the bladder wall (21 mGy), kidneys (11 mGy), and red marrow (9.0 mGy). All other organs receive less than 4 mGy. These results reflect the fact that Tc-99m pyrophosphate is taken up mainly by bone and is excreted by the renal system. The mean effective dose equivalent is 6.1 mSv. Although the absorbed dose to a given organ varies by up to ±50%, the effective dose equivalent varies among patients by less than ±15%. It is not possible to correlate the dose data to a specific patient characteristic, because of the small number of patients and the large variety of diseases present in the patients. The errors in the absorbed doses do not include the systematic errors inherent to the MIRD S values.

It is difficult to say how much the accuracy of the absorbed doses is improved by when comparing the results of the present study to the published data, because the published data by Subramanian and Krishnamurthy are based on a different model. They assumed that the activity in soft tissue is only due to the blood activity. Also, they assumed that 50% of the injected activity was taken up into the bone, and that no more than 1.9% of the injected activity was taken up into the kidneys. The bone and kidney uptake were estimated from human and animal studies. The bladder activity was calculated from the urinary excretion, and assumed that the urine activity retained in the bladder after voiding was

negligible. The absorbed doses calculated in the present study are probably more accurate because they are based on direct measurements of the counts over the whole body, kidneys, bladder, bone and soft tissue, as well as on cumulative urine collections. However, gross assumptions are still used in the calculation of the soft tissue and bone activities, which have a large impact on the dose calculations.

The major problems in the dosimetry of a Tc-99m phosphorous bone imaging radiopharmaceutical that are still unsolved is how to determine the highly non-uniform distribution of activity in the skeleton, and to deal with the fact that the activity is distributed on the bone surface and not throughout the total bone volume. These two problems make it very difficult to quantify the activity in bone directly from counts measured over the bone.

APPENDIX I - PATIENT DATA

The patient data are shown in four blocks on the next two pages (patients 1-7, 8-14, 15-21, and 22-26), with the patient number shown at the top of each column. There are 26 patients (11 female, 15 male). Reading down the rows are shown the sex, age, weight, height, patient depth over the chest, injected activity, number of scans obtained in the patient study, and the time of each scan. The mean and standard deviation are shown in the last two columns. The following two pages show the disease state of the patients, based on their medical records. The five columns show the disease state, bone function, renal function, diagnosis, and medication. Bone and renal function are indicated by "N", "A", or "?" which corresponds to normal, abnormal, and unknown. Abnormal bone function is described by an excess uptake of activity in a bone region, based on a whole body scan report done for each patient. Tests for renal function were not done for all patients, as indicated by the "?" symbol. Normal renal function was partially indicated by the tests for serum urea, serum creatinine, urine creatinine, and creatinine clearance.

APPENDIX I - PATIENT DATA

patient	1	2	3	4	5	6	7
sex	F	M	M	F	M	F	M
age	81	60	66	42	79	51	68
wt(kg)	72	107	89	51	83	53	52
ht(cm)	155	230	183	165	185	157	173
dp(cm)	23	29	23	20	25	23	23
act(MBq	720	738	700	740	701	685	711
#scans	3	4	4	4	4	4	3
time, 1	1.7	1.8	1.6	1.9	1.9	2.3	1.6
2	4.7	4.8	4.5	4.8	4.5	4.9	4.7
3	7.4	7.4	7.3	7.5	7.5	7.5	---
4	---	25.5	25.5	26.0	26.0	25.5	24.2

patient	8	9	10	11	12	13	14
sex	F	M	M	M	F	F	F
age	44	55	76	77	56	81	43
wt(kg)	48	102	100	82	78	70	95
ht(cm)	160	183	175	163	153	180	163
dp(cm)	20	29	33	23	24	25	28
act(MBq	740	685	695	680	700	663	724
#scans	3	4	3	4	3	4	4
time, 1	1.5	1.6	1.8	1.8	2.5	1.6	1.5
2	4.1	3.8	4.8	5.0	5.0	4.6	4.4
3	---	6.0	7.5	7.3	---	7.5	7.2
4	22.1	24.6	25.7	25.7	23.5	26.0	25.7

sex = male (M) or female (F)
age (years), wt = weight (kg)
ht = height (cm), dp = depth over chest (cm)
act = injected activity (MBq)
#scans = number of scans obtained
time = time of each scan (hours after injection)

APPENDIX I - PATIENT DATA

patient	15	16	17	18	19	20	21
sex	F	M	M	F	M	M	F
age	70	93	68	18	35	64	73
wt(kg)	50	75	65	68	65	106	34
ht(cm)	167	178	171	170	164	183	152
dp(cm)	20	23	23	20	23	28	23
act(MBc	740	722	730	676	660	657	700
#scans	4	4	4	3	4	3	4
time, 1	1.4	1.8	1.6	1.3	1.8	1.7	1.7
2	4.3	4.4	4.5	3.5	4.4	5.4	4.7
3	6.9	7.3	7.5	---	7.5	7.7	7.5
4	25.5	25.7	25.5	23.7	25.5	---	25.7

patient	22	23	24	25	26	mean	stdev
sex	F	M	M	M	M	26 patients	
age	19	85	55	43	47	60	19
wt(kg)	64	69	80	63	66	73	19
ht(cm)	169	185	176	169	190	173	16
dp(cm)	23	23	25	23	18	24	3
act(MBc	700	700	613	702	740	701	31
#scans	3	3	4	4	4	---	---
time, 1	2.2	2.0	1.6	1.9	2.7	1.8	0.3
2	5.1	5.2	4.1	4.5	5.4	4.6	0.5
3	---	---	6.5	7.3	9.0	7.4	0.6
4	24.4	23.8	27.7	25.3	26.2	25.2	1.1

sex = male (M) or female (F)
age (years), wt = weight (kg)
ht = height (cm), dp = depth over chest (cm)
act = injected activity (MBq)
#scans = number of scans obtained
time = time of each scan (hours after injection)

APPENDIX I - PATIENT DATA					
NO.	DISEASE	BONE	RENAL	DIAGNOSIS	MEDICATION
1	cancer	N	A	carcinoma of right breast	serpasil esidrix
				urinary tract infection	keflex, serax
2	infection	A	N	infection in right foot, diabetic	aldomet, clindamycin
					cytoxan, lasix
3	cancer	N	A	carcinoma of bladder	
				left ureteric obstruction	
4	infection	N	A	meningitis	cloxacillin, cefoxitin
				anemia, very high serum protein	ferrous sulfate, cortisporin
5	cancer	N	N	adenocarcinoma of right lung, diabetic	voltaren
6	arthritis	A	?	rheumatoid arthritis, chronic vasculitis	prednisone, entrophen
				leg ulcers, infected with herpes zoster	tobramycin, ticarcillin
7	vascular	N	A	left brain stroke, diabetic, carotid artery stenosis	
				ulcer in left leg, peripheral vascular disease	
8	cancer	A	N	carcinoma of left breast, cyst with	tylenol, serax
				perforation and chemical peritonitis	
9	infection	A	?	cellulitis on right foot	cloxacillin, hydralazine, clind
				diabetic, overweight	digoxin, allopurinol, proprano
10	cancer	N	N	adenocarcinoma of rectum, polynephritis,	ampimycin, gentamycin
				anemia, hypertension, atrial fibrulation, rectal polyps	
11	cancer	?	?	cancer of hard palate, diabetic	insulin
				hypertension, mild aortic stenosis	
12	arthritis	A	N	rheumatoid arthritis	tylenol, naproxen
13	cancer	A	N	carcinoma of esophagus, metastases to kidne	digoxin, k-lyte, lasix
				and brain (aphagia); hypercalcemia, atrial	filtration

APPENDIX I - PATIENT DATA					
NO.	DISEASE	BONE	RENAL	DIAGNOSIS	MEDICATION
14	cancer	A	N	metastatic carcinoma of right breast	
15	cancer	N	N	enlarged inguinal nodes bilaterally	decadron, levo-dromoran, mo
				right buttock soft tissue mass, history of ly	imodium eltroxin, allopurinol,
16	cancer	A	A	carcinoma of prostate	morphine, atropine
					stilphostrol, serax
17	cancer	A	N	adenocarcinoma of lung	ferrous sulfate, tylenol
				multiple bony metastases, anemia	
18	infection	A	N	sacroilieitis	ampicillin, gentamicin
					metronidazole, cytoxan, tylen
19	infection	A	A	infected foot ulcer, diabetic, hypertension	aldomet, cloxacillin, clindamy
				chronic renal failure, right arm fistula	hydrochlorothiazide, lasix
20	cancer	N	?	adenocarcinoma of prostate	tylenol, serax, aldomet
				history of hypertension, obesity	trazadone, lorazepam
21	cancer	N	N	metastatic carcinoma of thyroid	colace, morphine
				metastases to left neck	
22	cancer	N	N	recurrent liposarcoma of right ankle	serax, lorazepam
23	arthritis	N	?	polymyalgia, temporal arthritis,	prednisone, chlorthalidone
				peripheral vascular disease	entrophen
24	infection	N	A	cataract of left eye	
				history: diabetic, kidney transplant	
25	cancer	N	N	small bowel obstruction due to ileocecal int	serax, flagyl, ampicillin
				secondary to small bowel, history of lympho	demerol, tylenol
26	infection	N	N	renal abscess, anemia	ampicillin, gentamicin
				chronic pyelonephritis	

APPENDIX II - TIME-ACTIVITY DATA AND DOSE DATA OF 25 PATIENTS

The time-activity data and dose data for 25 patients are shown on the following six pages in three blocks (patients 1-11, 12-21, and 22-26). Note that patient number 2 in Appendix I was not used in generating the results. The patient number is shown at the top of each column. The data consists of three parts: whole body retention and urinary excretion data, time-activity data, and dose data. The results for each patient covers two pages. On the first page, reading down the rows, are shown the whole body retention, urinary excretion, and the sum of these two parameters for each of the four scans, all expressed as a percentage of the injected activity. The four scans were obtained at about 1.5, 4.5, 7.5 and 25.5 hours after injection. Eight of the 25 patients were only scanned three times. Following this is the time-activity data, which consists of the correlation coefficient, initial activity, and half life for the kidneys (KI), bladder (BL), bone (BO), soft tissue (ST), whole body (BODY), upper spine (USP), lower spine (LSP), and intestine (INT). The initial activities are expressed as a percentage of the injected activity, and the half lives are expressed in hours. On the following page are shown the dose data, specifically the absorbed doses to 20 target organs. The absorbed dose to the testes is zero for females, and the absorbed dose to the ovaries and uterus is zero for males. The mean, standard deviation, and percentage error are shown in the last three columns.

APPENDIX II - TIME-ACTIVITY DATA AND DOSE DATA OF 25 PATIENTS										
patient	1	3	4	5	6	7	8	9	10	11
WBR, 1	100%	91%	97%	87%	79%	88%	87%	98%	100%	100%
2	86%	83%	73%	84%	74%	84%	78%	94%	87%	97%
3	79%	77%	73%	77%	72%			91%	84%	92%
4		63%	55%	63%	60%	63%	59%	74%	62%	76%
UE, 1	0%	9%	3%	13%	21%	12%	13%	2%	0%	0%
2	11%	19%	4%	14%	22%	13%	18%	7%	0%	0%
3	11%	25%	11%	22%	28%			10%	0%	0%
4		40%	37%	35%	43%	30%	32%	23%	0%	6%
WBR+UE	100%	100%	100%	100%	100%	100%	100%	100%	100%	100%
2	97%	101%	77%	98%	97%	97%	96%	101%	87%	97%
3	90%	103%	84%	99%	100%	0%	0%	101%	84%	92%
4	0%	103%	92%	98%	103%	93%	91%	97%	62%	82%
correlation coefficient										
KI	-0.97	-0.99	-0.93	-0.96	-0.95	-0.99	-0.99	-0.98	-0.98	-1.00
BL	-0.99	-0.98	-0.95	-0.96	-0.99	-0.94	-1.00	-0.90	-0.95	-0.98
BO	-0.99	-0.99	-1.00	-0.98	-0.96	-0.97	-0.99	-0.85	-0.85	-0.95
ST	-1.00	-0.99	-0.99	-0.99	-0.99	-1.00	-0.98	-1.00	-0.99	-0.99
BODY	-1.00	-1.00	-1.00	-1.00	-1.00	-1.00	-1.00	-1.00	-1.00	-1.00
USP	-0.97	-1.00	-1.00	-0.99	-0.99	-1.00	-1.00	-1.00	-1.00	-1.00
LSP	-0.98	-0.99	-1.00	-0.99	-0.99	-1.00	-1.00	-0.99	-0.99	-1.00
INTEST	-1.00	-0.97	-1.00	-1.00	-1.00	-1.00	-1.00	-1.00	-0.99	-1.00
initial activity										
KI	2%	1%	2%	2%	4%	1%	2%	2%	4%	1%
BL	22%	2%	12%	5%	5%	13%	4%	7%	18%	8%
BO	36%	41%	49%	31%	25%	20%	44%	18%	20%	32%
ST	54%	48%	32%	53%	48%	58%	36%	75%	62%	63%
BODY	102%	90%	102%	89%	81%	90%	87%	97%	100%	101%
halflife										
KI	5.7	6.6	5.5	9.7	3.9	6.6	8.3	6.4	6.4	7.8
BL	1.6	4.7	2.8	4.0	3.5	4.5	3.2	3.0	2.6	3.6
BO	7.4	6.1	5.4	6.4	7.2	8.0	5.7	8.2	7.5	6.9
ST	3.9	4.5	4.7	4.6	4.6	4.4	4.4	4.8	4.7	4.8
BODY	5.1	5.2	5.2	5.4	5.4	5.5	5.5	5.5	6.0	5.9
USP	7.3	5.8	5.6	5.6	6.2	6.2	5.4	5.3	5.2	5.8
LSP	7.7	5.9	5.7	5.4	6.1	6.9	6.1	5.6	5.9	6.2
INTEST	4.1	4.7	6.0	6.0	5.4	5.7	5.4	6.6	5.4	5.5

APPENDIX II, TIME-ACTIVITY DATA AND DOSE DATA OF 25 PATIENTS										
patient	1	3	4	5	6	7	8	9	10	11
absorbed	doses									
Adrena	2.6	2.5	2.3	2.9	2.6	2.6	2.6	3.2	3.3	3.0
Bladder	19.3	12.6	24.6	17.2	17.6	34.2	16.5	16.2	29.2	18.2
Bone s	64.3	60.6	64.8	49.3	44.5	39.3	61.5	37.6	38.1	54.7
GI (sto	1.9	1.9	1.6	2.1	2.0	2.1	1.7	2.7	2.4	2.4
GI (sm	2.5	2.4	2.2	2.7	2.5	2.9	2.2	3.3	3.2	3.0
GI (ULI	2.3	2.2	2.0	2.5	2.3	2.7	2.0	3.1	2.9	2.8
GI (LLI	3.0	2.7	2.9	3.0	2.8	3.7	2.6	3.5	3.7	3.4
Kidneys	8.8	6.9	8.8	13.3	10.9	7.1	13.0	8.4	16.0	6.5
Liver	2.0	2.0	1.7	2.2	2.0	2.1	1.8	2.7	2.5	2.4
Lungs	2.0	2.0	1.7	2.0	1.9	2.0	1.7	2.5	2.2	2.4
Marrow	9.8	9.3	9.5	8.3	7.5	7.3	9.2	7.6	7.5	9.2
Other t	2.1	2.0	1.9	2.2	2.0	2.3	1.9	2.6	2.4	2.5
Ovaries	2.8		2.7		2.7		2.4			
Pancrea	2.4	2.3	2.0	2.6	2.4	2.4	2.2	3.1	2.9	2.8
Skin	1.4	1.3	1.2	1.4	1.3	1.4	1.2	1.7	1.5	1.6
Spleen	2.2	2.1	1.9	2.5	2.2	2.3	2.1	2.9	2.9	2.5
Testes		1.8		2.0		2.5		2.5	2.5	2.4
Thyroid	1.5	1.5	1.3	1.5	1.4	1.5	1.3	1.9	1.6	1.8
Uterus	3.8		4.0		3.7		3.2			
Total b	3.0	2.9	2.8	2.9	2.7	2.9	2.7	3.2	3.1	3.3

APPENDIX II, TIME-ACTIVITY DATA AND DOSE DATA OF 25 PATIENTS										
patient	12	13	14	15	16	17	18	19	20	21
WBR, 1	100%	87%	88%	89%	100%	96%	100%	99%	100%	100%
2	83%	83%	76%	84%	96%	87%	73%	99%	79%	90%
3		83%	68%	83%	93%	90%		101%	81%	84%
4	68%	70%	57%	73%	73%	85%	60%	97%		72%
UE, 1	0%	13%	12%	11%	0%	4%	0%	1%	0%	0%
2	0%	13%	24%	16%	0%	9%	23%	2%	0%	0%
3		13%	26%	16%	0%	12%		2%	0%	0%
4	0%	13%	35%	26%	0%	17%	35%	6%		12%
WBR+UE	100%	100%	100%	100%	100%	100%	100%	100%	100%	100%
2	83%	96%	100%	100%	96%	97%	96%	100%	79%	90%
3	0%	96%	94%	99%	93%	102%	0%	104%	81%	84%
4	68%	83%	92%	99%	73%	103%	95%	102%	0%	83%
correlation coefficient										
KI	-1.00	-1.00	-0.94	-0.74	-0.99	-0.89	-0.90	-0.98	-0.94	-0.88
BL	-0.87	-0.99	-0.99	-0.99	-0.87	-0.98	-0.88	-0.99	-0.95	-1.00
BO	-0.92	-0.78	-0.99	-0.95	-0.97	-0.99	-0.96	-0.98	-0.99	-1.00
ST	-1.00	-1.00	-0.97	-0.99	-1.00	-0.97	-0.96	-1.00	-0.99	-0.99
BODY	-1.00	-1.00	-1.00	-1.00	-1.00	-1.00	-0.99	-1.00	-1.00	-1.00
USP	-1.00	-1.00	-0.99	-0.98	-0.99	-1.00	-1.00	-0.99	-0.97	-0.99
LSP	-1.00	-0.98	-0.99	-0.97	-0.98	-0.99	-0.99	-0.95	-0.94	-1.00
INTEST	-1.00	-1.00	-0.98	-1.00	-1.00	-1.00	-0.98	-0.99	-1.00	-1.00
initial activity										
KI	2%	4%	9%	2%	2%	7%	3%	2%	2%	2%
BL	42%	4%	6%	5%	12%	4%	23%	1%	9%	0%
BO	30%	17%	40%	29%	22%	55%	34%	33%	33%	61%
ST	41%	73%	36%	53%	64%	32%	40%	65%	69%	35%
BODY	100%	87%	84%	88%	100%	95%	93%	99%	100%	102%
halflife										
KI	7.2	7.6	2.5	13.6	5.5	2.9	4.7	5.3	7.3	7.3
BL	2.1	3.2	3.6	3.5	7.1	4.0	2.4	5.8	0.7	5.6
BO	7.3	10.9	6.2	6.9	6.8	6.5	6.7	7.4	9.5	5.6
ST	4.7	3.8	4.0	4.9	5.1	4.6	4.3	5.2	3.1	4.6
BODY	6.0	6.0	5.5	5.7	6.0	5.7	5.3	5.9	6.0	5.8
USP	5.5	5.5	6.4	6.5	6.0	6.9	5.8	6.3	6.6	4.5
LSP	6.2	5.7	5.9	6.9	6.3	6.9	6.1	7.7	6.8	5.2
INTEST	6.3	6.2	4.9	6.0	5.7	6.2	5.1	6.5	3.9	6.0

APPENDIX II, TIME-ACTIVITY DATA AND DOSE DATA OF 25 PATIENTS										
patient	12	13	14	15	16	17	18	19	20	21
absorbed	doses									
Adrena	2.6	3.4	2.5	3.2	3.0	2.7	2.4	3.3	2.9	2.7
Bladder	42.5	13.3	19.2	14.5	45.2	11.5	32.2	6.9	10.2	8.5
Bone s	53.3	45.7	59.9	50.4	37.7	85.7	54.8	60.2	76.1	82.1
GI (sto	1.9	2.4	1.6	2.3	2.5	1.7	1.7	2.6	2.0	1.8
GI (sm	2.8	2.8	2.1	2.8	3.6	2.2	2.5	3.1	2.5	2.2
GI (ULI	2.5	2.7	1.9	2.6	3.3	2.0	2.2	2.9	2.4	2.1
GI (LLI	3.9	3.0	2.6	3.0	4.6	2.5	3.3	3.2	2.8	2.4
Kidneys	10.5	17.9	14.1	16.2	7.6	12.5	9.7	7.3	9.8	11.4
Liver	1.9	2.5	1.7	2.4	2.5	1.8	1.8	2.7	2.1	1.9
Lungs	1.8	2.2	1.6	2.1	2.4	1.9	1.7	2.6	2.1	1.9
Marrow	8.7	8.1	8.9	8.6	7.7	11.9	8.6	10.0	11.2	11.5
Other t	2.3	2.3	1.8	2.3	2.8	2.0	2.0	2.6	2.2	2.0
Ovaries	3.8	2.9	2.4	2.9			3.1			2.2
Pancrea	2.3	2.9	2.1	2.8	2.9	2.3	2.1	3.1	2.5	2.3
Skin	1.3	1.5	1.1	1.5	1.7	1.3	1.2	1.7	1.4	1.3
Spleen	2.2	2.8	2.0	2.7	2.8	2.1	2.0	2.8	2.3	2.1
Testes					3.2	1.7		2.2	1.9	
Thyroid	1.4	1.6	1.2	1.6	1.8	1.5	1.3	2.0	1.7	1.5
Uterus	6.0	3.6	3.4	3.6			4.8			2.5
Total b	3.0	3.0	2.6	3.0	3.3	3.2	2.8	3.5	3.2	3.1

APPENDIX II, TIME-ACTIVITY DATA AND DOSE DATA OF 25 PATIENTS										
patient	22	23	24	25	26	mean	stdev	stdev/mean		
WBR, 1	100%	99%	95%	100%	83%	94%	7%	7%	WBR, 1	
2	89%	98%	90%	82%	82%	94%	32%	34%	2	
3			94%	73%	71%	104%	67%	65%	3	
4	67%	75%	73%	60%	58%	94%	92%	98%	4	
UE, 1	0%	1%	5%	0%	17%	6%	7%	116%	UE, 1	
2	0%	2%	8%	0%	17%	23%	53%	224%	2	
3			11%	13%	25%	41%	89%	219%	3	
4	0%	5%	29%	21%	31%	51%	106%	208%	4	
WBR+UE	100%	100%	100%	100%	100%	100%	0%	0%	WBR+UE	
2	89%	99%	98%	82%	99%	102%	30%	29%	2	
3	0%	0%	104%	86%	97%	89%	74%	84%	3	
4	67%	79%	101%	81%	89%	109%	88%	81%	4	
correlation coefficient									correlation co	
KI	-0.98	-0.85	-0.97	-0.99	-1.00	-0.95	0.06	-6%	KI	
BL	-0.96	-0.98	-0.97	-0.94		-0.96	0.04	-4%	BL	
BO	-1.00	-0.99	-0.85	-0.97	-0.98	-0.95	0.06	-6%	BO	
ST	-0.98	-0.96	-1.00	-0.99	-0.99	-0.99	0.01	-1%	ST	
BODY	-1.00	-1.00	-1.00	-1.00	-1.00	-1.00	0.00	0%	BODY	
USP	-1.00	-0.93	-0.98	-1.00	-1.00	-0.99	0.02	-2%	USP	
LSP	-1.00	-0.84	-0.99	-1.00	-1.00	-0.98	0.03	-4%	LSP	
INTEST	-0.99	-0.96	-1.00	-1.00	-1.00	-0.99	0.01	-1%	INTEST	
initial activity									initial	activity
KI	2%	1%	2%	2%	2%	3%	2%	68%	KI	
BL	5%	1%	5%	37%		10%	11%	109%	BL	
BO	71%	61%	12%	32%	25%	35%	15%	44%	BO	
ST	25%	38%	78%	36%	52%	50%	16%	31%	ST	
BODY	100%	100%	96%	101%	85%	95%	7%	7%	BODY	
halflife									halflife	
KI	5.2	12.3	5.1	8.3	6.0	6.7	2.5	38%	KI	
BL	3.7	5.3	4.4	2.2		3.7	1.4	38%	BL	
BO	5.5	5.3	9.0	6.6	6.8	7.0	1.3	19%	BO	
ST	4.5	5.4	5.1	4.8	4.6	4.6	0.5	10%	ST	
BODY	6.0	5.9	5.5	5.5	5.6	5.7	0.3	5%	BODY	
USP	5.7	6.3	5.8	5.8	5.7	5.9	0.5	9%	USP	
LSP	6.1	6.3	5.5	6.0	5.6	6.1	0.6	9%	LSP	
INTEST	5.3	7.8	5.6	5.9	5.6	5.7	0.7	13%	INTEST	

APPENDIX II, TIME-ACTIVITY DATA AND DOSE DATA OF 25 PATIENTS										
patient	22	23	24	25	26	mean	stdev	stdev/mean		
absorbed	doses								absorbed	doses
Adrena	2.3	3.0	3.4	2.5	2.6	2.8	0.3	12%	Adrenals	
Bladder	15.9	10.3	18.4	42.0	24.0	20.9	11.1	53%	Bladder	wall
Bone s	93.0	78.5	29.2	52.1	42.3	56.3	16.8	30%	Bone	surface
GI (sto	1.4	2.0	2.8	1.8	2.0	2.1	0.4	19%	GI (stom	wall)
GI (sm	2.0	2.5	3.5	2.7	2.7	2.7	0.4	17%	GI (small	intes
GI (ULI	1.8	2.4	3.3	2.4	2.5	2.5	0.4	17%	GI (ULI	wall)
GI (LLI	2.6	2.7	3.7	3.7	3.2	3.1	0.6	18%	GI (LLI	wall)
Kidneys	6.9	12.0	9.6	12.1	8.9	10.7	3.2	30%	Kidneys	
Liver	1.6	2.1	2.9	1.8	2.1	2.1	0.4	17%	Liver	
Lungs	1.7	2.1	2.6	1.7	1.9	2.0	0.3	15%	Lungs	
Marrow	12.5	11.4	6.8	8.5	7.4	9.0	1.6	18%	Marrow	(red)
Other t	1.9	2.2	2.7	2.1	2.1	2.2	0.3	12%	Other	tissue (
Ovaries	2.3					2.8	0.5	17%	Ovaries	
Pancrea	1.9	2.6	3.3	2.2	2.4	2.5	0.4	15%	Pancreas	
Skin	1.2	1.4	1.8	1.3	1.3	1.4	0.2	13%	Skin	
Spleen	1.7	2.3	3.1	2.2	2.3	2.4	0.4	16%	Spleen	
Testes		1.9	2.6	2.5	2.2	2.3	0.4	17%	Testes	
Thyroid	1.4	1.6	2.0	1.3	1.5	1.5	0.2	15%	Thyroid	
Uterus	3.0					3.8	1.0	26%	Uterus	(nongra
Total b	3.1	3.3	3.2	2.9	2.7	3.0	0.2	7%	Total	body

REFERENCES

Abdel-dayem HM, Alker GJ (1974) Improving the Tc-99m phosphate bone scan. J Nucl Med 15:1229

Alazraki N (1984) The musculoskeletal system, Chapter 8. In Textbook of Nuclear Medicine, Volume II, 2nd Edition. Edited by J Harbert, AFG da Rocha. Philadelphia, Lea & Febiger

Arnold JS (1982) Mechanisms of fixation of bone imaging radiopharmaceuticals, Chapter 5. In Studies of Cellular Function Using Radiotracers. Edited by MW Billinghurst. Boca Raton, Florida, CRC Press

Bevan JA, Tofe AJ, Benedict JJ (1980) Tc-99m HMDP (hydroxymethylene diphosphonate): A radiopharmaceutical for skeletal and acute myocardial infarct imaging. J Nucl Med 21:961

Billinghurst MW (1973) Chromatographic quality control of Tc-99m labeled compounds. J Nucl Med 14:793

Blau M (1976) Problems of dose calculations for technetium-99m bone scanning agents. In Radiopharmaceutical Dosimetry Symposium, HEW Publication (FDA) 76-8044.

Castronovo FP, Guiberteau MJ, Berg G, et al. (1977) Pharmacokinetics of technetium-99m diphosphonate. J Nucl Med 18:809

Citrin DL, Bessent RG, McGinley E, et al. (1975) Dynamic studies with Tc-99m HEDP in normal subjects and in patients with bone tumors. J Nucl Med 16:886

Davis MA, Jones AL (1976) Comparison of agents for skeletal imaging. Semin Nucl Med 6:19

Dillman LT, von der Lage FC (1975) Radionuclide decay schemes and nuclear parameters for use in radiation dose estimation. MIRD pamphlet 10. New York. Society of Nuclear Medicine.

Eckelman WC, Reba RC, Kubota H, et al. (1974) Tc-99m pyrophosphate for bone imaging. J Nucl Med 15: 279

Eckelman WC (1984) Radiopharmaceutical chemistry, Chapter 10. In Textbook of Nuclear Medicine, Volume I, 2nd Edition. Edited by J Harbert, AFG da Rocha. Philadelphia, Lea & Febiger

Ericson J (1984) Imaging systems, Chapter 6. In Textbook of Nuclear Medicine, Volume I, 2nd Edition. Edited by J Harbert, AFG da Rocha. Philadelphia, Lea & Febiger

Fleming JS (1979) A technique for the absolute measurement of activity using a gamma camera and computer. Phys Med Biol 24:176

Fogelman I, Bessent JGT, Citrin DL, et al. (1978) The use of whole body retention of Tc-99m diphosphonate in the diagnosis of metabolic bone disease. J Nucl Med 19:270

Genant HK, Bautovich GJ, Sing M, et al. (1974) Bone seeking radionuclides: an in vivo study of factors affecting skeletal uptake. Radiology 113:373

Harbert J, da Rocha AFG (Eds) (1984) Textbook of Nuclear Medicine, Vol I. Philadelphia, Lea & Febiger

Hine GJ, Sorenson JA (Eds) (1981) Instrumentation in nuclear medicine, Vol 2. New York, Academic Press.

Hladik WB III, Nigg KK, Rhodes BA (1982) Drug induced changes in the biologic distribution of radiopharmaceuticals. Semin Nucl Med 12:184

Hosain P (1973) Technetium-99m labeled pyrophosphate: a simple and reproducible bone scanning agent. Br J Radiol 46:724

Huda W (1986) Nuclear medicine dose equivalent: a method for determination of radiation risk. J Nucl Med Tech 14:199-201

ICRP 23 (1975) Report of the task group on reference man, adopted by the International Commission on Radiological Protection, October 1974. New York, Pergamon Press.

ICRP 26 (1977) Recommendations of the International Commission on Radiological Protection. Oxford, Pergamon Press.

ICRP 30 (1978) Limits for intakes of radionuclides by workers. International Commission on Radiological Protection.

ICRP 45 (1985) Quantitative bases for developing a unified index of harm. Oxford, Pergamon Press.

ICRU 32 (1979) Methods of assessment of absorbed dose in clinical use of radionuclides. International Commission on Radiation Units and Measurents, Washington DC.

ICRU 40 (1986) The quality factor in radiation protection. Bethesda, Maryland.

Jones AG, Francis MD, Davis MA (1976) Bone scanning: radionuclide reaction mechanisms. Semin Nucl Med 6:3

Krishnamurthy GT, Huebotter RJ, Walsh CF, et al. (1975) Kinetics of Tc-99m labeled pyrophosphate and polyphosphate in man. J Nucl Med 16:109

Lentle BC, Scott JR, Noujaim AA, Jackson FI (1979) Iatrogenic alterations in radionuclide biodistributions. Semin Nucl Med 9:131

Loevinger R, Berman M (1976) A revised chema for calculating the absorbed dose from biologically distributed radionuclides. MIRD pamphlet 1, revised. New York, Society of Nuclear Medicine.

Perez R, Kohen Y, Henry R, et al. (1972) A new radiopharmaceutical for Tc-99m bone scanning. J Nucl Med 13:788

Potsaid MS, Guiberteau MJ, McKusick KA (1977) Quality of bone scans compared to itme between dose and scan. J Nucl Med 18:787

Rock RC, Walker WG, Jennings CD (1986) Nitrogen metabolites and renal function, Chapter 11. In Textbook of Clinical Chemistry, edited by NW Tietz. Toronto, WB Saunders

Roedler HD (1981) Accuracy of internal dose calculations with special consideration of radiopharmacetucial biokinetics. In Radiopharmaceutical Dosimetry Symposium, HEW Publication (FDA) 80-8166

Rohen JW, Yokochi C (1983) Color atlas of anatomy. A photographic study of the human body. Ikagu-Shoen Medical Publishers, New York

Rollo FD (Ed) (1977) Nuclear medicine physics, instrumentation, and agents. St. Louis, CV Mosby

Rosenthall L, Kaye M (1976) Observations on the mechanism of Tc-99m labeled phosphate complex uptake in metabolic bone disease. Semin Nucl Med 6:59

Schultz CL, Roberts JG, Webber CE, et al. (1987) Whole body retention of Tc-99m imidodiphosphate: a measurement of total body bone turnover rate. Nuc J Can 1:119

Snow RM, Weber DA (1975) Time dependent image quality using Tc-99m pyrophosphate. J Nucl Med 16:879

Snyder WS, Ford MR, Warner GG, Watson SB (1973) "S", absorbed dose per unit cumulated activity for selected radionuclides and organs. MIRD pamphlet 11. New York, Society of Nuclear Medicine.

Snyder WS, Ford MR, Warner GG (1977) Estimates of specific absorbed fractions for photon sources uniformly distributed in various organs of a heterogeneous phantom. NM/MIRD Pamphlet 5, Revised. New York, Society of Nuclear Medicine.

Subramanian G, McAfee JG (1971) A new complex of Tc-99m for skeletal imaging. Radiology 99:192

Subramanian G, McAfee JG, Blair RJ, et al. (1975) Technetium 99m methylene diphosphonate - a superior agent for skeletal imaging: comparison with other Technetium complexes. J Nucl Med 16:744

Thomsen K, Nilas L, Mogensen T, Christiansen C (1986) Determination of bone turnover by urinary excretion of Tc-99m MDP. Eur J Nucl Med 12:342

Tothill P, Galt JM (1971) Quantitative profile scanning for the measurement of organ radioactivity. Phys Med Biol 16:625

United States Pharmacopeia XX revised (1975) US Pharmacopeia Convention, Rockville, MD, p765-6

Weber DA, Keyes JW, Benedette WJ, et al. (1974) Tc-99m pyrophosphate for diagnostic bone imaging. Radiology 113:131

Wilson MA (1981) The effect of age on the quality of bone scans using Tc-99m pyrophosphate. Radiology 139:703

Yano Y, McRae J, Van Dyke DC, et al. (1973) Technetium 99m labeled stannous ethane-1-hydroxy-1-diphosphonate: a new bone scanning agent. J Nucl Med 14:73